PROTEOMICS INSIGHTS INTO MOLECULAR MECHANISMS OF TRIPTOLIDE AGAINST COLORECTAL CANCER

LI JINGLIN

(B.Sc. Nankai University)

A THESIS SUBMITTED FOR THE DEGREE OF DOCTOR OF PHILOSOPHY

DEPARTMENT OF BIOLOGICAL SCIENCES

NATIONAL UNIVERSITY OF SINGAPORE

2016

"Declaration

I hereby declare that this thesis is my original work and it has been written by me in its entirety. I have duly acknowledged all the sources of information which have been used in the thesis.

This thesis has also not been submitted for any degree in any university previously."

Signature: 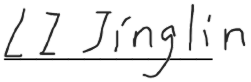

LI Jinglin

31 March, 2017

Acknowledgements

It is my greatest pleasure to express deepest appreciation to my supervisor Dr. Lin Qingsong for his support and guidance. Words cannot express my gratitude to him for his trust and unconditioned support for my research and my career. His timely suggestions, meticulous scrutiny and mentorship encourage me to a great extent to accomplish this task as well as motivate me throughout my PhD life.

I would like to thank to all lab members in our lab: Zhengjun, Jigang, Teck Kwang, Xing Fei, Yew Mun, Chin Xia, Lili, Zhou Hu, Siok Yuen and Xin Shan. They provided a warm and professional research environment. They are teachers and advisors, who helped me a lot during these years. Special thanks to Dr. Wang Jigang for continuous help and advice in my research.

I extend my thanks to the staffs in Protein and Proteomics Center: Teck Kwang, Xianhui, for their technical expertise and help.

I would like to thank to Dr. Wang Shu, Dr. Jayaraman Sivaraman, Dr. Henry Mok, Dr. Gong Zhiyuan, and Dr. Kim Chu-Young for their guidance and advice.

I would like to express my sincere gratitude to NUS, MOE for the NUS Research Scholarship for supporting my PhD study.

Finally, I am grateful for the understanding, encouragement and continuous support from my family, friends and loved ones.

Table of Contents

Declaration……...……....i
Acknowledgements……...……...ii
Table of Contents……iii
Summary……...……..vi
List of Tables……..……...…vii
List of Figures……...……...viii
List of Abbreviations……..……x
Chapter 1 Introduction 1
1.1 An overview of colorectal cancer 2
1.1.1 Cancer 2
1.1.2 Hallmarks of cancer 3
1.1.3 Colorectal Cancer 5
1.2 Triptolide as a therapeutic agent against cancers 8
1.2.1 Chemotherapy 8
1.2.2 Derivation and history of triptolide 9
1.2.3 The structure of triptolide 9
1.2.3.1 C-14-hydroxyl group 10
1.2.3.2 α, β-unsaturated-5-membered-lactone ring 11
1.2.3.3 C-5, 6 functional group 12
1.2.3.4 Epoxy groups 12
1.2.4 Literature review of triptolide's properties 14
1.2.4.1 Inflammatory and immunosuppressive activities 14
1.2.4.2 Antitumor activity 14
1.2.4.3 Clinical applications of triptolide and its derivatives 17
1.3 Drug target identification of triptolide using proteomics approaches 21
1.3.1 Introduction of proteomics 21
1.3.2 Mass Spectrometry 22
1.3.2.1 Ionization techniques 23
1.3.2.2 Mass analyzers 23
1.3.2.3 Tandem mass spectrometry 24
1.3.3 The methods of separation and comparison of whole proteome 24
1.3.3.1 Gel-based proteomics and two-dimensional gel electrophoresis (2-DE) 25
1.3.3.2 Difference Gel Electrophoresis (DIGE) 26
1.3.3.3 Liquid Chromatography (LC) - Mass Spectrometry (MS) 26
1.3.3.4 Stable Isotope Labeling with Amino acids in Cell culture (SILAC) 27
1.3.3.5 Isotope Coded Affinity Tag (ICAT) 27
1.3.3.6 Isobaric Tag for Relative and Absolute Quantitation (iTRAQ) 28
1.4 Identifying cellular direct target of triptolide using chemical proteomics

approaches....29
1.4.1 The development of chemical proteomics....29
1.4.2 Activity Based Protein Profiling (ABPP)....30
1.4.3 Tagging strategies for chemical proteomics....32
1.4.3.1 Isotope tags....32
1.4.3.2 Fluorophores....33
1.4.3.3 Affinity tags....34
1.4.3.4 Tandem biorthogonal tagging....35
1.4.4 Previous studies of direct targets and their limitations....36
1.5 Aims of my projects....39
Chapter 2 Materials and Methods....42
2.1 Cell Culture....43
2.2 Cell Proliferation Assay....43
2.3 Cell Cycle Analysis....43
2.4 Proteomics Sample Preparation....43
2.5 ITRAQ labeling....44
2.6 Strong Cation Exchange (SCX) Chromatography and Desalting....46
2.7 2D LC Analysis and Tandem Mass Spectrometry (MS/MS)....46
2.8 Peptide and Protein Identification and Bioinformatics Analysis....47
2.9 Validation of Proteomics Data using Western Blot....47
2.10 Immunocytochemistry Staining....48
2.11 *In situ* fluorescence labeling using triptolide probe....49
2.12 Proteome labeling with triptolide probe....49
2.13 Pull down and MS analysis of triptolide-bound proteins....50
2.14 Immunofluorescence staining using triptolide probe....51
2.15 Protein synthesis evaluation....51
2.16 Preparation of recombinant PRDX I....52
2.17 *In vitro* Labeling of PRDX I....52
2.18 Binding sites mapping by MS/MS....53
2.19 Docking simulation of target-triptolide compound....53
2.20 Peroxiredoxin function study....54
2.21 Evaluation of Reactive Oxygen Species (ROS) level....55
2.22 Wound healing assay....55
Chapter 3 Studies of global alteration of proteins in HCT116 with triptolide treatment by using iTRAQ approaches....56
3.1 Introduction....57
3.2 Results....58
3.2.1 Anti-tumor properties of triptolide....58
3.2.1.1 Proliferation assay and cell morphology analysis....58
3.2.1.2 Cell cycle and apoptotic analysis by flow cytometry....62
3.2.2 ITRAQ results....65
3.2.3 GO analysis of significantly altered proteins....68
3.2.4 IPA analysis....70
3.2.5 Validation of significantly altered proteins....76

3.2.5.1 Bromodomain-containing protein 4 (BRD4) 76
3.2.5.2 β-catenin 79
3.2.6 Proteins specifically regulated by triptolide in cancer cells 81
3.3 Discussion 83
Chapter 4 Identifying direct binding targets of triptolide using combination of clickable ABPP and iTRAQ 86
4.1 Introduction 87
4.2 Results 89
4.2.1 Proliferation inhibition activity of triptolide probe 89
4.2.2 *In situ* proteome profiling of triptolide targets 91
4.2.3 Pull down and iTRAQ labeling 92
4.2.4 GO analysis 94
4.2.5 Cellular immunofluorescence image 96
4.2.6 Network analysis by IPA 97
4.2.7 Identification of binding targets *via* in-gel digestion and MS/MS ... 101
4.2.8 Validation and functional analysis of triptolide's target – PRDX I ... 102
4.2.8.1 Expression and purification of recombinant PRDX I 103
4.2.8.2 Validation of triptolide-PRDX I binding using fluorescence labeling 104
4.2.8.3 Competition assay 105
4.2.8.4 Identification of binding sites 106
4.2.8.5 Molecular modeling 109
4.2.8.6 Inactivation of PRDX I induced by triptolide 110
4.2.9 Validation and functional analysis of triptolide target – Annexin A1 ... 111
4.2.9.1 Identification of binding sites of ANXA1 by MS/MS 112
4.2.9.2 Docking simulation model of ANXA1-triptolide complex ... 115
4.3 Discussion 116
Chapter 5 Discussion and Conclusion 127
5.1 Discussion 128
5.2 Future Work 133
5.2.1 More cell models and other possible strategies 133
5.2.2 Function study of triptolide's binding targets 135
5.3 Conclusion 136
Reference 138
Appendices I: Significantly regulated proteins by triptolide with 6 hrs of treatment 149
Appendices II: Significantly regulated proteins by triptolide with 48 hrs of treatment 154
Appendices III: Direct binding targets of triptolide by pull down assay 159
List of Publication 170
Conference Presentation 170

Summary

Triptolide, a diterpene triepoxide extracted from traditional Chinese medicinal plant, *Leigongteng*, has been shown to have strong anti-tumor activities. However, the molecular mechanisms of triptolide against colorectal cancer remains largely elusive to date. In my study, triptolide was demonstrated to interfere with ROS, actin cytoskeleton, cell migration, cell adhesion, protein synthesis and induce alteration of transcription factors in colorectal cancer cell line HCT 116. In my first project, protein alterations of HCT 116 cells treated with triptolide were profiled at a global level, by using Isobaric Tags for Relative and Absolute Quantitation (iTRAQ) labeling followed by MS/MS analysis. The study of networks provides some insight into the molecular mechanisms of triptolide against colorectal cancer. In my second project, direct binding targets of triptolide were identified, by using combination of Activity-based Protein Profiling (ABPP) and proteomic approaches. Peroxiredoxin I and Annexin A1 were validated to be the direct binding targets of triptolide. Proteomics approaches allow the study of altered proteins by triptolide and binding targets of triptolide at a global level, which provides some insight into the mechanism of action of triptolide and aid to identify potential targets for cancer therapy. Furthermore, construction of important protein networks might offer fruitful information for future research on colorectal cancer treatment. Revealing the direct targets of triptolide will also aid to design derivatives that might be less toxic with fewer side effects.

List of Tables

Table 1.1 Clinical evaluation of triptolide and its derivatives 20

Table 1.2 Direct binding targets of triptolide currently found 38

Table 3.1 Functions and top networks of differentiated proteins 70

List of Figures

Figure 1.1 A genetic model of colorectal cancer development **7**

Figure 1.2 Chemical structure of triptolide 10

Figure 1.3 Chemical structures of different analogues of triptolide 13

Figure 1.4 Components of activity-based probe (ABP) 32

Figure 1.5 Click chemistry catalyzed by Copper (I) 36

Figure 2.1 Schematic representation of workflow if iTRAQ labeling showing biological replicates 45

Figure 3.1 Triptolide showed strong anti-proliferative effects and induced cell morphology change of colorectal cancer cell line HCT 116 but did not interfere with the proliferation of colorectal epithelial cell line CCD 841. 60

Figure 3.2 Triptolide induced cell morphology change of colorectal cancer cell line HCT 116 61

Figure 3.3 Effects of triptolide on cell cycle phases and apoptosis 63

Figure 3.4 Workflow of iTRAQ 65

Figure 3.5 The percentage at different variation levels of total 2382 proteins 67

Figure 3.6 Cellular localization (Upper) and biological process (Bottom) of differentially regulated proteins 69

Figure 3.7 Functions of significantly regulated proteins by IPA analysis 72

Figure 3.8 Networks of significantly altered proteins using Ingenuity Pathway Analysis (IPA) method 73

Figure 3.9 Wound Healing Assay 75

Figure 3.10 Triptolide inhibited expression of BRD4 with 48 hrs of treatment 77

Figure 3.11 Quantitative immunocytochemistry analysis for expression of BRD4 in HCT 116 treated with DMSO or different concentrations of triptolide 79

Figure 3.12 Validation of key proteins altered by triptolide treatment using Western blot analysis 81

Figure 3.13 Comparison of BRD4 and β-catenin in normal and cancer cell lines CCD 841 and HCT 116 82

Figure 4.1 Chemical structure of triptolide probe 89

Figure 4.2 Triptolide probe showed strong inhibitory activity against cell proliferation with 48 hrs of treatment 90

Figure 4.3 *In situ* proteome labeling of HCT 116 cells using triptolide probe 91

Figure 4.4 The workflow of identification of triptolide targets by combination of ABPP and iTRAQ approaches 93

Figure 4.5 Molecular function (Upper) and cellular localization (Bottom) of targets of triptolide 95

Figure 4.6 Quantitative cellular immunofluorescence images of triptolide targets 96

Figure 4.7 Functions (Upper) and canonical pathways (Bottom) analysis of triptolide's binding targets 98

Figure 4.8 Triptolide was shown to interfere with protein synthesis 99

Figure 4.9 The top networks of binding targets were analyzed by Ingenuity Pathway Analysis (IPA) 100

Figure 4.10 Identification of target bands by MS/MS 102

Figure 4.11 Validation of triptolide-PRDX I binding activity using fluorescence labeling 105

Figure 4.12 Validation of triptolide's target PRDX I by competition assay 106

Figure 4.13 Identification of binding sites of protein PRDX I by MS/MS 108

Figure 4.14 Docking simulation of triptolide-PRDX II complex 109

Figure 4.15 Peroxidase activity assay indicated the inhibitory activity of triptolide against peroxidase activity of PRDX I 111

Figure 4.16 Identification of binding sites of ANXA1 with triptolide, using MS/MS analysis 114

Figure 4.17 Docking simulation of triptolide-ANXA1 complex 116

Figure 5.1 Overall proteome picture depicting activities of triptolide against colorectal cancer based on proteomics approaches 128

List of Abbreviations

2-DE	Two-dimensional electrophoresis
5-FU	5-Fluorouracil
ABP	Activity-based probe
ABPP	Activity-based protein profiling
AHA	Azidohomoalanine
ATCC	American Type Culture Collection
BSA	Bovine serum albumin
CID	Collision-induced dissociation
C_p	Peroxidase cysteine
C_R	Resolving cysteine
Cu	Copper
Cyn	Cyanine
Da	Dalton
dCTPP	dCTP Pyrophosphatase
DIGE	Difference in gel electrophoresis
DMSO	Dimethyl sulfoxide
DTT	Dithiothreitol
E.*coli*	*Escherichia coli*
ER	Endoplasmic Reticulum
ESI	Electrospray ionization

GO	Gene ontology
HPLC	High performance liquid chromatography
IC_{50}	Half the maximal inhibitory concentration
ICAT	Isotope Coded Affinity Tags
IPA	Ingenuity Pathway analysis
IPG	Immobilized pH gradients
IEF	Isoelectric focusing
iTRAQ	Isobaric Tag for Relative and Absolute Quantitation
LC	Liquid chromatography
MALDI	Matrix-assisted laser desorption ionization
MMTS	Methylmethanethiosulphate
MS	Mass spectrometry
mTOR	Mammalian target of rapamycin
PAGE	Polyacrylamide gel electrophoresis
PBS (-T)	Phosphate buffered saline (-Tween)
PRDX	Peroxiredoxin
PTM	Post-translational modification
PVDF	Polyvinylidene fluoride
RA	Rheumatoid arthritis
ROS	Reactive oxygen species
SAR	Structure activity relationship
SDS	Sodium dodecyl sulphate

TBTA	Tris[(1-benzyl-1H-1,2,3-triazol-4-yl)methyl]amine
TCEP	Tris(2-carboxyethyl)
TCM	Traditional Chinese Medicine
TPL	Triptolide
Tris	Trishydroxymethyl amino methane
Trx	Thioredoxin

Chapter 1 Introduction

1.1 An overview of colorectal cancer

1.1.1 Cancer

Cancer is characterized by rapid and uncontrolled growth of abnormal cells with the capability of spreading to distant sites of the body [1]. Other terms of cancer include malignant tumors and neoplasms [2]. Cancers are the leading causes of death in the world and the burden of cancers is increasing in developed countries [1]. The top four cancer sites (lung, breast, colorectum and stomach) account for about 42% of the total cancer diagnoses in the world [3]. In Singapore, about ten thousand cases of cancer per year were reported with the increasing rate [4]. High risk of cancers could be attributed to heredity, high fat intake and genetic factors [5].

The traits of cancer include sustaining proliferative signaling, promoting metastasis and invasion, resisting cell death and so on [6]. These characteristics are progressively acquired and provide driving forces in the process of cancer progression [7]. The growth of tumors is not only due to the uncontrolled proliferation but also because of the evasion of apoptosis. Apoptosis is a physiological suicide mechanism that controls the normal cell numbers [8]. However, cancer cells resist cell death through regulating both anti-apoptotic and pro-apoptotic signaling pathways [8, 9].

1.1.2 Hallmarks of cancer

Cancer begins when abnormal cells start to proliferate in an uncontrolled way. In the normal conditions, cell proliferation, cell division, apoptosis, autophagy, *etc.* are strictly regulated by the organism [10]. However, in the case of cancers, the regulation is interfered and cells begin rapid and uncontrolled growth, followed by invasion, and metastasis. Characteristics of cancer could be classified into ten hallmarks. They are: 1) Sustaining proliferative signaling, 2) Evading growth suppressors, 3) Resisting cell death, 4) Enabling replicative immortality, 5) Inducing angiogenesis, 6) Activating invasion and metastasis, 7) Genome instability and mutation, 8) Tumor-promoting inflammation, 9) Deregulating cellular energetic and 10) Avoiding immune destruction [6].

Cancers have the ability to sustain proliferation without external growth-promoting signals [11]. Through mutations, cancer cells acquire the ability to sustain growth signaling in alternative ways including producing transcription factors such as Myc and supplying growth factors [7]. At the same time, cancer cells could also escape from the regulation of multiple tumor suppressors. For example, transforming growth factor beta (TGFβ) are suppressed in the cancer cells [12].

Apoptosis is another important mechanism that regulates the normal growth of cells and eliminate the aged, mutant, and damaged cells. However, cancer cells have

the mechanism to escape from the programmed cell death. Cancer cells resist cell death *via* mutations. For example, the mutations of oncogene B-cell lymphoma 2 (Bcl-2) leads to cell resistance to apoptosis in cancer cells [13].

Normal cells usually have limited cell cycle due to senescence and apoptosis. Telomeres, a special DNA polymerase, protect the ends of chromosome and are involved in the unlimited proliferation [14]. The lengths of telomeric DNA are shortened progressively with the division of cells [15]. However, cancer cells could escape these regulation, growing and dividing immortally. Telomeres are maintained via the continuous addition of telomeres by enzyme telomerase [6].

Cancer cells also induce angiogenesis [16]. In cancer cells, the supply of oxygen and nutrients become scarce due to the unlimited proliferation. Therefore, tumor cells promote the formation of new blood vessels by turning on the angiogenic switch, which is activated due to the changes of angiogenic inducers and inhibitors [7].

The main cause of cancer deaths is metastasis [13]. Besides the capability of unlimited proliferation, evasion of growth suppression, as well as resistance to cell death, the ability of invasion and metastasis allows abnormal cells spread to surrounding tissues. It begins by initiating the escape of cancer cells form from their original sites to nearby blood and lymphatic vessels during intravasation [6]. Next, in the phase of extravasation, cancer cells exit the capillaries and enter organs [17]. The

activation of invasion is triggered by proteins involved in cell motility, adhesion, and cell migration [18].

In addition, instability of genome leads to random mutations and contributes to genetic alteration. The genome instability is the basis for the genetic alteration that lead cancer cells to the above hallmarks [7]. Therefore, genome instability is one of the main enabling characteristics of cancer cells. Another enabling characteristic is tumor-promoting inflammation. It provides bioactive molecules to the tumor microenvironment, supporting the other cancer characteristics above [13].

Another two hallmarks include reprogramming energy metabolism to support rapid cell growth and proliferation, and evading immune destruction, which prevents cancer cells from attacking by immune system. These two capabilities are considered as emerging hallmarks of cancer according to Hanahan and Weinberg [6].

1.1.3 Colorectal Cancer

Colorectal cancer (CRC) is the second most common cancer with the third leading mortality rate in developed countries [1]. In Singapore, colorectal cancer is the most common cancer in Singaporean males and second most common cancer amongst Singaporean females [19, 20]. In addition, colorectal cancer leads to death within 5 years after diagnosis among half of the patients. Besides heredity, high fat intake, polyps in the large intestine and ulcerative colitis, gene mutations play

important roles as risk factors of colorectal cancer. For example, mutations in the tumor suppressor genes such as Adenomatous polyposis coli (APC), p53, and SMAD4 cause the cells growing and spreading uncontrollably.

The multi-step molecular mechanism of colorectal cancer development has been well-elucidated by Fearon and Vogelstein [21]. Colorectal cancer begins from colorectal polyps. Abnormal cells start to divide in an uncontrolled way. The mutation of APC, which is involved in the Wnt pathway, is involved in the development of cancerous traits. Abnormal cells escape from the normal checks and balances that control cell growth. As polyps grow, additional genetic mutations occurred, leading to transition from normal cells to adenoma then to carcinoma. Three stages of adenoma formation are described in Figure 1.1. Genetic alterations such as mutations of KRAS, DCC and p53 occur during the development of colorectal cancer. When these precancerous tumors invade other layers of the large intestine (such as the muscular layer), the precancerous polyp becomes cancerous.

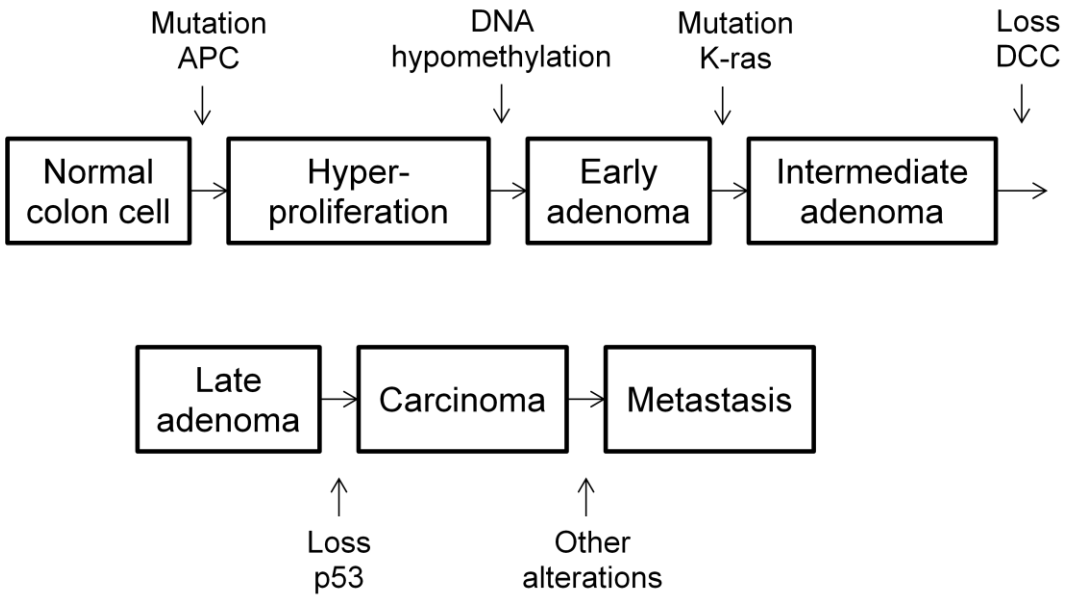

Figure 1.1 A genetic model of colorectal cancer development. Multi-step development of colorectal cancer from normal epithelium to carcinoma. Several genetic factors such as APC, p53, KRAS are involved in the progression of colon cancer. This model was proposed by Fearon and Vogelstein [21].

Several therapeutic approaches like surgery and radiotherapy have shown some anti-cancer effects. However, each of them has side effects. For example, besides the difficulty for the early diagnosis of colorectal cancer for surgery [22], cancers often recur after surgery [23]. Among the organism sites, liver and lung are commonly subjected to recurrence. Thus, resection of liver and lung metastasis is needed to protect patients from recurrence [24]. Other side effects include susceptibility to infection, abdominal cramps, excoriation of perianal skin and anemia, neutropenia and hair loss. Due to above limitations, an increasing attention has been paid on the development of targeted chemotherapy for the treatment of colorectal cancer.

1.2 Triptolide as a therapeutic agent against cancers

1.2.1 Chemotherapy

Chemotherapy for treating against cancers was introduced into the clinical application since more the 50 years ago [25]. Chemotherapeutic drugs have been successfully applied to treat some tumors, such as leukemia, breast, colorectal and lung cancer [26][27]. Among the chemotherapies, novel natural anti-cancer compounds have drawn the attention of scientists all over the world, especially those in East Asia. Natural products have been studied as cancer chemotherapy for the past 40 years [28][29]. Several plants, such as etoposide, *Podophyllum peltatum*, *Catharanthus roseus* were shown to effectively treat small-cell lung caner [30], acute lymphocytic leukemia [31] and so on. The folk medicine's significant contribution results in the exploration the large-scale screening of native plants for cancers [28]. One of such chemotherapy is triptolide, a natural plant-derived compound.

1.2.2 Derivation and history of triptolide

Triptolide, a diterpene triepoxide, was purified from traditional Chinese medicine herb *Tripterygium wilfordii hook F*, commonly known as thunder god vine or *Leigongteng* in Chinese. *Leigongteng* was used to treat inflammatory disease such as rheumatoid arthritis in China [32]. Its clinical therapeutic effects stimulated the isolation of triptolide in 1972 [33]. Right after its isolation, triptolide was revealed to have strong anti-leukemic activity, which stimulated extensive studies regarding to its

other antitumor properties. Owing to numerous studies, triptolide has been demonstrated to induce apoptosis of hepatocellular carcinoma, promyelocytic leukemia, cervical adenocarcinoma, lung cancer, pancreatic carcinoma and oral cancer cells [34-38].

1.2.3 The structure of triptolide

Compounds derived from natural products, especially those originating from plants, have played important roles in disease treatment in the drug discovery history [39]. Diterpenoids from plant exert an extensive range of important physiological functions and give hope for the development of new therapeutic agents against cancer, inflammation and cardiovascular disease as secondary metabolites [40-42]. Recently, p50, a crucial regulator of NF-κB signaling, was identified as the cellular target of Eriocalyxin B (EriB), an *ent*-kaurene diterpenoid isolated from *Isodon eriocalyx var. Laxiflora* [43]. EriB was shown to induce cancer cell apoptosis *via* binding Cysteine 62 of p50, which was the same binding site for another diterpenoid, andrographolide [44, 45]. However, the diterpenoids form several structurally diverse types and have a wide spectrum of activities, leaving open the exploration of their biological functions and binding targets.

As shown in Figure 1.2, triptolide contains natural reactive electrophile and three epoxide groups. The Structure Activity Relationship (SAR) of triptolide was subsequently analyzed. Several systematic structural modifications of triptolide were

conducted in the previous studies, focusing on the C-14-hydroxyl group, the C5, 6-positions of the triptolide, the epoxide groups as well as the lactone ring.

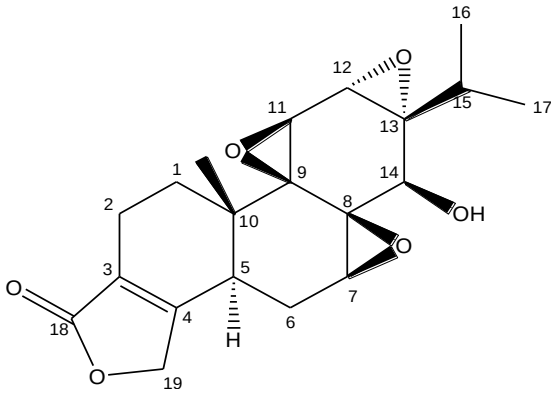

Figure 1.2 Chemical structure of triptolide. Chemical structure of triptolide was depicted with the software Chemdraw.

1.2.3.1 C-14-hydroxyl group

According to Structure Activity Relationship (SAR) of triptolide, the position C-14β-OH was demonstrated to be associated with cytotoxicity of triptolide. Previous studies indicated that hydrogen-bonded C-14 of triptolide may account for its antitumor effect [46]. This position is also related to the water solubility. Due to the poor water-solubility of native triptolide, for a long time, the modification's aim was to improve the triptolide's water solubility by carboxylation of C-14β-OH to introduce water-solubility-enhancing moieties [47]. In addition, most of these derivatives were enzymatically converted into triptolide when they were utilized *in vivo*, retaining most of triptolide's effects [48]. Another study found that replacing the C-14-hydroxyl group with fluoride or with a chiral epoxy group, containing α oxygen configuration retains the cytotoxicity of triptolide [49]. In their study, two series of

C-14-spirotriptolide derivatives (Figure 1.3A and 1.3B) were designed not to form intramolecular hydrogen bonds. After evaluation, the novel derivative (Figure 1.3A) has strong anti-tumor activity and potential low systemic toxicity, making it a candidate of promising anticancer drug. These above achievements challenge the traditional understanding that C-14β-OH cannot be altered for retaining of toxic activity by triptolide analogues [46]. Therefore, C-14β-OH group was demonstrated to be one of the sites that could be modified without changing the property of native triptolide.

1.2.3.2 α, β-unsaturated-5-membered-lactone ring

The five-membered unsaturated lactone ring was identified as the most important group for the function of triptolide. Some studies synthesized triptolide analogues with furan ring instead of the five-membered unsaturated lactone ring (Figure 1.3D) or with the lactone ring opened [50]. Although these analogues showed enhanced efficiency of uptake due to the improved water solubility, triptolide analogues with a transbutenolide (Figure 1.3C) was shown to be slightly toxic. Another analogue (Figure 1.3D) with the furan ring completely lost toxic activity. These investigations suggest that the five-membered unsaturated lactone is necessary and critical for the anti-tumor activity of triptolide and the C18 carbonyl group might play significant roles in the interplay between triptolide and its targets.

1.2.3.3 C-5, 6 functional group

For a long time, there is little research focusing on C-5, 6 modification because of the lack of modification sites. In 2005, Fu's group reported that (5R)-5-hydroxytriptolide (Figure 1.3E) possessed strong anti-inflammatory and immunosuppressive activities [51]. In addition, the introduction of the hydroxyl group at C-5 led to a significant elimination in side effects. Therefore, modification in C-5,6 function group did not change the property of triptolide.

1.2.3.4 Epoxy groups

According to the analysis of SAR of triptolide, three epoxy groups of triptolide were demonstrated to play critical roles in determining therapeutic activities of triptolide. Among them, the C-12, 13-epoxide group is the most important modification site due to its small steric impact. Therefore, the C-12, 13-epoxide group is sensitive to nucleophilic attack, which may cause ring-opening [52]. By comparison, the C-7, 8-β-epoxide group is not as sensitive as the C-12, 13-epoxide group towards nucleophilic attack. The inhibitory activity of triptolide derivatives with ring-opening at the C7 was significantly decreased *in vitro* [53]. Moreover, three analogues modified in the position of C9, 11-β-epoxide were synthesized by Zhou *at al*. Their further work demonstrated that C-9, 11-olenfin analogues were effective against SKOV-3 and prostate cancer PC-3 cell lines [54]. These results indicated that modification of the C-12, 13-epoxide group and C-7, 8-β-epoxide significantly reduce

triptolide's activity. On the other hand, the C-9, 11-β-epoxide group could be recognized as a potential modification site.

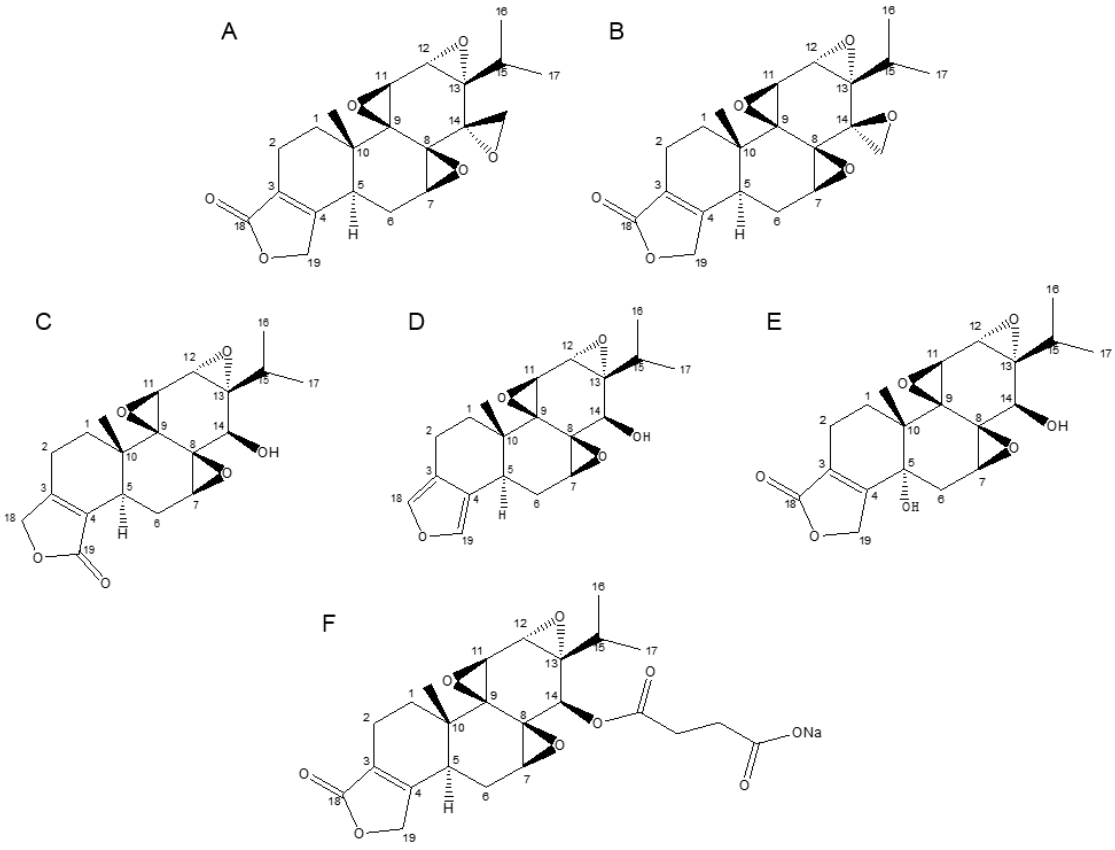

Figure 1.3 Chemical structures of different analogues of triptolide. Different analogues of triptolide were synthesized to examine the influence of different modification sites on its anti-cancer property. (A, B) Derivatives with modification on C 14 have strong anti-tumor activity, making C 14 as a promising modifiable site. (C, D) The properties of compounds with the modification on five-membered unsaturated lactone ring change greatly, making the unsaturated lactone ring necessary for the anti-tumor activity of native triptolide. (E) (5R)-5-hydroxytriptolide, which has modification on C-5, 6, possesses strong anti-inflammatory and immunosuppressive activities, making it as a suitable site for modification. (F) Omtriptolide (PG-490-88Na, F60008) which has the modification on C 14, has entered clinical trials as a pro-drug to treat advanced solid tumors, verifying that C 14 is suitable for modification.

1.2.4 Literature review of triptolide's properties

1.2.4.1 Inflammatory and immunosuppressive activities

For more than two centuries, *leigongteng* was used to treat against a variety of inflammatory and autoimmune diseases in ancient China [55]. Its main functional component, triptolide, has been revealed responsible for those activities in patients with rheumatoid arthritis. Triptolide was also shown to be the main component for treatment against autoimmune and inflammatory diseases in various animal models [56]. Hoyle's group identified that triptolide inhibits lung inflammation in the NIH Clinical Collection, using acute lung injury model [57].

Moreover, triptolide was shown to impair the function of T-cell *in vivo* and *in vitro* [58]. Triptolide was also demonstrated to inhibit the T-cell proliferative responses to stimuli and interferes with the transcription of interleukin-2 through either Ca^{2+}-dependent or Ca^{2+}-independent pathways [59]. As for numerous pro-inflammatory mediators, triptolide suppresses the production of TNF-α, IL-4, IL-6, IL-8, cyclooxygenase (COX)-2 and interferon (IFN)-α [59-61]. In addition, triptolide inhibits B-cell proliferation and immunoglobulin production, suggesting that it interferes with humoral immunity [58].

1.2.4.2 Antitumor activity

Triptolide has broad and potent anti-tumor activities. It was demonstrated to

inhibit proliferation as well as to induce apoptosis in various cancer cell lines with IC_{50} (half-maximal inhibitory concentration) values in nano-molar range [62].

The mechanisms of anti-proliferation and pro-apoptosis activity of triptolide have been studied in the past forty years. Triptolide was demonstrated to inhibit expression of numerous transcription factors like NF-κB [59], TFIIH subunit XPB [63], heat shock transcription factor 1 (HSF1) [64], and so on *via* the inhibition of RNA polymerase II [62]. Triptolide's inhibitory effect on RNA polymerase affects the transcription machinery indirectly, causing a rapid depletion of short-lived mRNA of transcription factors. The global transcriptional inhibition could provide the explanation for the finding that triptolide decreased diverse proteins involved in various biological functions.

1). Triptolide decreases expression level of proteins involved in apoptosis such as anti-apoptotic proteins Bcl-2 [65], Mcl-1, the IAP family members cIAP2 and XIAP [66]. Triptolide was also shown to induce caspase-dependent apoptosis mediated by mitochondria-mediated pathways [34]. In gastric cancers, triptolide was shown to induce tumor suppressor p53, p21, Bcl2-associated X protein (Bax) and increase the activity of caspases [65, 67].

2) Triptolide exerted inhibitory effects on oncogenic proteins, such as Myc, Src [68] and heat shock protein 70 (HSP70) [64]. Molecular chaperones play important

roles in balancing cell stress, survival and cell death mechanisms. The inhibitory effect of triptolide on the heat shock response makes cancer cells sensitive to stress-induced cell death. Triptolide also decreased mRNA and protein levels of HSP70 in MiaPaCa-2 and PANC-1 cell lines [64].

3) Triptolide was shown to exert epigenetics effects on cancer cells. In the previous study, triptolide was demonstrated to decrease methylation of histone H3K9 and H3K27 through inhibiting histone methyltransferases EZH2 and SUV39H1, respectively. Meanwhile, triptolide also increased the histone H3 and H4 acetylation through reducing histone deacetylase 8 (HDAC8) [69]. These regulated molecules were reported to be responsible for epigenetic effects and anti-myeloma mechanism of triptolide.

4) Triptolide was reported to suppress proteins involved in anti-tumor related signal pathways. Besides NF-κB signal pathway, triptolide also suppresses the expression of mitogen-activated protein kinase phosphatase-1 (MKP-1), which inactivates ERK-1/2, MAPK and c-Jun N-terminal kinase-1/2 (JNK-1/2). MKP-1 plays critical roles in suppressing the proliferative and metastatic abilities of non-small cell lung cancer (NSCLC) [70]. Triptolide also decreases PI3K activity in human fibrosarcoma HT-1080, which causes the augmentation of JNK1 phosphorylation through Akt or PKC-independent pathway [71].

5) Triptolide induces chemotherapeutic agents-induced apoptosis. It is reported that triptolide could inhibit the growth of colon carcinoma and human KB oral cancer cells. In addition, the anti-tumor activity is much stronger when introducing the co-treatment of triptolide and 5-FU. The growth of these cells was significantly inhibited and the activity is much stronger, compared to using the agents individually, especially when used at low dose [72]. The proposed explanation is that triptolide inhibits NF-κB activity and sensitized colon cancer cell lines to 5-FU by activating expression of caspase 3 and Bax as well as by inhibiting Bcl-2. In addition, in pancreatic cancer model, combination of triptolide with ionizing radiation (IR) reduces cell survival to 21% and induces tumor cell apoptosis [73]. Triptolide also enhances the cytotoxicity induced by cisplatin in gastric cancer cells *in vitro* and *in vivo* [74].

1.2.4.3 Clinical applications of triptolide and its derivatives

Since 1960s, *Leigongteng* has been evaluated in the clinic, mainly focused on autoimmune and inflammatory diseases [75], including graft-versus-host diseases, systemic lupus erythematosus, rheumatoid arthritis, nephropathies, Behcet's disease, Crohn's disease, ankylosing spondylitis and autosomal dominant polycystic kidney disease [76, 77].

1) Triptolide has entered clinical trials to treat leukemia and rheumatoid arthritis in China (Table 1.1). In the leukemia patients, 30 μg kg^{-1} triptolide showed

therapeutic effects and caused no obvious side effects. However, when at 40 μg kg^{-1}, triptolide caused severely toxic effects, such as phlebitis and gastrointestinal abnormalities, leading to the suspension of the regimen [78]. Ten years later, its clinical anti-leukemia effects were evaluated again. 30-40μg kg^{-1} daily was used as regimen on 45 patients. Among them, 18 patients has complete remission and 6 patients have partial remission [79].

The clinical influence of triptolide for treatment against rheumatoid arthritis was evaluated at 0.5-0.75 mg day^{-1} in 15 patients. However, it showed serious toxicities, including leucopenia, urinary abnormalities, liver and myocardial damage although it displayed significant improvement for rheumatoid arthritis. The high toxicities make 47% withdrawal in the treatment group [75] [80].

Therefore, triptolide has shown severe toxicities at higher concentrations. In addition, triptolide has a very poor water solubility. These properties restrict its clinical application. Thus, modification of the molecular structure of triptolide with the goal of producing safer and water-soluble analogues while retaining or improving anti-tumor efficacy of triptolide is very important [81]. Several derivatives of triptolide were developed. So far, there are two derivatives shown to have strong anti-tumor activities with less toxicity and greater water solubility. In addition, they have entered the clinical trials. For the treatment against relapsing acute leukemia as well as advanced solid tumors, Omtriptolide has demonstrated to be effective. The

Phase I clinical trials of Omtriptolide on refractory or relapsing acute leukemia and advanced solid tumors was completed [52] [79]. In addition, Omtriptolide has also entered the Phase I clinical trials for its treatment against prostate cancer [79]. Moreover, (5R)-5-hydroxytriptolide (LLDT-8) also has entered Phase II for its treatment against rheumatoid arthritis [82].

2) Omtriptolide (PG-490-88Na, F60008) is one of the derivatives of triptolide (Figure 1.3F). It is designed to be highly water soluble. In addition, it could be converted into triptolide in the serum [83]. Omtriptolide has shown to inhibit proliferation of tumors in mice bearing COLO 205 (colorectal cancer) and HT-29 (colorectal cancer) xenografts. It also eradicated tumors in mice bearing H23 (non-small cell lung cancer) and COLO 205 xenografts [84]. In the phase I clinical trial on patients with refractory or relapsing acute leukemia, patients were given Omtriptolide once a day for 5 consecutive days, more than 5.7 mg m^{-2} day^{-1}. The maximum tolerated dose was demonstrated to be 7 mg m^{-2} day^{-1}, larger than which the cerebellar toxicity would occur [78]. In the phase I clinical trial on patients with advanced solid tumors, 20 patients were given 9 dose between 0.5 mg m^{-2} and 18 mg m^{-2}. The dose tolerance was demonstrated to be 18 mg m^{-2}. By far, the phase I studies of omtriptolide on patients with advanced solid tumors and relapsing acute leukemia were completed. In addition, omtriptolide has entered Phase I for treatment against human prostatic epithelial cells [79]. There studies make Omtriptolide a promising pro-drug for the further evaluation in the clinical trials.

3) (5R)-5-hydroxytriptolide displayed promising anti-inflammatory activity in clinical trials [85]. In the Phase II clinical trials, its oral administration (0.125, 0.25, and 0.5 mg/kg) consistently attenuated the severity of collagen-induced arthritis (CIA). More importantly, compared to triptolide, (5R)-5-hydroxytriptolide displayed a much lower toxicity both *in vitro* and *in vivo*. Its CC_{50} value is 256.6 ± 73.8 nmol/L, while the CC_{50} value of triptolide is 2.1 ± 0.3 nmol/L in murine splenocytes. Its higher safety property makes it more suitable as a promising anti-tumor drug candidate. It is now ready to enter the Phase II clinical trials on patients with rheumatoid arthritis [82, 86, 87]. The safety and side effects of it need to be further elucidated.

Table 1.1 Clinical evaluation of triptolide and its derivatives. Analogues of triptolide that entered the clinical trials were listed. The disease model, regimen, response, toxicity and phase status were demonstrated.

Compound	Disease	Regimen	Response	Toxicity	Status	Ref
Triptolide	Leukemia	5-40 μg kg^{-1}	effective at 30 μg kg^{-1}	toxicity at 40 μg kg^{-1}		[88]
	Rheumatoid Arthritis	0.5-0.75 mg day^{-1}	improvement	serious toxicity		[80]
Omtriptolide (PG490-88Na, F60008, Figure 1.3F)	Acute Leukemia	0.15-13 mg m^{-2} day^{-1}	effective at 5.7 mg m^{-2} day^{-1}	Dose-limited toxicity	Phase I completed	[52]
	Prostate Cancer	No further information	No further information	No further information	Phase I ongoing	[79]
	Advanced Solid Tumors	0.5-18 mg m^{-2}	effective at 12-18 mg m^{-2}	hematological damage	Phase I completed	[79]
(5R)-5-hydroxytriptolide (Figure 1.3E)	Rheumatoid Arthritis	0.125-0.5 mg day^{-1}	effective	low toxicity	Phase II ongoing	[82]

Triptolide's derivatives had entered clinic trials and showed inhibition effects on tumors. In addition, one of the promising pro-drugs, Omtriptolide, exerts its function *via* converted to native triptolide *in vivo*. Therefore, the knowledge of triptolide's mechanisms becomes very important. Previous studies have explored triptolide's possible mechanisms; however, as tumor grows in a complex and multi-step way, the detailed mechanisms of its anti-tumor activity remain unclear. With the development of proteomics, a global picture of the regulated molecular proteins will definitely provide some insights on the mechanisms of its anti-tumor functions.

1.3 Drug target identification of triptolide using proteomics approaches

1.3.1 Introduction of proteomics

With the investigation of the Human Genome Project (HGP) and whole genome sequences of various organisms, genomics have established a firm foundation for modern biological investigation to unravel the blueprint of life [89]. Massively parallel measurement strategies aim to understand the complicated biochemical circuitry which is responsible for disease processes and physiologic homeostasis [90]. The large-scale "omics" studies, including proteomics, aim to accelerate the study of cellular and metabolic functions of molecules responsible for controlling normal development. In the last decade, many attentions turned towards proteomics research because proteins are very crucial for cellular and metabolic functions. In addition, in

many cases, there is not a direct correlation between gene expression and protein expression patterns. Some post-translational modifications on the proteins, such as phosphorylation and glycosylation play important roles during the life process.

Proteome, as the name suggests, refers to as the entire proteins expressed in cells, tissues and organisms [91]. Proteomics can be defined as the large scale study of the protein properties, including expression level, post-translational modification, interaction [92]. This kind of study is extremely important for us to obtain an integrated view of cellular processes, disease processes, and network of proteins at the global level [92], therefore unveiling the mechanism of biological perturbations such as disease and drug treatment, accelerating the development of diagnostic techniques and therapeutic approaches [93].

1.3.2 Mass Spectrometry

With the development of Mass spectrometry (MS), the study of proteomics advances further. Initially, the conventional proteomics was only to identify and characterize proteins. Protein was identified most frequently by Edman degradation of isolated peptide fragments [94]. When correlating sequences obtained from experiment in which peptides were analyzed with the sequence database, even the short and imperfect sequences could be utilized for identification of proteins due to the growth of database. Subsequently, the sequence information required for mapping sequence database could be easily and overwhelmingly generated by mass

spectrometry. Mass spectrometry identifies a molecule by measuring the mass-to-charge (*m/z*) ratio. A classical mass spectrometer consists of three parts: ionizer, mass analyzer and detector.

1.3.2.1 Ionization techniques

The ionization methods include Matrix-Assisted Laser Desorption Ionization (MALDI) and Electrospray Ionization (ESI). MALDI matrix absorbs laser energy and transfers the energy to the acidified analyte. The rapid laser heating leads $[M + H]^+$ ions of analyte into the gas phase, generating singly charged ions [95].

Unlike MALDI, ESI generates ions from solution at atmospheric pressure when passing through a small capillary. Electrostatic spraying of a sample solution generated an aerosol of multi-charged droplets [94]. Then, ions become free of solvent and make their way to the analyzer [95]. Multiple charging allows mass spectrometers with limited *m/z* ranges to analyze molecules with higher molecular weight.

1.3.2.2 Mass analyzers

The basic types of mass analyzer include time-of-flight (TOF), quadrupole (Q), Fourier transform-ion cyclotron resonance (FT-ICR), ion traps and OrbiTrap. They have different properties to identify a molecule according to their *m/z* value. For example, in the TOF analyzer, ions are accelerated by high voltage. All ions with

same charge could obtain the same kinetic energy after acceleration. The lower *m/z* ions have higher speed [51]. Therefore, by measuring the time it takes to reach the detector, its *m/z* value could be determined. These mass analyzers can be used alone or combined in hybrid analyzers.

1.3.2.3 Tandem mass spectrometry

MS/MS includes two stages of MS. In the first MS, ions of certain *m/z* are isolated from other ions emanating from the ion source. These isolated ions are called parent ions or precursor ions. The ions are then further fragmented, commonly using the method, Collision Induced Dissociation (CID). The resulting ions are called product ions or daughter ions, which are then analyzed by the second stage of MS/MS.

On top of the mass spectrometry analysis, quantitative and comparative studies become available due to the advancement in chromatography and isotope labeling methods. The quantitative studies enable the wider application, such as biomarker discovery, drug treatment, drug efficacy and toxicity, and disease mechanism studies.

1.3.3 The methods of separation and comparison of whole proteome

Separation is critical for the mass spectrometry analysis. A variety of separation techniques were used depending on the nature of the protein samples and the choice

of proteomics approaches. The widely used approaches for proteome profiling include gel-based proteomics and LCMS-based proteomics.

1.3.3.1 Gel-based proteomics and two-dimensional gel electrophoresis (2-DE)

In two-dimensional polyacrylamide gel electrophoresis (2-D PAGE), the set of proteins were firstly separated by isoelectric focusing (IEF), corresponding to their isoelectric points (pI) in the first dimension, followed by SDS-PAGE according to their molecular weight in the second dimension (rotate 90 ℃). Subsequently, the resultant regulated proteins spots were excised and identified using mass spectrometry.

However, this method has some limitations. The fraction created by 2-D PAGE is quite limited for the total number of proteins [93]. There are several reasons for that: 1) many low-abundance proteins might not be detectable by staining in 2D-PAGE technique, 2) missing polypeptides might not enter the gel because they could not be resolved by the limited range of pH or molecular weight, *etc*. In addition, the staining process might also result in the variation from gel to gel, making it hard to differentiate the real expression changes, although the staining methods for sensitivity and limited dynamic range are optimized [96]. In addition, the fatal limitation for the 2D-PAGE is the poor reproducibility due to different amount of proteins transferred from IEF to SDS-PAGE.

1.3.3.2 Difference Gel Electrophoresis (DIGE)

In the method of DIGE, control and treatment samples were labeled with size-matched and charge-matched fluorescent dyes such as Cyanine2, Cyanine3 and Cyanine5 prior to 2-D Electrophoresis. The labeled proteins were then mixed and separated by running gel [97]. Then, the gel was scanned with different excitation wavelengths of individual fluorescent dyes [98]. This technology minimizes the variations among gels [99]. This technique allows up to three samples directly compared in a single gel. In the experiments which comprise several gels, an internal standard in each gel could be introduced to improve the accuracy of protein quantification of samples [100].

However, these gel-based techniques were challenged with the achievement of LC-based approaches. Non-gel- and LC-based technologies produce good reproducibility and aid to identify the low-abundant proteins with the high-throughput screening.

1.3.3.3 Liquid Chromatography (LC) - Mass Spectrometry (MS)

LC-MS is commonly used proteomic method to analyze solution-based sample [101]. LC allows combination of stationary and mobile phases for separating peptides [24]. The two or more multimodal separation improve the resolution and provide greater number of peptides [101]. In 2-D LC separation, peptides are usually

separated firstly by SCX, followed by C18 reversed phased chromatography [102]. Several tagging strategies based on LC-MS, such as SILAC, ICAT, as well as iTRAQ could be utilized to label different samples to study the quantification of proteins.

1.3.3.4 Stable Isotope Labeling with Amino acids in Cell culture (SILAC)

SILAC is a simple and *in vivo* metabolic labeling method for quantitative proteomics. It depends on "light" and "heavy" forms of amino acids in proteins in pair samples. One group of cells were cultured with natural amino acids, in the "light" form. The other group of cells were cultured with amino acids modified with ^{13}C labeled L-arginine or ^{13}C, ^{15}N-labeled L-lysine, in the "heavy" form. The proteins with abundance changes can be identified by mass spectrometry. Since there is an early introduction of isotope, SILAC could increase efficiency and reproducibility. It becomes popular also because of a relatively accurate comparison of expression level of proteins and post-transcription modifications [96].

However, there were some limitations and challenges of this technique. 1) SILAC was only applied to cells but not tissues and *in vivo*. 2) The continuous usage of labeled amino acids induces a high budget for the biological experiment.

1.3.3.5 Isotope Coded Affinity Tag (ICAT)

The core of ICAT is the usage of tags that could attach to cysteine residues. The tags are the heavy and light pairs differed in isotopic composition [93]. Therefore, in

the quantitative proteomics field, control and treated samples could be labeled with the heavy and light ICAT reagents respectively, followed by combination and identification by MS/MS. However, ICAT could not identify proteins without cysteine residues. In addition, only two samples could be compared using ICAT, making it limited for application.

1.3.3.6 Isobaric Tag for Relative and Absolute Quantitation (iTRAQ)

The biological system is usually complex. In some cases, groups with different conditions need to be compared with multiple groups. However, neither SILAC nor ICAT is powerful enough to compare eight samples simultaneously like iTRAQ.

ITRAQ is a non-gel-based technique used in proteomics to study quantitative changes of up to eight samples simultaneously. ITRAQ reagents were designed as isobaric tags which consist of reporter groups (ranging from 113-119, and 121 for 8-plex iTRAQ reagents), their mass balance group and the peptide reactive group (PRG) [103]. The mass at 120 is ruled out to avoid contamination from phenylalanine immonium ion whose m/z is 120.08. The peptides labeled with different isobaric tags are mixed and separated by Liquid Chromatography (LC) and identified by tandem mass spectrometry (MS/MS), to be identified as a single MS peak (identical m/z). The quantification of the peptide abundance can be calculated by the relative areas of the reporter peaks. After performing iTRAQ labeling and LC-MS/MS, bioinformatics analysis such as Gene Ontology (GO) and Ingenuity Pathway Analysis (IPA) can

provide clues for exploring the signaling pathway [104]. The proteins found to be differentially altered and/or associated with the biological process/disease of interest will be chosen for functional validation and exploration for successive downstream signaling pathways. The workflow of iTRAQ labeling and protein identification will be discussed in the Chapter 3.

1.4 Identifying cellular direct targets of triptolide using chemical proteomics approaches

1.4.1 The development of chemical proteomics

Numerous proteomics methods have be developed in the identification of drug therapeutic targets, screening of enzyme inhibitors, as well as discovery of tumor biomarkers [105, 106]. Although studies on drug-induced downstream signaling pathways have provided some insights, studies of protein targets are required because target-identification and mechanism-of-action studies play vital roles in drug discovery [88]. However, the traditional proteomics approaches only focus on measuring quantitative alterations in protein abundance, which do not necessarily correlate with protein activities [47], neither do they provide functional interpretation of proteins in the physiologically relevant environment [47]. Thus, additional combinatory and interdisciplinary techniques could be utilized in the application of drug treatment, especially in the study of protein function and protein – protein

interaction, protein – ligand interaction.

The emerging multidisciplinary methods, chemical proteomics provides an opportunity to reveal the protein activity as well as the interaction between protein and small molecules. Chemical proteomics utilizes the synthetic small molecules, which could covalently bind to the catalytic residues in an enzyme active site. Thus, proteins could be tagged, enriched and detected. This kind of probes could monitor different properties of proteins, such as protein activity, protein location, protein-protein interaction and post-transcriptional modification.

1.4.2 Activity Based Protein Profiling (ABPP)

Many drugs exert pharmacological functions by binding their targets and may inhibit their activities, the study of function or activity of their binding targets is extremely important. In addition, hydrolytic and proteolytic enzymes have been shown up-regulated in many tumor cells [47]. As enzymes regulated essential cellular processes, they have become vital therapeutic targets for many human diseases including cancers [107]. However, it is difficult to investigate the functional roles of enzymes in cancers by traditional proteomics because those strategies do not provide functional understanding of proteins in the physiologically relevant environment *in vivo* [47]. Moreover, proteins' abundance does not truly reflect their activities because most enzymes are expressed as inactive zymogens or reside in complexes with their endogenous inhibitors [47].

To circumvent these limitations, Activity-based protein profiling (ABPP) could be utilized to unravel the enzyme activities and to identify the targets of small molecules [46]. The main advantage of ABPP over the traditional proteomics approaches is that it could profile the active sites of enzymes. Activity-based protein profiling (ABPP) combined with bio-orthogonal click chemistry is a novel functional proteomics technology to directly examine the functional state of enzymes both *in vitro* and *in vivo* [46, 47, 53, 108]. The ABPP method can mainly detect the functionally active form of the targets because most of the regulatory mechanisms for enzyme activities involve changes of the proteins' active sites.

The core of ABPP technology is a small molecule called activity-based probe (ABP). ABP was designed to contain three basic elements: 1) A reactive group, which could target and covalently bind to the active sites of the enzyme, 2) a reporter tag and 3) a linker, which connect the reporter tag, as well as the reactive group (Figure 1.4). The reactive group was designed to contain the electrophile and could interact with active-site residues of target proteins, forming a stable covalent bond. The reporter tag could be 1) fluorophore for visualization, 2) biotin for enrichment and purification, and 3) isotope tag for identification.

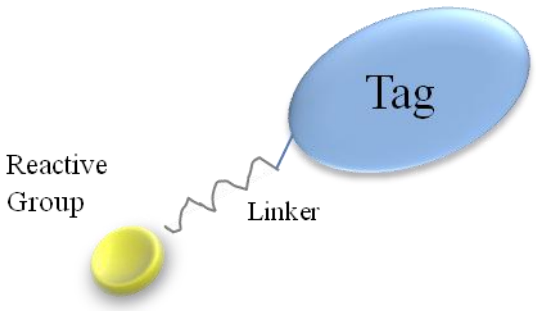

Figure 1.4 Components of activity-based probe (ABP). ABP contains a reactive group, a tag that could be a fluorophore such as cyanine 3 for fluorescence detecting, or a biotin for enrichment, and a linker.

1.4.3 Tagging strategies for chemical proteomics

The core of chemical proteomics is the integration of synthetic chemical molecular into the proteins of interest. The design of synthetic molecules depends on different purposes, such as protein enrichment, visualization, purification, *etc*. The commonly used probe contains isotope tags, fluorophores, affinity tags or tandem bio-orthogonal tagging.

1.4.3.1 Isotope tags

The radioactive isotopes, like ^{3}H and ^{125}I, could be integrated into probes. Tritium can replace hydrogen in probes without changing the structure of small probes. Therefore, radioactive probes could be used to monitor alterations in enzyme activity. Some studies utilized the isotope-labeled drugs to study and identify the targets of drugs [109].

There are several advantages using this strategy. First, the replacement of normal

iodine or hydrogen does not affect the whole structure of the small molecule, retaining the original permeability and function of the native molecule. Secondly, the radioactive isotopes could provide sensitive signal for detection, easier to be identified compared with fluorophores. However, some big challenges exist, including 1) difficulty to enrich its targets from proteomes, and 2) restricted handling and dealing with the radioactive reagents.

1.4.3.2 Fluorophores

There are diverse types of fluorophores with a relatively broad range of absorbance and emission spectra for chemical proteomics strategies, providing efficient ways for most imaging applications. Nowadays, with large amount of commercially available fluorophores, the scope of chemical proteomics increases dramatically. Among the various types of fluorophores, cyanine dyes display high absorption coefficients, narrow absorption and high quantum yields, making them appropriate for majorities of biological applications. In addition, Cy-dyes are hydrophobic, making them freely penetrate cell membranes for protein localization.

Fluorophores allow the early detection of the tagged proteins, which could efficiently facilitate the further exploration such as identification and purification of the proteins of interest. They could also directly provide visualization of the location, the expression level of proteins from the whole proteome. Fluorescent tags could be detected by in-gel scanning with a laser scanner with high sensitivity and a greater

dynamic range. What is more, when using diverse fluorophores with different excitation/emission spectra, the results in a single gel could be obtained.

1.4.3.3 Affinity tags

The usage of affinity tags enables the enrichment of the proteins of interest. Especially in the chemical proteomics field, affinity tags were commonly and widely used for purification of labeled proteins, because purification and enrichment of probe-bound proteins are quite important for the identification of probe's targets. Among various affinity tags, biotin is the most commonly used affinity tag. Its binding to streptavidin is one of the strongest non-covalent interactions, making it feasible for the binding of low-abundant biotinylated proteins.

However, there are some limitations of this kind of tags. First, because biotin-labeled or biotinylated proteins are usually binding to an avidin resin, the bound proteins need to be eluted by using detergents or denaturants, resulting in eluting nonspecific-binding and endogenously biotinylated proteins. This might increase the possibility of the negative candidates for drug target screening. Another challenge of using biotin for protein enrichment is the size of biotin. Biotin is too large to permeate the cell membrane, making it hard to be used to pull down the proteins of interest *in vivo* and *in situ*. Recently a tandem biorthogonal labeling method was quickly developed to address these problems. It enables biotin/fluorophore tags to be added to the probe after the probe finds its targets.

Another strategy to exclude the nonspecific-binding or endogenously biotinylated proteins is the introduction of iTRAQ. The detail of these mechanisms will be discussed in the following sections.

1.4.3.4 Tandem biorthogonal tagging

The important part of tandem biorthogonal strategy is the usage of the small chemical functionalities. This kind of tags have minimal alteration of parent compound and cell permeability. The great advantage is that the tags could be later used for chemical modification with various reporter tags.

The most commonly used strategy is called “click chemistry” (Figure 1.5). In this strategy, an alkyne and an azide functional group are catalyzed by Cu (I) to form a triazole conjugate through cycloaddition. This reaction is highly biocompatible with chemical functionality in biomolecules such as proteins and metabolites. The reaction could also proceed in aqueous environment even containing strong denaturants. Therefore, this strategy was largely used in the chemical proteomics fields [47, 53, 108, 110]. Briefly, the alkyne-labeled probe is small enough to permeate the cell membrane. After binding its potential targets in the proteome, the probe-target compound as well as the whole proteome were then react with the azide-modified biotin/fluorophore for enrichment or visualization.

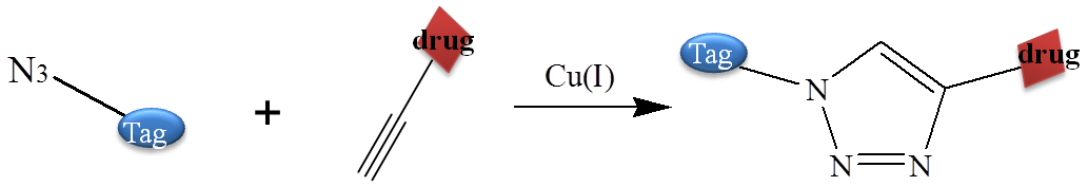

Figure 1.5 Click chemistry catalyzed by Copper (I). The drug probe was designed to contain alkyne, which could react with azide to form a triazole conjugate through cycloaddition. The tag could be a fluorophore or biotin. In our experiments, Cy3-azide or biotin-azide were used in click chemistry for fluorescence labeling or enrichment, respectively.

1.4.4 Previous studies of direct targets and their limitations

So far, only five proteins were identified as cellular targets of triptolide, as listed in Table 1.2. The first binding target of triptolide, Polycystin-2 (PC2), was identified by Crews' group in 2007, using tritium-labeled triptolide [109]. They found the specific [^{3}H] triptolide-binding activity through chromatographic purification, and identified PC2 as a putative target of triptolide. Although usage of tritium-labeled probes maintains the activity or property of the native triptolide, the tritiation could never be enriched and it needs more safety regulation matters.

After that, this group also identified dCTP Pyrophosphatase 1 (dCTPP1) as the direct binding target of triptolide [111], using a biotinylated photoaffinity derivative of triptolide as the probe. This improved strategy allows the candidate targets to be enriched. However, this biotin-conjugated triptolide probe contains a quite long linker thus might greatly alter the property of the native triptolide. Actually, the IC_{50} of this

probe is 168 μM, extremely higher than the IC_{50} of native triptolide. As a result, dCTPP1 might not be a physiologically associated target of triptolide.

In the same year, Liu's lab identified XPB as a target of triptolide, and recently in 2015, identified its binding site, Cysteine 342 [112, 113]. They utilized the "top-down" approach. Their research and previous literature [114] found that RNA Polymerase II (RNAPII) was inhibited by triptolide. Then their group analyzed the protein clusters that compose RNAPII. Among them, TFIIH was indicated to be inhibited by triptolide. Subsequently by screening the individual proteins in TFIIH, XPB was found to interact with triptolide directly. This method is a repeat of screening process from the complex to the individual proteins. However, the candidates need to be validated further, and this method might generate a large amount of negative results if applied to target screening in large scale. Therefore, this method's efficiency needs to be improved.

In addition, Yan Lu, *et al* identified TAB1 as the target of triptolide in macrophages. They utilized triptolide succinate (mTP) as the hapten derivative, followed by co-immunoprecipitation (coIP) with anti-TP. As a result, the specific band of candidate was excised and identified by mass spectrometry. Although their finding did not focus on binding targets of triptolide in cancers, it provided some insights on its binding mechanism and pharmacological functions.

Recently Yang's lab identified the triptolide's binding target – Peroxiredoxin I. Yang's lab utilized two chemical proteomics probes, fluorophore-conjugated probe and biotin-conjugated probe. However, both probes were bulky and not ideal to enter the cells. Actually, they extracted the proteins and incubated the proteins with the probes *in vitro*. Therefore, the application of these two probes was limited. In addition, the pull-down candidates might contain non-physiologically relevant targets.

Table 1.2 Direct binding targets of triptolide currently found. So far, there are only five proteins identified as the direct binding targets of triptolide.

Targets	Model	Material and Method	Reference
Polycystin-2	ADPKD	[^{3}H] triptolide-binding protein, fractionated by FPLC, MALDI-MS	Stephanie J, 2007
XPB	Hela	'top-down' approach	Denis V, 2011
dCTPP1	Hela	Biotin-conjugated triptolide Affinity pull down	Corson TW, 2011
TAB1	Macrophages	Chemical proteomics, TLP-mmc	Lu Y, 2014
Prx I	HCT116	Chemical proteomics, two TLP-probes	Qian Z, 2015

Some studies have shown that drugs exert their functions through interacting with multiple targets. One of the methods to study the multiple targets is chemical proteomics [115-117]. For example, multiple proteins ranging from anti-inflammatory to anticancer properties were identified as Artemisinin's binding target, by using proteomics approaches [118]. Therefore, the attempts to identify binding targets of triptolide indicated that triptolide's molecular targets have not been fully characterized and there are more possible binding targets with low affinity or low abundance remains unexplored. Considering the above limitations, and with the aim to provide a large scale of triptolide's target candidates at a global level, we propose

to utilize the chemical proteomics approaches to profile the direct binding targets of triptolide *in vivo*. Profiling the targets of triptolide and exploring the signaling pathways are mutually promotional to unravel the mechanisms of triptolide against colorectal cancer. In addition, revealing the direct targets of triptolide might aid to design derivatives that have fewer side effects and less toxicity.

1.5 Aims of my projects

Compounds derived from natural products, especially those originating from plants, have played invaluable roles in drug discovery process regarding to all disease types [39]. Diterpenoids from plant exert an extensive range of important physiological functions and give hope for the development of new therapeutic agents against cancer, inflammation and cardiovascular diseases [40-42].

Triptolide, a diterpene triepoxide extracted from natural plant, exerts strong anti-tumor activities. Previously numerous studies have demonstrated that triptolide has anti-proliferative and pro-apoptotic activity in various tumor models *in vitro* and *in vivo*. However, the detailed molecular mechanisms of triptolide against colorectal cancer remains largely elusive to date. Fortunately, the current achievement in the fields of proteomics and bioinformatics provide the opportunity to study protein changes at a global level, facilitating the exploration of the cellular signaling pathway with triptolide's treatment. Particularly, isobaric tags for relative and absolute

quantitation (iTRAQ) is a non-gel-based technique used in proteomics to study quantitative changes in up to eight samples simultaneously. Until now, only a few limited studies in the area of colorectal cancer treatment have exploited this high-throughput technique. The previous works focused on individual proteins, which might not provide an overall picture of the regulated proteins at a global level.

On the other hand, identification of the binding targets of a drug is very important in exploring its mechanism as well as refining the drug in the clinic trials with minimal side effects. However, only five proteins so far have been identified as direct binding targets of triptolide, using methods with some limitations described above. Therefore, in our study, the chemical proteomics method will be utilized, which could profile the target candidates with high confidence at a global level.

Therefore, the aims of my projects include two parts: 1) to profile the protein alterations with triptolide's treatment at a global level, revealing the signaling pathways of the regulated proteins 2) to identify the direct binding targets of triptolide. These studies might shed some lights on the mechanism of triptolide against colorectal cancer cells. An understanding of the direct binding targets of triptolide and the signaling pathways will aid to unravel its mechanism.

For my first objective, the regulated proteins in colorectal cancer cell line HCT 116 treated with triptolide will be profiled at proteome level by iTRAQ and analyzed

using bioinformatics approaches. These approaches could generate an overall picture of protein level changes, which provides some insights into the mechanism of triptolide against colorectal cancer. For my second objective, the specific targets of triptolide will be identified using Activity-based Protein Profiling (ABPP) combined with bio-orthogonal “click chemistry”. The mechanism of the drug’s binding activity with targets will also be evaluated. These methods will provide us with a profile of potential binding targets at a global level.

Chapter 2 Materials and Methods

2.1 Cell Culture

Human colorectal cancer cell line HCT 116 was obtained from American type culture collection (ATCC) and cultured in McCoy's 5A Medium supplemented with 10% fetal bovine serum (FBS) and 1% antibiotic-antimycotic at 37℃ in 5% CO_2 mixed with air.

2.2 Cell Proliferation Assay

HCT 116 cells were seeded at a density of 8,000 cells per well of a 96-well plate and allowed to adhere overnight. Cells were treated with 1% DMSO as control or triptolide at different concentrations ranging from 2 nM to 50 nM, in 6 replicates. After 48 hrs of incubation, the medium was removed and cells from each condition were fixed, stained and rinsed thoroughly. A staining solution contained 20% methanol and 0.5% crystal violet. After air-drying, 100 μl of 1% SDS in PBS was added to each well to solubilize the dye completely. The absorbance value was read at 590 nm. In another experiment to study time-effects, cells were treated with selected concentrations (10 nM and 25 nM) of triptolide for 24, 48 and 72 hrs.

2.3 Cell Cycle Analysis

HCT 116 cells were synchronized with serum-free medium overnight and then treated with 1% DMSO or 25 nM of triptolide for 6, 12 or 48 hrs, in three biological replicates. To harvest, a number of 1×10^6 cells of each condition were then scraped

without wash. 70% ice-cold absolute ethanol was added into cell pallets by gentle pipetting. After being fixed overnight at -20℃, cells were then spun down and stained with 1 ml propidium iodide (50 μg/ml; Sigma-Aldrich) containing RNase A (50 μg/ml; Sigma-Aldrich) for 3 hrs at room temperature in tinfoil-covered tubes. Next, analysis of DNA content was carried out on a FACScan flow cytometer.

2.4 Proteomics Sample Preparation

Samples were prepared by sonicating the harvested cells with a lysis buffer containing 0.5 M triethylammonium bicarbonate (TEAB) and 1% SDS, pH 8.5. The lysates were then centrifuged at 12,500 g for 30 min to remove cell debris. Protein quantitation was performed using RCDC Protein Assay Kit (Bio-Rad); 100 μg of each sample was used for iTRAQ labeling.

2.5 ITRAQ labeling

ITRAQ labeling was carried out using commercial reagents (iTRAQ^{TM} Reagent 8-Plex kit, Applied Biosystem) based on the manufacturer's protocol. Cell lysates were reduced with tris-(2-carboxyethyl) phosphine (TCEP), alkylated with methyl methane-thiosulfonate (MMTS), and diluted 20 times before digesting overnight by trypsin (w/$CaCl_2$; Promega; 1:10 (w/w)) at 37℃. Equal amount of digested peptides was reconstituted with 0.5 M TEAB. A pair of whole cell lysates of HCT 116 cells treated with DMSO and 25 nM of triptolide for 6 hrs was labeled with 113 and 114

iTRAQ labeling reagents, respectively. Another pair of its biological replicates of the same samples was labeled with 117 and 118 iTRAQ labeling reagents, respectively. For another comparison, a pair of whole cell lysates of HCT 116 cells treated with DMSO and 25 nM of triptolide for 48 hrs was labeled with 115 and 116 iTRAQ reagents, respectively. Another pair of its biological replicates of the same samples was labeled with 119 and 121 iTRAQ reagents, respectively. Once the peptides were added with respective isobaric tags, they were incubated at room temperature for 2 hrs before mixing (Figure 2.1).

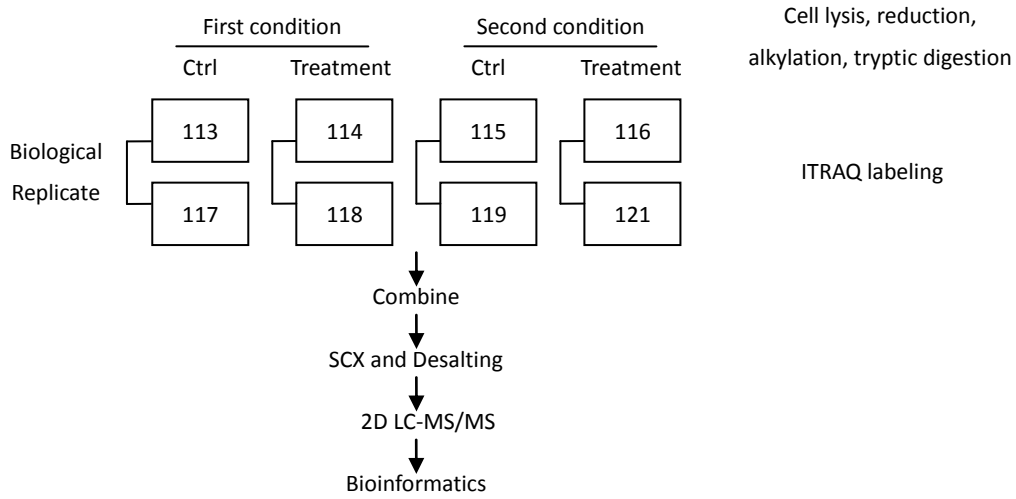

Figure 2.1 Schematic representation of workflow of iTRAQ labeling showing biological replicates. In our experiment, proteome from HCT 116 cells treated with DMSO either with 25 nM of triptolide for 6 or 48 hrs were reduced and digested. Subsequently, the digested peptides from each sample were labeled with respective isobaric tags and mixed. Strong Cation Exchange (SCX) chromatography followed by desalting was applied to facilitate the identification and quantification of the respective samples by 2D LC-MS/MS.

2.6 Strong Cation Exchange (SCX) Chromatography and Desalting

SCX was carried out to remove interfering substances such as dissolution buffer, organic solvent, reducing agent and excess iTRAQ reagents. Cation exchange system provided in the iTRAQ Method Development Kit (AB SCIEX) was utilized. The labeled peptide mixture was diluted 10 times with Cation Exchange Buffer-Load. The pH was checked and brought down in the range of 2.5 to 3.3. The cation-exchange cartridge was conditioned by injecting 1 ml of the Cation Exchange Buffer-Clean and 2 ml of Cation Exchange Buffer-Load. Then the diluted sample mixture was injected slowly into the cartridge. The cartridge was washed with 1 ml Cation Exchange Buffer-Load and finally the peptides were eluted with 500 µl of Cation Exchange Buffer-Elute and collected in a new tube. This fraction was then desalted using Sep-Pak C18 cartridges (Waters, Milford, MA). Subsequently the sample was lyophilized and dried. The desalted and dried sample was reconstituted with 98% H_2O, 2% acetonitrile and 0.05% formic acid for 2D LC-MS/MS analysis.

2.7 2D LC Analysis and Tandem Mass Spectrometry (MS/MS)

Peptide separation was performed on Ultimate 3000 LC system (Dionex-LC-Packing, Sunnyvale, CA) connected to SCX NanoEase trap column (PolyLC inc, PolySULFOETHYLA^{TM}) for the first dimension. Peptides were separated using step gradients of mobile A (10 mM K_2HPO_4, 25% ACN, pH=3) and mobile B (10 mM K_2HPO_4, 25% ACN and 250 mM KCl, pH=3) as follows: 0% of

mobile B for 10 min, 0-36% for next 80 min, 36-70% for the next 30 min, and 100% for last 5 min and 0% for another 15 min, at a flow rate of 0.5 ml/min. Then twenty eluting fractions were desalted with Sep-Pak C18 cartridges (Waters, Milford, MA) for second-dimension reverse phase (RP) chromatography. The MS analysis was performed using a 5600 TripleTOF analyzer (AB SCIEX, Foster City, CA).

2.8 Peptide and Protein Identification and Bioinformatics Analysis

ProteinPilot Software 2.0.1 (AB SCIEX) was exploited for protein identification and relative iTRAQ quantification. A strict unused score cutoff > 1.3 was used as the qualification criteria, which corresponds to a protein confidence level of > 95%. Four sets of fold change of treatment to control for both early and late time points were averaged. Gene Ontology (GO) studies classified the significantly altered proteins as per their molecular function, cellular component and the biological process. To better analyze the data generated, protein list of these proteins was uploaded into Ingenuity Pathway Analysis (IPA) software. The top biological processes, molecular functions as well as networks including the significantly altered proteins were established.

2.9 Validation of Proteomics Data using Western Blot

SDS-PAGE was performed to run equal amount of whole proteins extracted from harvested cells. The proteins were then transferred onto PVDF (Polyvinylidene fluoride) membranes (Bio-Rad). The blots were blocked using 5% BSA in PBS with

0.1% Tween 20 (PBST). The membranes were incubated with rabbit anti-BRD4 mAb (Santa Cruz Biotechnology), rabbit anti-GAPDH mAb (Santa Cruz Biotechnology), rabbit anti-Cyclin D1 mAb (Santa Cruz Biotechnology) and rabbit anti-CDK4 mAb (Santa Cruz Biotechnology) overnight. HRP-conjugated anti-mouse IgG (1:5000) from GE Healthcare, or HRP-conjugated anti-rabbit IgM (1:5000) from Pierce Biotechnology were used as secondary antibodies. Subsequent visualization was performed using ECL substrate (Santa Cruz Biotechnology, Inc.) with GAPDH as the loading control.

2.10 Immunocytochemistry Staining

HCT 116 cells were seeded on 6-well plate covered with autoclaved coverslips and grown until 50%. Full medium was then changed to medium with 1% DMSO or difference concentrations of triptolide (25 nM, 50 nM and 100 nM). After incubating for 48 hrs, cells were then fixed with 4% paraformaldehyde in PBS (pH 7.4) for 10 min at room temperature. The coverslips were then washed with cold PBS and permeabilized for 10 min with PBS containing 0.25% Triton X-100. Subsequently, coverslips were washed and blocked with 1% BSA for 1 hr and incubated with rabbit monoclonal anti-BRD4 antibody (Santa Cruz Biotechnology; diluted 1:500) overnight at 4 degrees. Cells were then incubated with Alexa Fluor-555 conjugated donkey anti-rabbit IgG (Abcam) for 1 hr in the dark and mounted on glass slides with DAPI

mounting solution (Santa Cruz Biotechnology). The immunofluorescence was analyzed under Leica DMI6000 B.

2.11 *In situ* fluorescence labeling using triptolide probe

HCT 116 cells were seeded into 6-well plates and allowed to adhere overnight at 37℃. Then cells were treated with medium containing 1% DMSO or increasing concentrations (5-500 μM) of triptolide-probe for 12 hrs. Cells were harvested and suspended in 150 μL of PBS containing 0.16% SDS and proteinase inhibitor. After cell lysis by sonication, the lysate was centrifuged at 12,500×g for 30 min. Concentration of proteins in supernatant was calculated by using Bradford assay. Equal amount of sample was incubated with Cy3-azide (20 μM), Tris (2-carboxyethyl) phosphine (TCEP) (1 mM, 100×fresh stock in water), Tris [(1-benzyl-1H-1, 2, 3-triazol-4-yl) methyl] amine (TBTA ligand) (100 μM, 100×stock in DMSO), and $CuSO_4$ (1 mM, 100×stock in water) at 37 ℃ for 4 hrs. Subsequently, the clicked proteins were precipitated by cold acetone and air-dried. Proteins were dissolved with 1×SDS loading buffer and separated by SDS gel electrophoresis on 12% polyacrylamide gel. After SDS-PAGE, gel was visualized using Typhoon 9410 laser scanner (GE, healthcare; Buckinghamshire, UK).

2.12 Proteome labeling with triptolide probe

HCT 116 cells were grown in T175 flasks until reaching 80-90% confluence,

followed by treatment with 1% DMSO or 100 μM triptolide-probe for 12 hrs, in two biological replicates. Cells were then suspended in 5mL of 800 μM PBS containing 1.2% SDS, followed by sonication. Next, samples were centrifuged at 12,500×g for 30 min and the supernatant was applied to protein quantitation. Equal amount of proteins was incubated with Biotin-azide (20 μM), TCEP (1 mM, 100×fresh stock in water), TBTA ligand (100 μM, 100×stock in DMSO), and $CuSO_4$ (1 mM, 100×stock in water) at 37 ℃ for 4 hrs. Subsequently, the clicked proteins were precipitated by cold acetone and stored at -80℃ until further use. After the proteins were fully precipitated, samples were centrifuged; Acetone in the supernatant was completely removed.

2.13 Pull down and MS analysis of triptolide-bound proteins

The precipitated proteins were dissolved in 1 mL of PBS containing 0.1% SDS and incubated with 70 μl of avidin beads (Sigma-Aldrich) with gentle mixing overnight at 4℃. The beads were washed with 1% SDS in PBS thrice, with 6 M urea thrice, and with PBS thrice. Each of these steps started with gentle centrifugation (800 rpm, 3 min), followed by removal of supernatant, and addition of 12 mL of above-mentioned washing solution with gentle shaking for 10 min. A small amount of enriched bead-bound proteins were separated by SDS-PAGE and visualized by silver staining. By comparison of the enriched target bands with control samples, the bands of triptolide-bound proteins were excised, followed by in-gel digestion and

identification by LC-MS/MS.

2.14 Immunofluorescence staining using triptolide probe

HCT 116 cells were seeded on Corning Disposable Sterile Suspension Culture Dishes (Corning Glass Works, N. Y.) and grown until 70% confluence. Full medium was then changed to medium containing 1% DMSO or 100 μM of triptolide probe. After incubation for 12 hrs, medium was removed and cells were then fixed with 4% paraformaldehyde in PBS (pH 7.4) for 10 min at room temperature. Next, cells were washed with cold PBS and permeabilized with PBS containing 0.25% Triton X-100. Next, cells were clicked with Cy3 alkyne. Briefly, cells were incubated with fresh-made click chemistry reaction solution containing 20 μM Cy3-azide, 1 mM TCEP, 100 μM TBTA and 1 mM $CuSO_4$ at room temperature for 2 hrs. The immunofluorescence was visualized using Leica DMI6000 B.

2.15 Protein synthesis evaluation

HCT 116 cells were cultured in L-methionine-free medium for 30 min to remove the previous methionine reserves. Then cells were labeled with 50 μM AHA with DMSO or 100 nM triptolide. After 12 hrs' incubation, cells were harvested and the amount of AHA incorporated into the protein could be detected using the click reaction as described before. AHA signal intensity was further analyzed using flow cytometry.

2.16 Preparation of recombinant PRDX I

Human gene of PRDX I (GenBank Accession No. NP_859048.1) was subcloned into pET28a to generate a 6×His-tagged fusion protein. After confirming DNA sequence with 100 % identities, the construct was transformed into *E.coli* strain *BL21* for protein purification. Briefly, *BL21* containing the desired plasmid was cultured in LB medium containing 100 μg/mL kanamycin at 37 °C until OD_{600} of 0.7 was reached. Then protein expression was induced by incubating with 0.4 mM Isopropyl β-D-1-thiogalactopyranoside (IPTG) at 37 ℃ for 2 hrs and then at 16 ℃ overnight. Subsequently, cells were harvested by centrifugation (4,500 rpm, 15-20 min) and suspended in lysis buffer (B-PER Reagent PI) by rotating for 20 min. Cell pellets were removed by centrifugation at 15,000g for 15-20 min. The protein in the supernatant was then bound to the beads (Ni^+ (His-Pr)) with rotation at 4 ℃ for 1 hr and then washed three times with wash buffer (50 mM Tris, pH 8.0). Next, protein was eluted with elution buffer (50 mM Tris, pH 8.0, 100 mM NaCl, 250 mM Imidazole and 10% Glycerol).

2.17 *In vitro* Labeling of PRDX I

The recombinant PRDX I was reconstituted with PBS. Equal amount of proteins (1 μg) was incubated with 1 μl triptolide probe with a final concentration of 0, 10, 25, 50 and 75 μM at 37 °C for 4 hrs. For the competition assay, protein was pre-treated

with 10×triptolide for 4 hrs and then incubated with triptolide probe. After incubation, PRDX I-probe complex was precipitated by acetone, and then applied to click chemistry reaction, SDS-PAGE and fluorescence scanning.

2.18 Binding sites mapping by MS/MS

The recombinant PRDX I was reconstituted with PBS. Equal amount of proteins (50 μg) were incubated with 1 μl of 10 mM triptolide or 1% DMSO in 100 μL of PBS at 37 ℃ for 4 hrs. Subsequently, samples were exchanged against 50 mM NH_4HCO_3 for removing salt and unbound drug by using PD-10 Desalting Columns (GE Healthcare). Then protein was reduced and cysteine blocked, followed by trypsin digestion. The digested sample was applied to LC-MS/MS. For identification of triptolide-modified sites, the mass spectra were converted into Mascot generic format (MGF). Triptolide-modified residue mass difference 360.2 amu was specified as a parameter for modification searching. The same method was also utilized to study the binding sites mapping of Annexin A1.

2.19 Docking simulation of target-triptolide compound

The dimeric PRDX II (PDB: 1QMV) was used for docking simulation, using Autodock version 4.2 (http://autodock.scripps.edu/) with the Lamarckian Genetic algorithm (LGA). Water was moved and polar hydrogen atoms were added. Next, the 3D chemistry structure of triptolide was obtained by using Chem3D Ultra. After grid,

triptolide was manually docked into PRDX II as a flexible ligand. Each docking simulation was repeated 10 times and the molecular modeling with minimum energy was adopted. The interaction of PRDX II-triptolide compound was analyzed using Pymol. The same method was also used for the study of Annexin A1-triptolide complex. The full-length Annexin A1 (PDB: 1MCX) was utilized.

2.20 Peroxiredoxin function study

Peroxiredoxin I function was tested by using Peroxidase Activity Assay Kit purchased from Sigma-Aldrich based on the manufacturer's protocol. Briefly, 20 μg of PRDX I was incubated with 0, 100, 500 μM and 1 mM of triptolide at room temperature for 1 hr. Next, fluorescent peroxidase substrate and 12.5 mM H_2O_2 substrate was added. Samples were then transferred into 96-well black plate with clear bottoms and incubated at 37 ℃. The fluorescence intensity was measured (λ_{ex}=535/λ_{em}=585 nm) for every 2 min (after 30 min, interval becomes 5 min until 60 min). The amount of H_2O_2 reduced by PRDX I was calculated according to the H_2O_2 standard curve. Peroxidase activity of a sample was determined by the following equation:

$$Peroxidase\ Activity = Amount\ of\ H_2O_2\ reduced/\ (Reaction\ Time) \times V.$$

Peroxidase activity reported as nmole/min/mL = milliunit/mL, where one unit of peroxidase is defined as the amount of enzyme that reduces 1.0 mmole of H_2O_2 per minute at 37 ℃.

2.21 Evaluation of Reactive Oxygen Species (ROS) level

HCT 116 cells were treated with 100 nM triptolide or DMSO for 12 hrs, followed by incubation with CM-H_2DCFDA, an indicator for ROS. The ideal Ex/Em for it is about 495/525 nm. The fluorescence intensity was finally analyzed by flow cytometry.

2.22 Wound healing assay

HCT 116 cells were seeded in 6-well plate in 3 biological replicates, and cultured until 100% confluency. Subsequently a wound was produced by gently scraping the cells with a yellow pipette tip. After removing the scraped cells with PBS twice, medium with DMSO as the control or triptolide were added into the well. The wounded cell cultures were then incubated at 37 ℃ in the humidified and equilibrated (5% v/v CO2) incubation. After 12 hours of treatment, the cells of the control and treatment were then photographed under microscope. The distances of migration covered from the initial time to the 12 hours were measured.

Chapter 3 Studies of global alteration of proteins in HCT116 with triptolide treatment by using iTRAQ approaches

3.1 Introduction

Triptolide, an extract from traditional Chinese medicine, has been investigated for many of its potential therapeutic uses, including the reduction of tumor progression and solid tumor masses. It has entered clinical trials based on its potent anti-tumor effects on prostate cancer and acute myeloid leukemia [79, 119]. Extensive scrutiny of its mechanism of action in the past few decades has yielded important insights. So far, triptolide has been demonstrated to directly induce apoptosis of human hepatocellular carcinoma, promyelocytic leukemia, cervical adenocarcinoma, pancreatic carcinoma, T cell lymphoma, lung caner and oral cancer cells [34, 36-38, 120].

As described above, triptolide was demonstrated to have anti-proliferative and pro-apoptosic activity in various types of cancers. It was shown to induce apoptosis *via* activation of cysteine protease caspases 3, 8 and 9, and subsequent cleavage of DNA repair enzyme (ADP-ribose) polymerase in multiple myeloma cells [121]. Triptolide was also shown to decrease histone H3K9 and H3K27 methylations *via* down-regulating histone methyltransferase, which may be a potential anti-myeloma mechanism [122]. Vispe *et al.* concluded that triptolide was an original pharmacologic inhibitor of RNA Polymerase activity, indirectly affecting the transcription machinery, resulting in a rapid depletion of short-lived mRNA of transcription factors, including MYC and Src [114].

However, as a tumor grows in a complicated way, the whole mechanism of the anti-tumor function of triptolide remain unclear. With the development of proteomics and bioinformatics methods, we have the opportunity to study protein changes in a whole picture, facilitating the study of the cellular signaling pathways. Therefore, in our study, the regulated proteins in colorectal cancer cell line HCT 116 treated with triptolide were profiled at whole proteins level by iTRAQ labeling followed by MS/MS. An eight-plex iTRAQ workflow followed by 2D LC-MS/MS was adopted to identify differentially expressed proteins. These approaches will aid to discover therapeutic targets of triptolide.

3.2 Results

3.2.1 Anti-tumor properties of triptolide

3.2.1.1 Proliferation assay and cell morphology analysis

To explore anti-proliferative activity of triptolide, the proliferation assay was performed. HCT 116 and CCD 841 cells were treated with DMSO as the control or increasing concentrations of triptolide for 48 hrs, in six biological replicates. IC_{50} (concentration at which growth inhibition of 50 % of the cell population was achieved) of triptolide against HCT 116 cells was determined to be 10 nM, suggesting that triptolide has a strong inhibitory effect on HCT 116 cells proliferation with IC_{50} in nano-molar rang (Figure 3.1A).

By comparison, the proliferation of non-cancerous CCD 841 cells was not altered with triptolide's treatment in low concentrations. IC_{50} of triptolide on CCD 841 was demonstrated to be more than 500 nM. The CCD 841 is one of the colorectal epithelial cell lines. They are adherent and stretched cells, and grow as a disorganized and flattened layer. Comparison of colorectal normal cells with the colorectal cancer cells is essentially important. It could definitely provide some insights on the mechanism of triptolide against colorectal cancer cells.

Different concentrations of triptolide were chosen to study the effect of triptolide. In another independent cell proliferation assay, cells were treated with 10 nM and 25 nM of triptolide for 24, 48 and 72 hrs. From the result, the percentage of viable cells decreased exponentially with increasing dosage level and treatment duration of triptolide (Figure 3.1B), which indicates that triptolide has a potent anti-proliferative activity in both time- and concentration-dependent manners.

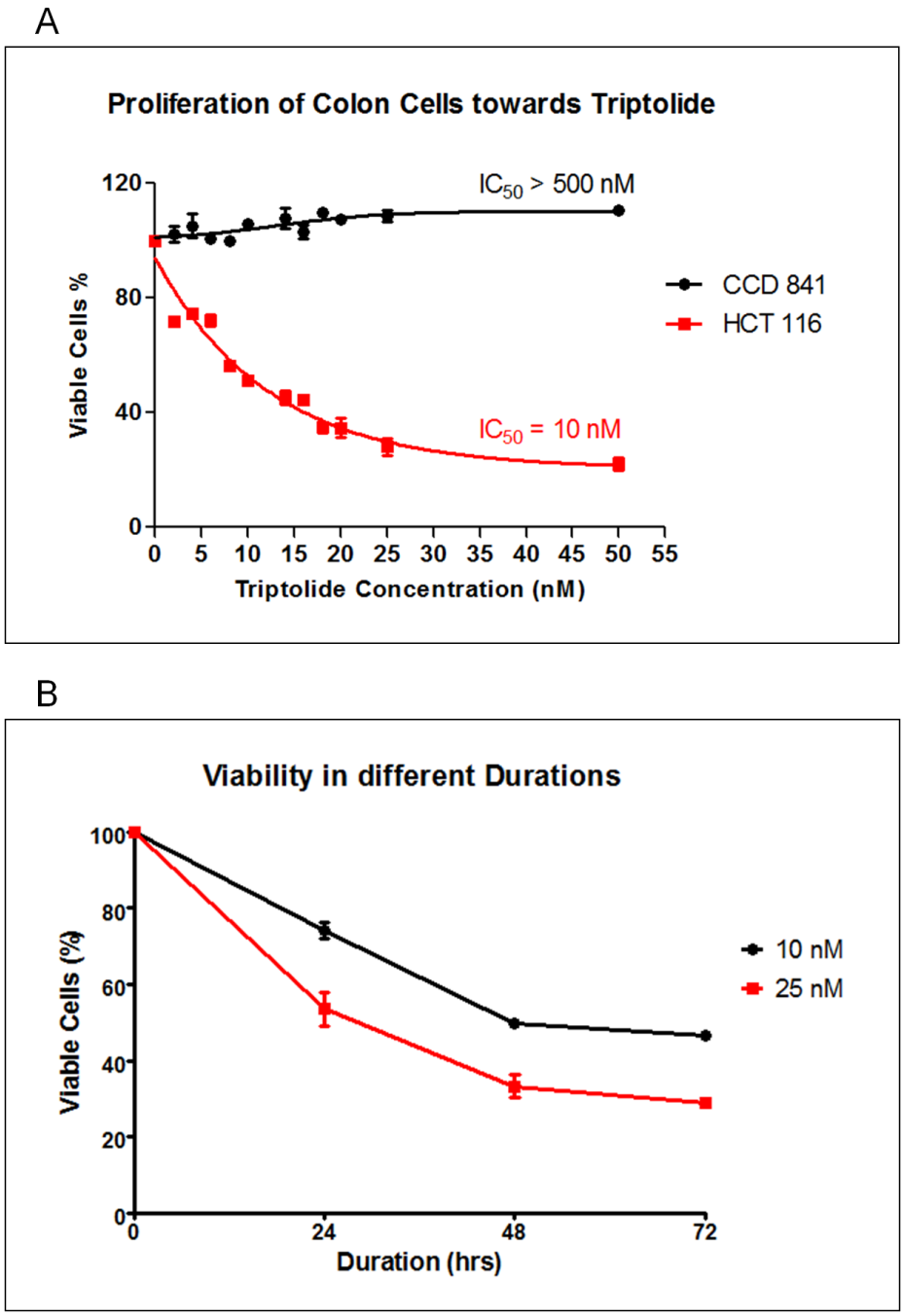

Figure 3.1 Triptolide showed strong anti-proliferative effects on colorectal cancer cell line HCT 116 but did not interfere with the proliferation of colorectal epithelial cell line CCD 841. (A) HCT 116 cells and CCD 841 were treated with increasing concentrations of triptolide. The IC_{50} of triptolide was determined to be 10 nM against HCT 116. The IC_{50} of triptolide against CCD 841 was more than 500 nM. (B) Cells were treated with 10 nM or 25 nM of triptolide for 24, 48 and 72 hrs, followed by the proliferation assay. Triptolide was shown to significantly attenuate cell proliferation in both time- and concentration-dependent behaviors.

To explore whether triptolide could alter cell morphology of HCT 116 cells, cells were treated with DMSO or 25 nM of triptolide for 48 hrs. The cell morphology was then observed under the microscope (Figure 3.2). Cell morphology image demonstrated that more than 20% of the total cells were detached with treatment. It suggested the presence of cell death with triptolide's treatment at the low concentration. The detached cells also lost characteristic of the ordinary HCT 116 cells, indicating triptolide induced cell morphology alteration with low concentration of treatment.

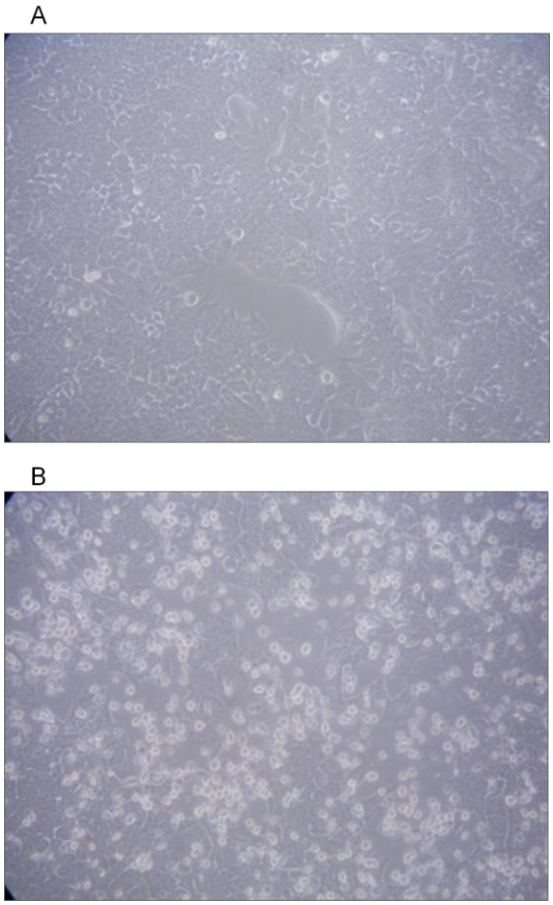

Figure 3.2 Triptolide induced cell morphology change of colorectal cancer cell line HCT 116. The image of cell morphologies of HCT 116 cells treated with 1 % DMSO (A) or 25 nM of triptolide (B) for 48 hrs were observed and compared under the microscope.

3.2.1.2 Cell cycle and apoptotic analysis by flow cytometry

To explore the function of triptolide on cell cycle of HCT 116 cells, flow cytometry analysis was then carried out. Cell distribution in three cell cycle phases were carefully calculated using software Flowing Software version 2.5.1. As shown in Figure 3.3A and 3.3B, Cell numbers in G_0 phase were increased with 6, 12 and 48 hrs of treatment, from 51.7% to 60.8%, 33.6% to 38.8, 58.9% to 66.5%, respectively. Flow cytometry assay indicated that triptolide induced G_0 phase cell cycle arrest and slowed down cell cycle shift from G_0 to S phase (Figure 3.3A).

In addition, to examine whether triptolide possesses pro-apoptotic activity on HCT 116 cells, the apoptotic analysis was then conducted by flow cytometry. Synchronized cells treated with DMSO or triptolide for 48 hrs were applied to the flow cytometric analysis in three biological replicates. Cell distributions in three cell cycle phases were also calculated using Flowing Software. As shown in Figure 3.3C, triptolide induced an obvious accumulation of cells in the sub G_0/G_1 region with 48 hrs of treatment (in red color), verifying that triptolide exerted the apoptotic activity on colorectal cancer cells.

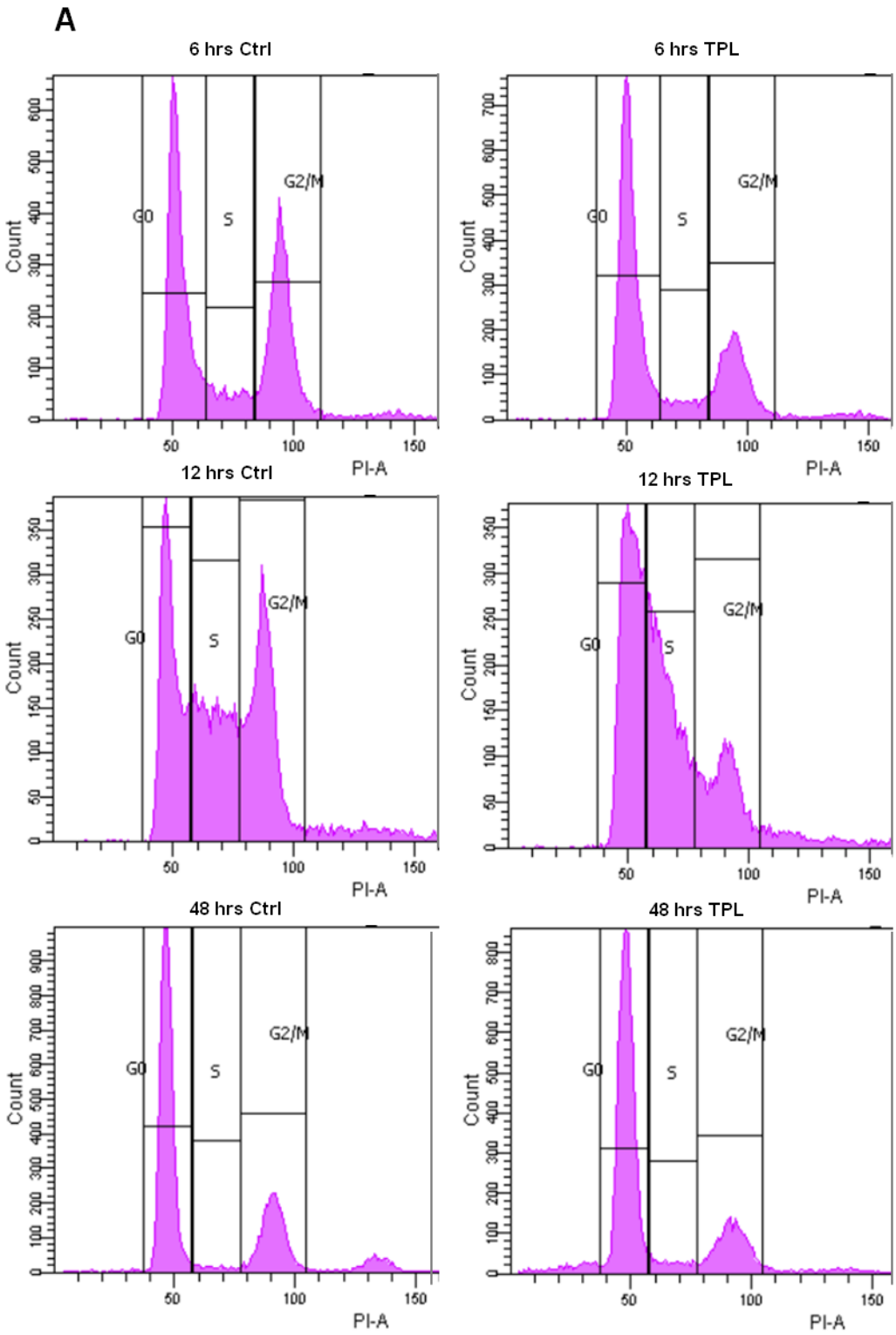
A
6 hrs Ctrl
6 hrs TPL
12 hrs Ctrl
12 hrs TPL
48 hrs Ctrl
48 hrs TPL
G0
S
G2/M
Count
PI-A

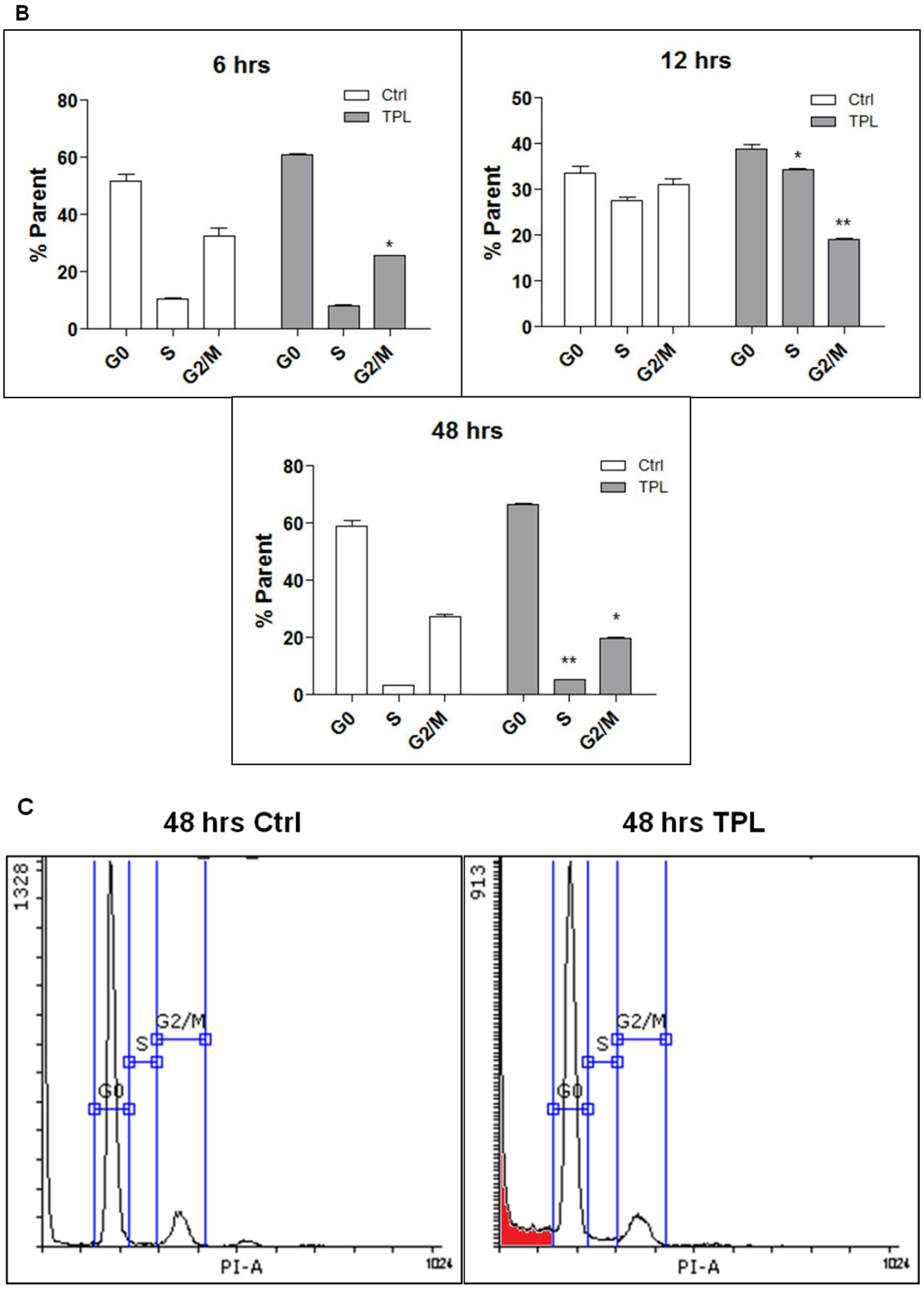

Figure 3.3 Effects of triptolide on cell cycle phases and apoptosis. The percentage of cells in phase G_0, S and G_2/M was showed (A) and summarized in (B), using Graphpad Prism 6 in three biological replicates. Triptolide was shown to cause G_0

phase arrest with 6, 12 and 48 hrs of treatment. (C) Cell apoptosis was evaluated using Flow Cytometry analysis. Cell cycle of HCT 116 cells were synchronized. Then cells incubated with 25 nM of triptolide for 48 hrs. Cell cycle analysis was performed by Propidium Iodide staining, followed by flow cytometry analysis. Accumulation of cells in sub G_0/G_1 region (labeled with red area) represented that triptolide induced apoptosis with 48 hrs of treatment.

3.2.2 ITRAQ results

To better understand the short-term and long-term effects of triptolide on colorectal cancer cells, proteins extracts from HCT 116 cells with 6 and 48 hrs of drug treatment were analyzed using 8-plex iTRAQ labeling followed by Strong Cation Exchange (SCX) and LC-MS/MS. The brief workflow of iTRAQ is describe in Figure 3.4. A strict cutoff of unused protein score was utilized, which corresponds to a 5% false discovery rate (FDR).

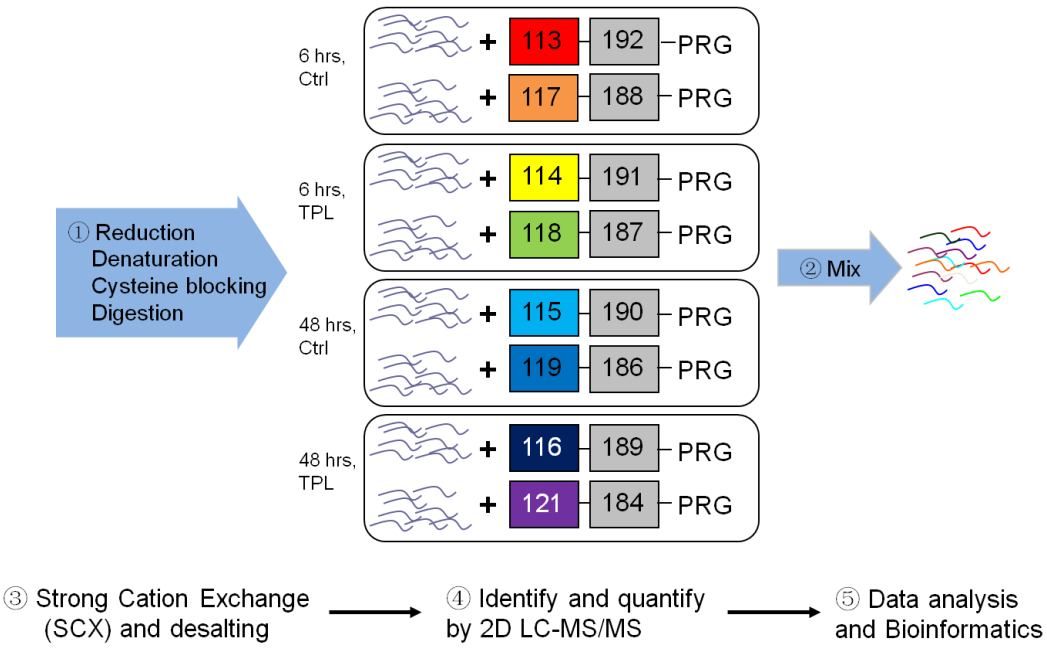

Figure 3.4 Workflow of iTRAQ. Proteins extracted from HCT 116 cells treated with DMSO or triptolide for 6 and 48 hrs were reduced and digested. Peptides with DMSO

treatment for 6 hrs were labeled with 113 and 117 iTRAQ reagents, in two biological replicates. Peptides with triptolide treatment for 6 hrs were labeled with 114 and 118 iTRAQ reagents, in two biological replicates. Similarly, peptides with DMSO treatment for 48 hrs were labeled with 115 and 119 iTRAQ reagents. Peptides with triptolide treatment for 48 hrs were labeled with 116 and 121 iTRAQ reagents. After mixing, SCX and desalting were performed. The peptides were finally identified by 2D LC-MS/MS.

Under this criterion, there were 2382 proteins identified. Subsequently, the final cutoff ratio for significantly up- or down-regulated proteins were determined using the method described in the previous literature [123]. The biological variation caused by random biological effects were then measured.

The biological effect caused the most likely source of variation compared to technical or experimental replicates [123]. This increased the need for fixing a cutoff with certainty that the protein alteration is real and thereby eliminated the need for other types of replicates [124]. The detailed method to determine cutoff value was described in the previous literature [123]. The proteins of the iTRAQ results were categorized into groups of variation ranging from 5% to 70% (Figure 3.5). Briefly, all peptide ratios were converted into $\log_2$ space. The average ratios of $\log_2$ values were then calculated, followed by being converted into linear space. Peptide ratios were then normalized and the normalized peptide ratios determine the variance. For example, at ±5% variation, 36.8% of the expression values from the 6 hrs of treatment and 19.2% of the expression values from the 48 hrs of treatment, respectively, fall into this range, suggesting that 36.8% and 19.2% of the proteins were identified and

quantified with criteria that variation of expression is less than 5%, respectively. Applying this cutoff method to our whole dataset, 17.3% and 22.1% variation corresponded to 88% coverage of protein for 6 and 48 hrs of treatment, respectively. Hence, the cutoff was determined to be 1.173 fold (±17.3% variation) for 6 hrs of treatment and 1.221 fold (±22.1% variation) for 48 hrs of treatment. With this criterion, 105 proteins were found to be significantly altered with 6 hrs of treatment and 115 significantly altered proteins were found with 48 hrs of treatment.

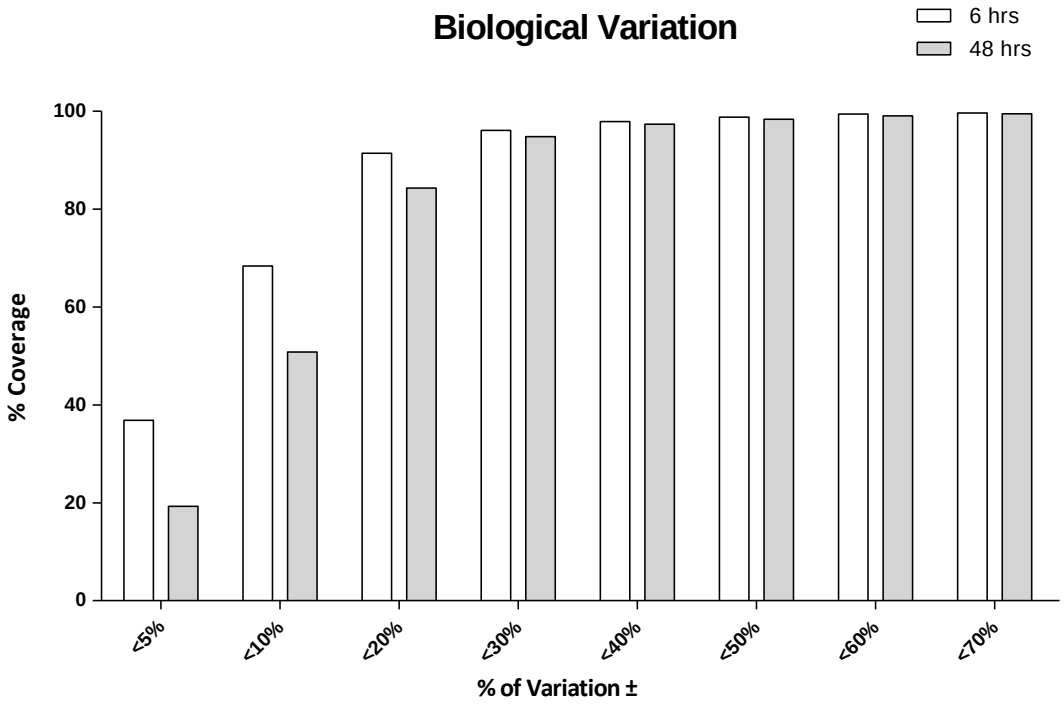

Figure 3.5 The percentage at different geometric standard deviation levels of total 2382 proteins. The X-axis represent percentage of geometric standard variation among four sets of iTRAQ ratios resulting from the comparisons between two controls and two treatments. Y-axis represents the corresponding percentage coverage. In our data, more than 88% of proteins had less than about 20% of variation. The cutoff thresholds for protein alteration were determined to be 1.173 fold (±17.3%) for 6 hrs of treatment and 1.221 fold (±22.1%) for 48 hrs of treatment.

3.2.3 GO analysis of significantly altered proteins

The list of significantly altered proteins was analyzed *via* Gene Ontology analysis. It classified the significantly changed proteins as per their cellular component, as well as biological process (Figure 3.6). The wide distribution of cellular location indicated the proteins were fully extracted and triptolide significantly interfered with proteins in the whole cell.

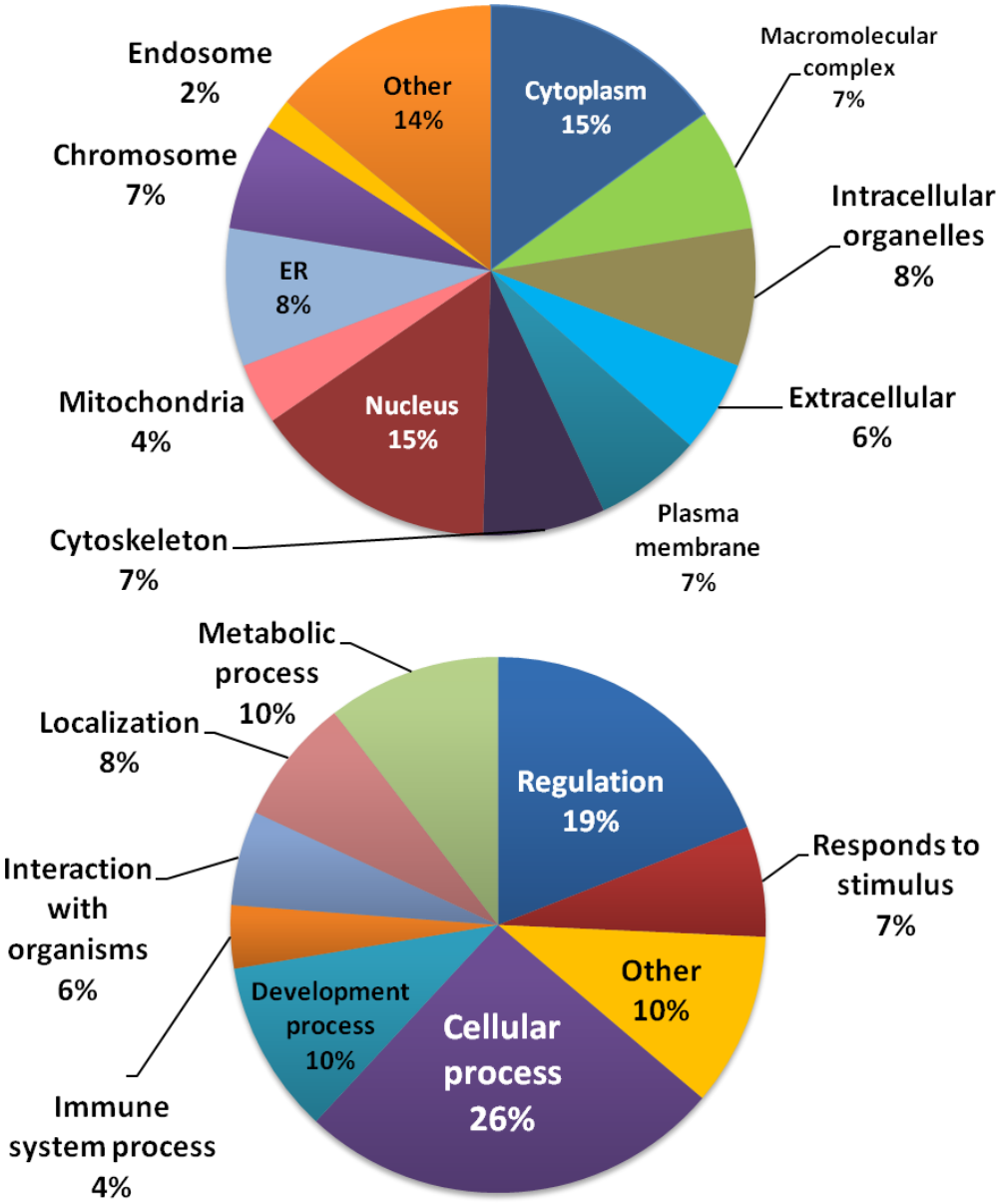

Figure 3.6 Cellular localization (Upper) and biological process (Bottom) of differentially regulated proteins. Two lists of significantly altered proteins from 6 and 48 hrs of treatment were uploaded to the software STRAP 1.5. The cellular components and biological processes were presented, providing an overview understanding of the property of the lists of significantly regulated proteins.

3.2.4 IPA analysis

The list of significantly changed proteins was then analyzed *via* Ingenuity Pathway Analysis (IPA) approach. IPA also ranked the molecular and cellular functions and top networks of significantly altered proteins (Table 3.1). The top functions of altered proteins were determined to be *cellular maintenance, cell morphology and molecular transport*. In addition, the associated top networks of these proteins were *cell death and survival*, *gene expression and protein synthesis*, and *cell cycle*. These data demonstrated that cell maintenance and morphology were interfered with triptolide. Cell death and survival ranked the top network of the altered proteins, which is consistent with our previous findings. Triptolide was also shown to alter the expression of proteins, which constitute the networks associated with cell death and cell cycle.

Table 3.1 Functions and top networks of differentiated proteins. IPA analysis provided a list of cellular functions and top networks constituted by the significantly altered proteins.

Molecular and Cellular Functions

Name	p-value	Molecule Numbers
Cellular Function and Maintenance	8.18E-05 - 4.59E-02	23
Cell Morphology	2.61E-04 – 4.55E-02	22
Molecular Transport	3.57E-04 – 4.06E-02	22

Top Networks

ID	Associated Network Functions	Score
1	Cell Death and Survival	47
2	Gene Expression, Protein Synthesis	47
3	Cell Cycle	29

Next, the functions of the proteins altered by short-term and long-term treatments were analyzed separately, which were illustrated in Figure 3.7. The top-ranked function of proteins in 6 hrs of treatment was *Cellular Assembly and Organization*. This finding indicated that as early as 6 hrs, triptolide had interfered with cells morphology and cell adhesion, which were enhanced by longer treatment. With 48 hrs of treatment, the top functions of the altered proteins were determined to be *Cellular Growth and Proliferation*, concordant with our previous proliferation assay. This comparison between short-term and long-term treatment periods demonstrated that triptolide exerts its anticancer activities such as interfering with cell adhesion as early as 6 hrs but with longer treatment, triptolide has strong anti-proliferative and pro-apoptotic functions on colorectal cancer cells.

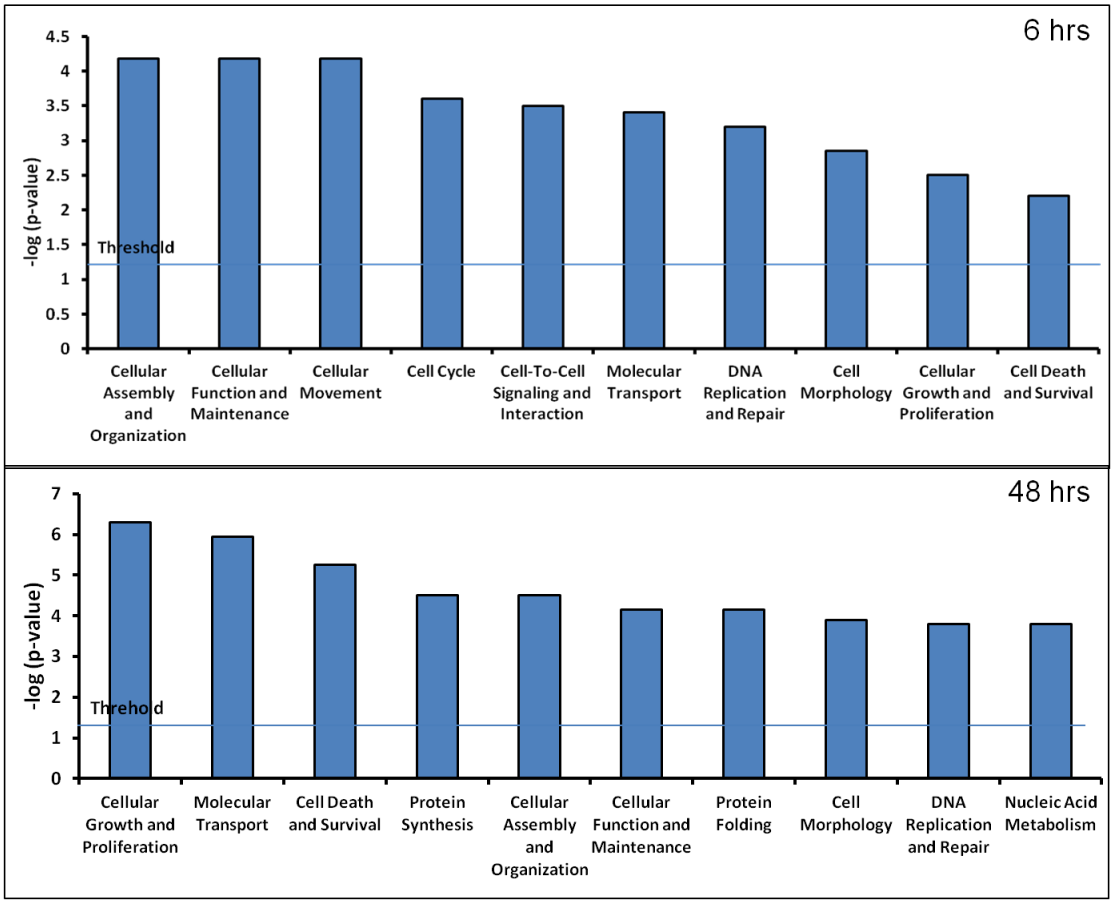

Figure 3.7 Functions of significantly altered proteins by IPA analysis. The list of significantly altered proteins were uploaded into IPA. These proteins were classified based on their functions and networks associated with cancer growth. The top functions of short-term treatment are *Cellular assembly* and top functions of long-term treatment is *Cellular Growth and Proliferation*.

Associated networks including *Cellular Assembly and Organization*, as well as *Metabolic Disease* of proteins with 6 hrs of treatment were illustrated in Figure 3.8A and Figure 3.8B, respectively. The top networks of 48 hrs of treatment, *Cell Death and Survival* and *Cell Morphology* were depicted in Figure 3.8C and Figure 3.8D, respectively. The red nodes in the network represent significantly up-regulated proteins from iTRAQ results and the green ones represent significantly down-regulated proteins.

A

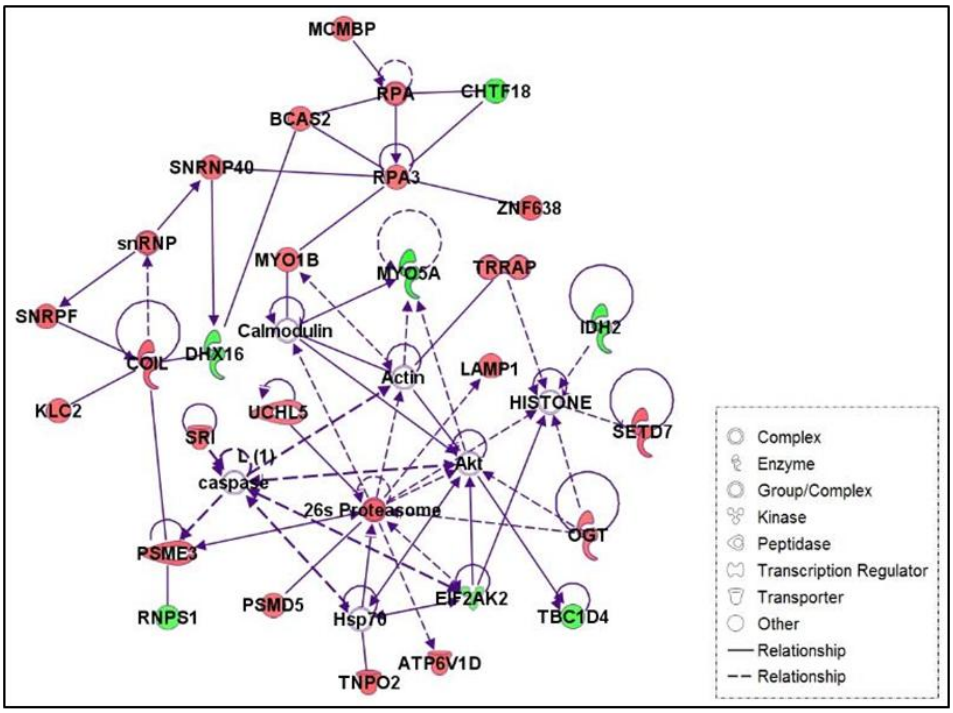
MCMBP
RPA
CHTF18
BCAS2
SNRNP40
RPA3
ZNF638
snRNP
MYO1B
MYO5A
TRRAP
SNRPF
Calmodulin
IDH2
COIL
DHX16
Actin
LAMP1
KLC2
UCHL5
HISTONE
SETD7
SRI
L (1)
Akt
caspase
26s Proteasome
OGT
PSME3
RNPS1
PSMD5
Hsp70
EIF2AK2
TBC1D4
ATP6V1D
TNPO2
Complex
Enzyme
Group/Complex
Kinase
Peptidase
Transcription Regulator
Transporter
Other
Relationship
Relationship

B

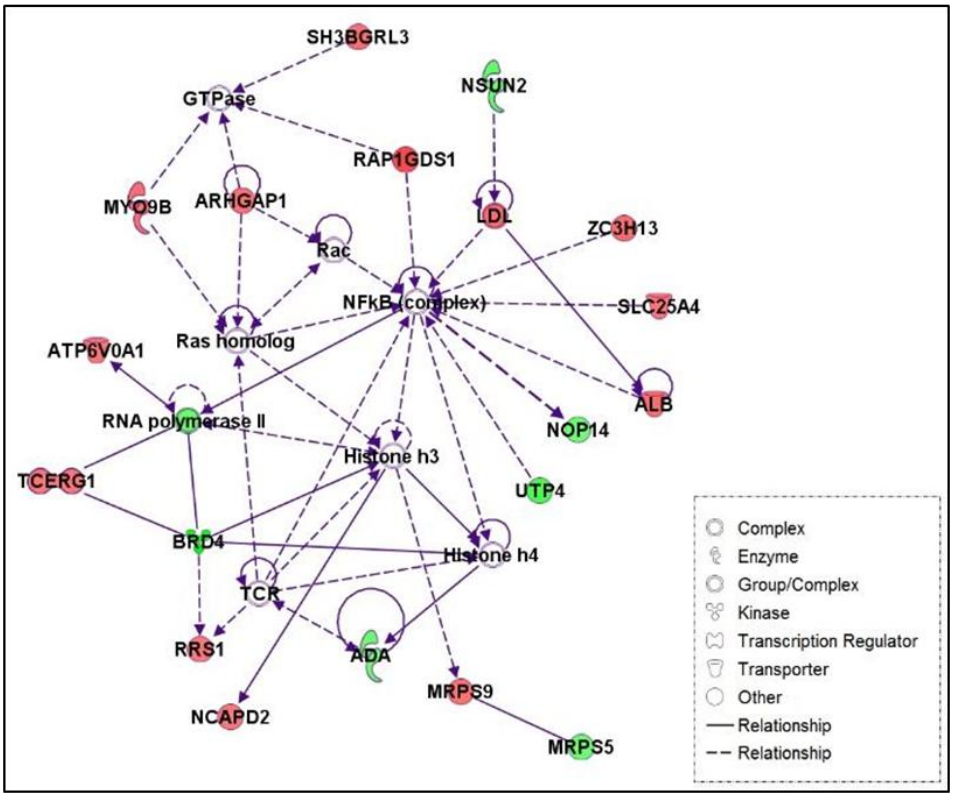
SH3BGRL3
NSUN2
GTPase
RAP1GDS1
MYO9B
ARHGAP1
LDL
ZC3H13
Rac
NFkB (complex)
SLC25A4
ATP6V0A1
Ras homolog
ALB
RNA polymerase II
NOP14
Histone h3
TCERG1
UTP4
BRD4
Histone h4
TCR
RRS1
ADA
MRPS9
NCAPD2
MRPS5
Complex
Enzyme
Group/Complex
Kinase
Transcription Regulator
Transporter
Other
Relationship
Relationship

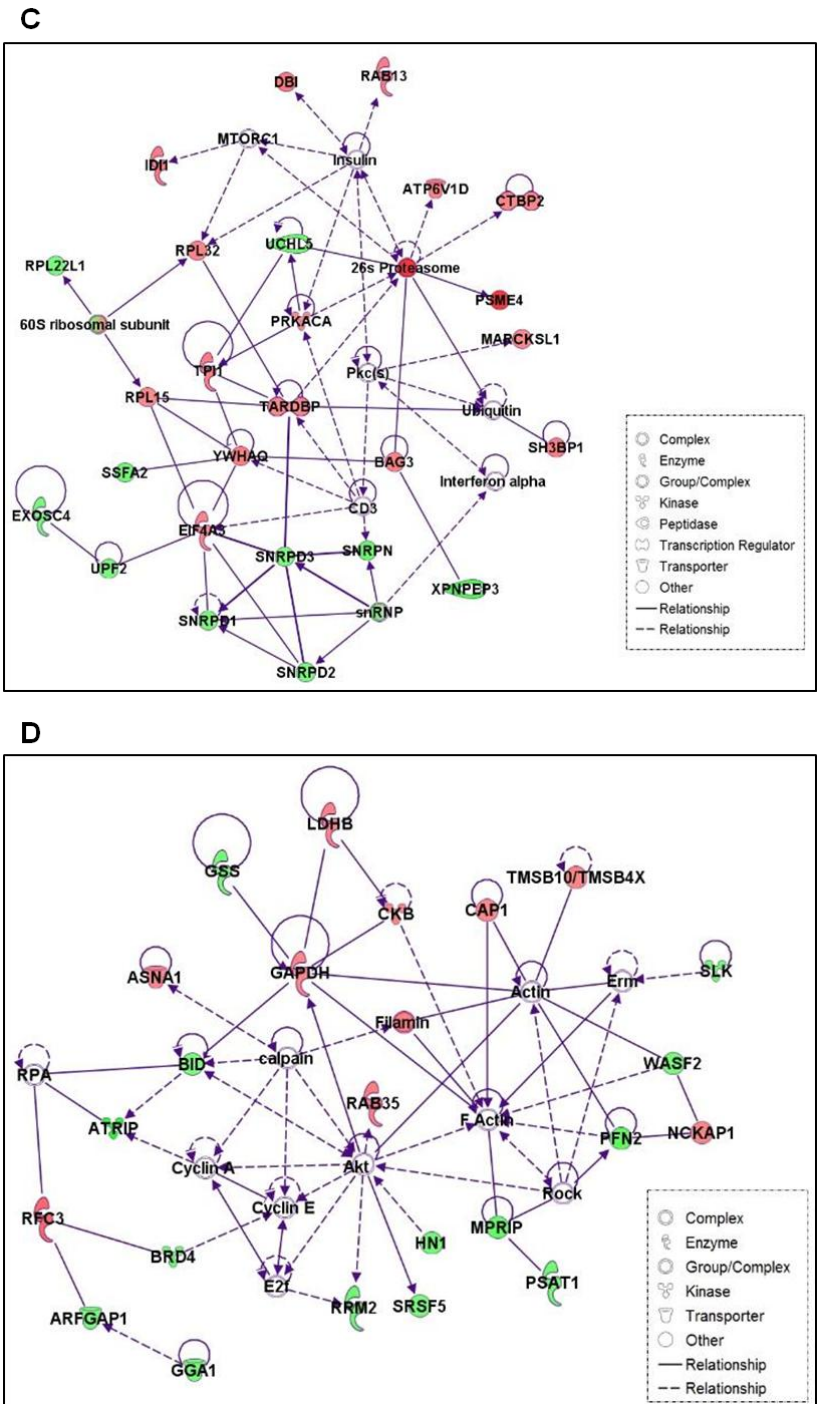

Figure 3.8 Networks of significantly altered proteins using Ingenuity Pathway Analysis (IPA) method. (A, B) In the 6 hrs of treatment, the top networks of *Cellular Assembly and Organization*, as well as *Metabolic Disease* were depicted, respectively. (C, D) In the 48 hrs of treatment, the top networks of *Cell Death and Survival* and *Cell Morphology* were depicted, respectively. The red nodes represent up-regulated proteins and green nodes represent down-regulated proteins based on our iTRAQ results. Lines with arrows represent the downstream signaling and lines alone represent binding and protein-protein interaction.

The top canonical pathway was determined to be *Remodeling of Epithelial Adherens Junctions*. This network might be related to cell adhesion and cell movement. Previous observation has demonstrated that 20% of cells were detached with triptolide treatment, which is in line with our canonical pathway analysis. To examine whether triptolide could also inhibit cell migration, the Wound Healing assay was then carried out. HCT 116 cells were treated with DMSO or triptolide until 100% cell confluency, followed by the creation of wounds with scratching. Cells were photographed at time 0 and 12 hrs. The initial edges of cells were labeled and the new edges of cells after treatment for 12 hrs were marked. The migration distances were measured and compared. As shown in Figure 3.9, the migration distances of cells treated with triptolide were much less than those of control samples. This suggests that triptolide also inhibits cell migration.

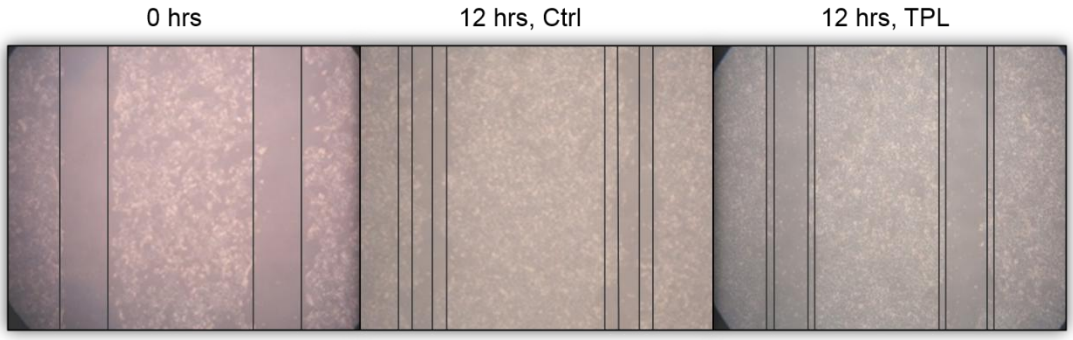

Figure 3.9 Wound Healing Assay. HCT 116 cells were cultured until 100% confluency and wounds were created by scratching. Then the cells were treated with DMSO and triptolide for 12 hrs. The distances of migration were calculated at time 0 and 12 hrs. The migration of HCT 116 cells treated with triptolide was less compared with control.

3.2.5 Validation of significantly altered proteins

3.2.5.1 Bromodomain-containing protein 4 (BRD4)

Bromodomain-containing protein 4 (BRD4) was first described as an unusual chromatin binding factor that remained bound to chromosomes throughout mitosis [125]. It belongs to the Bromo and Extra Terminal (BET) family of nuclear proteins that play important roles in numerous functions including transcription regulation, genome structure, chromatin boundary maintenance as well as cell cycle regulation [126]. In mammals, once bound to the hyperacetylated histones at the promoter, BRD4 recruits Positive Transcription Elongation Factor b (p-TEFb) to the 5'-end of genes to release paused RNA Polymerase II (RNAPII) into productive elongation [127]. BRD4 was also demonstrated to have a kinase activity capable of directly phosphorylating Ser2 of the RNAPII C-terminal domain (CTD), suggesting a direct role in transcription elongation [128].

In addition, RNA polymerase II was also decreased with triptolide treatment in our iTRAQ result, which is in line with a previous study [114]. RNA polymerase II (RNAPII) played important roles for promoter escape and the recruitment of the mRNA processing machinery during transcription. Its inhibition was demonstrated to causes a rapid depletion of short-lived mRNA.

BRD4 was demonstrated to be the upstream regulator of RNAPII. This fundamental role of BRD4 in the transcriptional regulation puts it to the center of numerous biological activities in cells, especially in tumor cells, which require extraordinary levels of transcription. As a matter of fact, BRD4 had been identified as a therapeutic target for acute myeloid leukemia, multiple myeloma and other cancers. [129, 130]

Therefore, our result suggested that triptolide interferes with transcription factors' expression through decreasing BRD4. BRD4 might be one of the potential targets of triptolide to exert its anti-tumor activity. It was selected for further validation by western blot analysis (Figure 3.10).

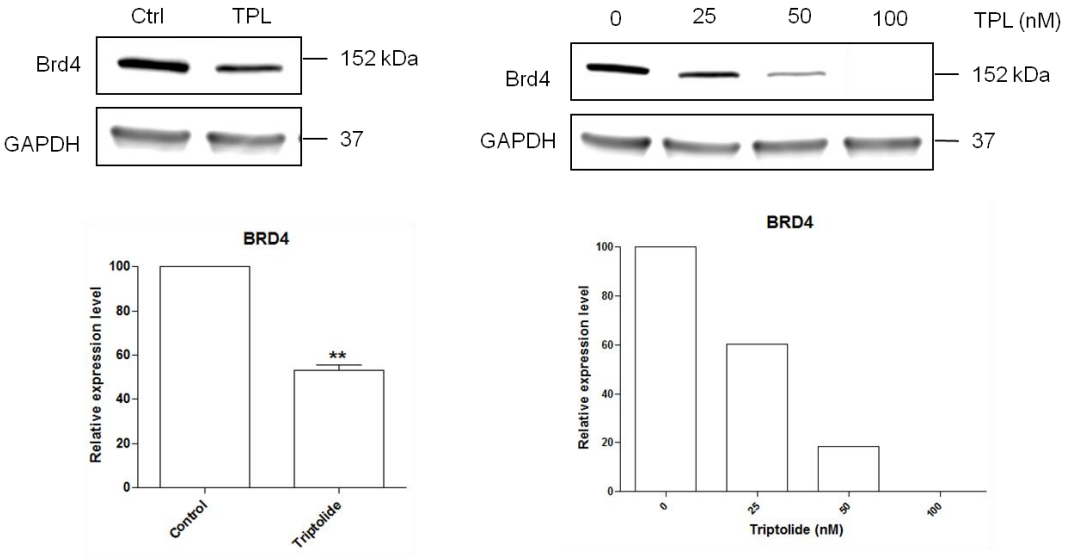

Figure 3.10 Triptolide inhibited expression of BRD4 with 48 hrs of treatment. (A) ITRAQ data was validated by Western blot. With 25 nM triptolide treatment, BRD4 was significantly decreased, which was in conformity with iTRAQ results. (B) HCT 116 cells were treated with DMSO or 25 nM, 50 nM and 100 nM of triptolide for 48 hrs. BRD4 protein was found to be decreased in a concentration-dependent manner.

To further validate the quantitative expression of BRD4 in colorectal cancer cells treated with triptolide or control, immunocytochemistry analysis was carried out. Intracellular levels of protein BRD4 in control and treated HCT 116 cells were shown in Figure 3.11. The level of protein BRD4 was decreased with the concentration of triptolide increased. Under the microscope, the cells treated with triptolide also showed alterations in cell morphologies. Cells were then analyzed by the quantitative analysis based on fluorescence intensity. Experiment was carried out twice to get the same trends of protein level change. This observation was also consistent with our western blot result and iTRAQ result, which indicates that BRD4 could be one of the targets of triptolide for exerting its pharmacological functions.

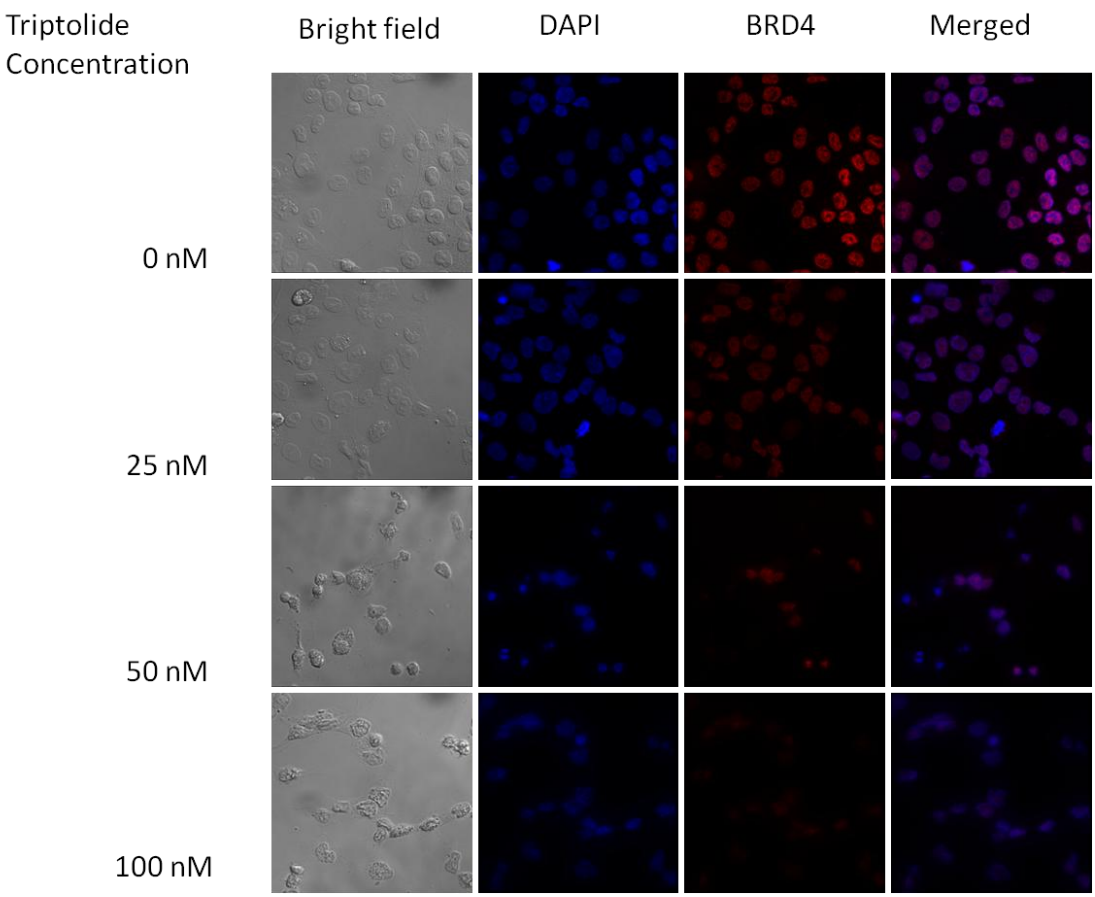

Figure 3.11 Quantitative immunocytochemistry analysis for expression of BRD4 in HCT 116 treated with DMSO or different concentrations of triptolide. Fluorescent image validated down-regulation of BRD4 in HCT 116 cells treated with triptolide for 48 hrs. Red channel represents BRD4 staining and blue channel represents DAPI.

3.2.5.2 β-catenin

β-catenin is known to regulate the coordination of cell-cell adhesion and gene transcription. β-catenin was firstly discovered for its roles in the cell adhesion [131] [132]. Cell-cell adhesion determines the cell morphology and regulates several cellular processes such as motility and survival [133]. Disruption of normal cell-cell adhesion might result in enhanced migration and proliferation, leading to invasion and

metastasis [133].

As a component of Cell-cell adherens junctions (AJs), β-catenin improves cell adhesion by binding to cadherin, and by mediating the interaction of adherens junction molecules with actin cytoskeleton. β-catenin also acts as an intracellular signal transducer in the Wnt signaling pathway, activating the transcription of several genes responsible for cellular proliferation and differentiation. Both roles of β-catenin indicate that it is important in the cell proliferation and survival.

What is more, the functions of β-catenin are deregulated in human malignancies. It was reported that mutations that activate the Wnt-β-catenin pathway enhance the stability of β-catenin and therefore activate gene transcription and alter cell migration [134] [135]. Due to its involvement in cancer development, inhibition of β-catenin receives the researchers' attention. Several works focus on targeting the upstream components of Wnt pathway or ARM domain of β-catenin, therefore influencing the β-catenin level.

In our experiment, β-catenin was shown to be down-regulated by triptolide, especially with 48 hours of treatment, as shown in Figure 3.12. The inhibition of β-catenin by triptolide suggested that triptolide might interfere with the Wnt-β-catenin pathway, inhibiting gene transcription. The down-regulated β-catenin suggested that triptolide might affect the cell migration through decreasing β-catenin.

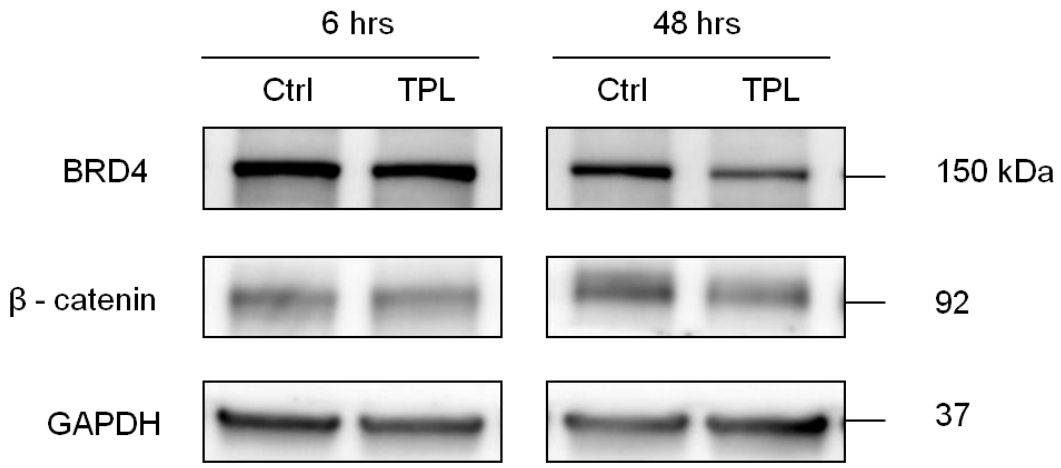

Figure 3.12 Validation of key proteins altered by triptolide treatment using Western blot analysis. Cells were treated with 25 nM of triptolide or DMSO for 6 or 48 hrs. Equal amount of proteins were loaded into SDS gel. Antibodies of BRD4 and β-catenin were utilized in each blot. BRD4 and β-catenin were showed to be significantly regulated with 48 hrs of treatment. GAPDH was used as the loading control.

3.2.6 Proteins specifically regulated by triptolide in cancer cells

As shown in the proliferation assay, viable cells of CCD 841 treated with up to 500 nM of triptolide is still 80 % of total cells. Therefore, the IC_{50} of triptolide towards CCD 841 is much greater than 500 nM. By contrast, the proliferation of HCT 116 cells was greatly affected by the inference of triptolide. With 10 nM triptolide's treatment, the viable cells of HCT 116 went down to 50 % of total cells. This big difference might be because triptolide binds and interferes with highly expressed or specifically expressed proteins in tumor cells. Therefore, to figure out the possible proteins that triptolide specifically targets or inhibits is quite important and might provide insights on the mechanism of triptolide's function against colorectal cancer

cells. In addition, these specific proteins might be the potential therapeutic targets of triptolide when it is applied in the clinical application.

Thus, to study whether triptolide interfere with the key proteins which play important roles in the tumor development, the significantly regulated proteins in the colorectal cancer cell line HCT 116 were then analyzed in normal colorectal cell line CCD 841 compared with HCT 116. As shown in the Figure 3.13, expression levels of BRD4 and β-catenin of CCD 841 cells were not changed, even with triptolide's treatment. These differences demonstrated that triptolide might specifically target and inhibit several key proteins expressed in colorectal cancer cell lines but not normal cells, explaining the different anti-proliferative properties of triptolide on different cell lines.

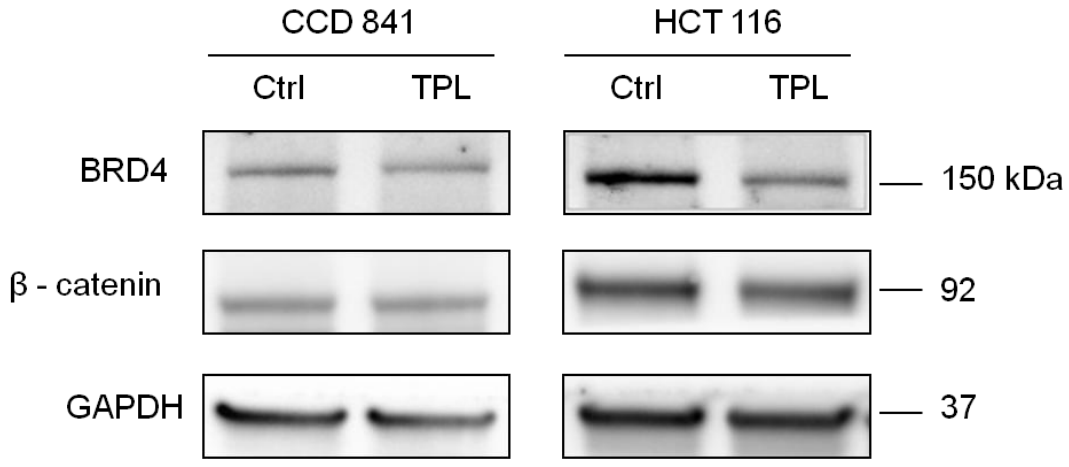

Figure 3.13 Comparison of BRD4 and β-catenin in normal and cancer cell lines CCD 841 and HCT 116. Triptolide was shown to down-regulate BRD4 and β-catenin in HCT 116 but it had no obvious effect on these proteins in CCD 841, which demonstrated that triptolide might specifically target these key proteins in cancer cells.

3.3 Discussion

Colorectal cancer (CRC) is the 2nd most common cancer with the 3rd leading mortality rate in developed countries [136]. Surgery may be the most common treatment for CRC when it has not spread. However, the early stage of colorectal cancer does not have symptoms. Therefore, chemotherapy becomes vitally important for CRC treatment when the cancer has penetrated the bowel wall and spread.

A number of natural compounds exhibit multi-targeted effects and have made a tremendous impact in drug discovery [137] [138]. One of the effective anti-cancer drugs, triptolide, was purified from traditional Chinese medicine herb, *Leigongteng*. Triptolide shows strong anti-proliferative activity, inhibiting the proliferation of all 60 US National Cancer Institute cancer cell lines with half-maximal inhibitory concentration (IC_{50}) values in the low nanomolar range (average IC_{50} = 12 nM).

Triptolide's derivates have entered clinical trials based on its potent anti-tumor effects on prostate cancer and leukemia models [79, 119]. It induces apoptosis in a number of cancer cell lines. So far, triptolide was demonstrated to directly induce apoptosis of human hepatocellular carcinoma, promyelocytic leukemia, cervical adenocarcinoma, pancreatic carcinoma, T cell lymphoma, lung cancer and oral cancer cells [34, 36-38, 120]. Extensive scrutiny of its mechanism of action in the past few decades has yielded important insights. However, the detailed mechanism of triptolide

against cancer cells remains unclear. Therefore, our study provided protein profiling of colorectal cancer cell HCT 116 upon triptolide treatment at a global level, by using proteomics approaches. In our study, triptolide was demonstrated to induce efficient apoptosis and inhibit cell growth of CRC cell line HCT 116. IC_{50} of triptolide on HCT 116 cells was found to be 10 nM with 48 hrs of treatment, which is close to the average level of those 60 cancer cell lines (12 nM). Its effective anti-proliferative activity on colorectal cancer cell also indicated that its derivatives might potentially enter clinic trials against colorectal cancer.

Our study evaluated significant altered proteins in HCT 116 treated with/without triptolide in the global protein landscape using quantitative labeling approach, iTRAQ. The high-throughput quantitative proteomics approach was able to identify significantly altered proteins at a global level. As expected, some significantly regulated proteins in our results, such as RNA Polymerase II and TAB1 were in line with earlier published reports [114, 139], demonstrating the reliability of our proteomics data.

At the molecular level, it is clear that RNA Poly transcription regulators play vital roles in malignant transformation. Previous study has revealed that triptolide exerted anti-tumor effects through inhibiting transcription machinery RNAPII [140][141]. Regulation of transcription by restricting the release of paused RNAPII appears to be the rate limiting step for the regulation of many genes [142]. Upstream regulator of

RNAPII, BRD4 promotes transcription by directly phosphorylating the C Terminal Domain of RNA Polymerase II. In our study, with triptolide's treatment, BRD4 was found to be down-regulated, whose alternation was further validated using Western blot analysis. Its down-regulation could be responsible for the inhibition of RNAPII and subsequent inhibition of transcriptional factors.

On the other hand, triptolide showed no effect on the proliferation of the epithelial colorectal cell line CCD 841, which suggested that triptolide might target some specifically or highly expressed proteins in HCT 116 cells. Then BRD4 and β-catenin levels of normal cell CCD 841 and cancer cell HCT 116 were compared. The levels of these two proteins did not change in the normal cells. As BRD4 has never be reported before, our study provides a novel insight into the mechanisms of action of triptolide.

Chapter 4 Identifying direct binding targets of triptolide using combination of clickable ABPP and iTRAQ

4.1 Introduction

Although studies on triptolide-induced downstream signaling pathways have provided some insights, studies of protein targets are critically important because target-identification and mechanism-of-action studies play vital roles in drug discovery [88]. So far, there were only five proteins identified as binding targets of triptolide. Polycystin-2 (PC2) was firstly identified by Crews' group in 2007 [109]. After that, their group also identified dCTP Pyrophosphatase 1 (dCTPP1) [111]. In the same year, Liu's lab identified XPB, later identified its binding site, Cysteine342 [112, 113]. Yan Lu, *et al.* identified TAB1 as the target of triptolide in macrophages. Recently, Yang's group identified Peroxiredoxin I as the binding target of three natural terpenoids: triptolide, celastrol and withaferin A [143]. However, the methods they utilized have their limitations. Triptolide's targets could not be easily enriched or could not be pulled down with *in vivo* studies However, identification of targets *in vivo* is vitally important. It could reflect the active conditions of the target candidates. Therefore, methods for identification of binding targets will be improved, which allows us to focus on the active proteins in the physiologically relevant environment.

Natural compounds commonly have multiple targets [138]. Numerous proteomic methods have been developed in identification of drug therapeutic targets, screening of enzyme inhibitors, as well as discovery of tumor biomarkers [105, 106]. However, the traditional proteomic approaches only focus on measuring quantitative changes in

protein abundance, which does not necessarily correlate with protein activity [47], neither do they provide functional understanding of native proteins in the physiologically relevant environment [47]. This limitation could be overcome by coupling Activity-Based Protein Profiling (ABPP) which uses probes to covalently bind to catalytic site of target enzymes *in vivo* with proteomic approaches [47, 53]. This chemical proteomics method could be utilized to identify targets of covalent drugs at a global level [46]. Moreover, ABPP combined with bio-orthogonal "click chemistry" is a widely used functional proteomics technology to determine the functional state of enzymes [53, 107, 108].

The core of the activity-based proteomics technology is a small molecule known as activity-based probe (ABP) that interacts with targeted proteins, forming stable covalent bonds. The position of triptolide to be modified cannot be pharmacopoeic, nor close to the binding sites, since disruption of major active sites will impede even abolish interaction with targets. The linker is supposed to be sufficiently flexible to ensure biotin or fluorescent dye cyanine 3 (Cy3) immobilized to streptavidin/avidin beads. Therefore, triptolide probe was designed to contain an alkyne tag in C_{14} coupled with triptolide through a long linker according by our collaborators (Figure 4.1).

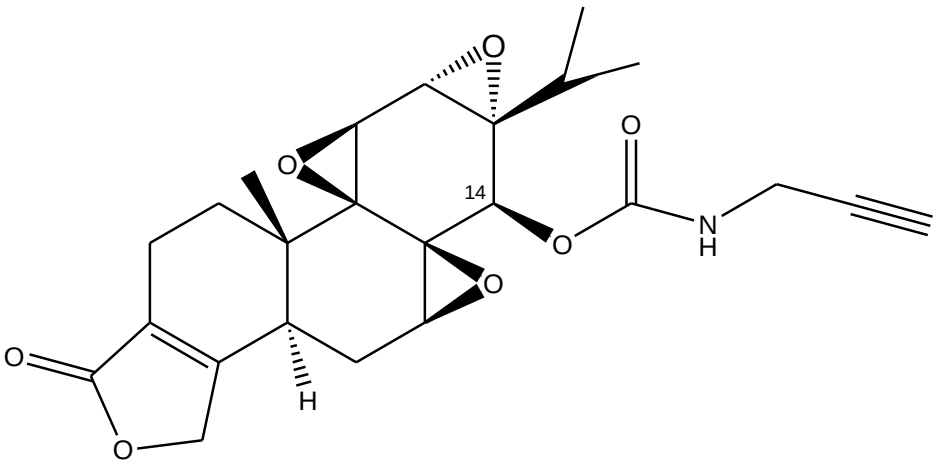

Figure 4.1 Chemical structure of triptolide probe. Triptolide was designed to contain an alkyne in the position of C_{14}, which is not critical for the toxicity of triptolide according to SAR.

However, the results from traditional chemical proteomics method may contain some non-specific protein targets. The non-specific targets can be ruled out by comparison of the protein profiles of probe-treated sample with the control sample. In my study, to discriminate specific protein targets from non-specific and endogenously biotinylated proteins, combination of ABPP and iTRAQ will be applied. The detailed workflow will be described in the result sections.

4.2 Results

4.2.1 Proliferation inhibition activity of triptolide probe

For evaluating the property of triptolide probe, proliferation assay was performed. HCT 116 cells were treated with different concentrations of triptolide probe in 4 replicates. As shown in Figure 4.2, The IC_{50} of triptolide probe was determined to be

2.2 μM, which is greater than the IC_{50} of native triptolide. The difference of IC_{50} of native triptolide and triptolide probe may be due to the introduction of longer moiety, influencing the interaction of probe with its targets. However, previous study that successfully identified the binding target, dCTPP1, utilized a probe with the IC_{50} of 168 μM [111], which is much greater than the IC_{50} of our probe. To explore and validate the binding activity of triptolide probe, the *in situ* proteome profiling assay was then performed.

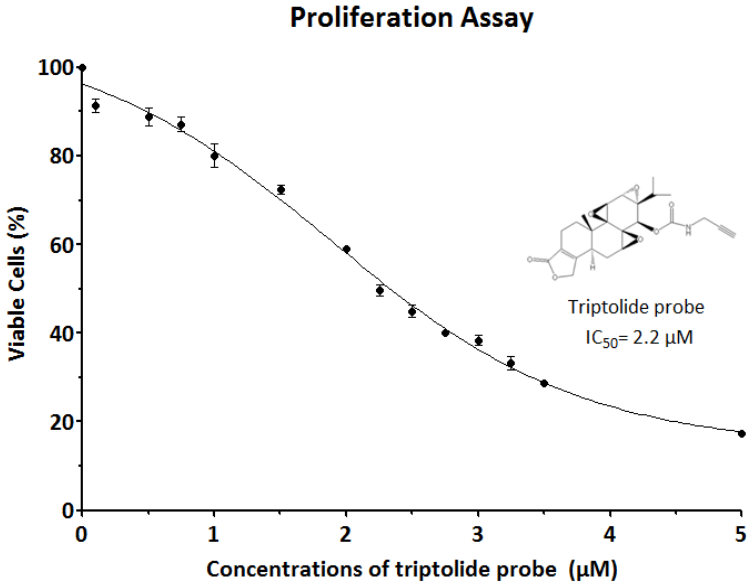

Figure 4.2 Triptolide probe showed inhibitory activity against cell proliferation with 48 hrs of treatment. HCT 116 cells were grown in 96-well plate and treated with increasing concentrations of triptolide probe for 48 hrs. The living cells were then washed by PBS and stained with crystal violet. After incubation for 10 min, crystal violet was completely removed and PBS containing SDS was added to dissolve it. As a result, IC_{50} of triptolide probe was determined to be 2.2 μM.

4.2.2 *In situ* proteome profiling of triptolide targets

For visualizing the cellular targets of triptolide, *in situ* proteome fluorescence labeling was performed. The probe-labeled proteomes of HCT 116 cells were applied to click chemistry and then visualized by fluorescence scanning. As shown in Figure 4.3, the fluorescence signals were enhanced with the concentration of triptolide probe increased. All samples were equally loaded, as verified by Coomassie blue staining (Figure 4.3). Therefore, the enhanced fluorescence signal bands represent the native cellular targets of triptolide. This data also demonstrated that our probe was suitable for the activity-based protein profiling approach, and it could be utilized for further experiments.

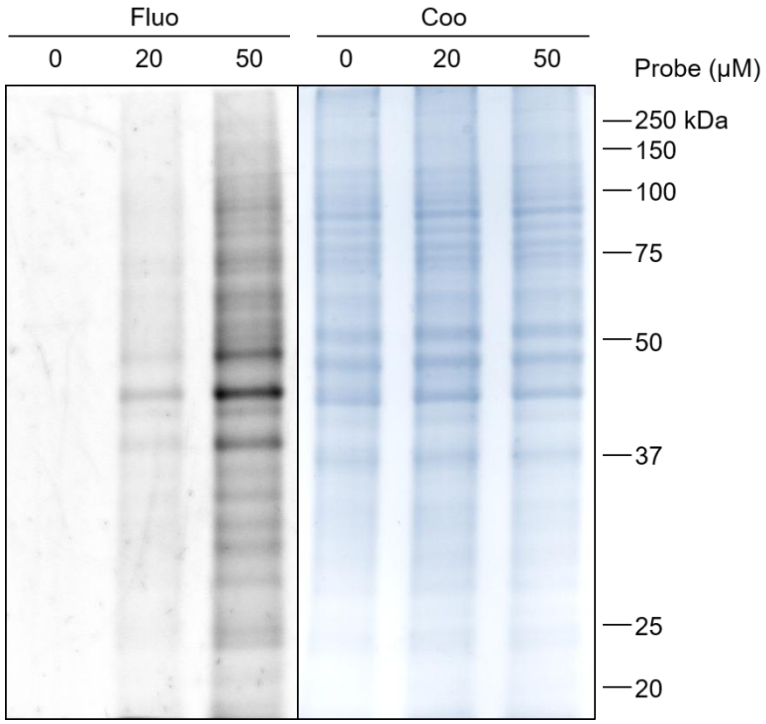

Figure 4.3 *In situ* proteome labeling of HCT 116 cells using triptolide probe. HCT 116 cells were treated with increasing concentrations of triptolide probe for 12 hrs. Click chemistry reagents were incubated with samples at 37 ℃ for 4 hrs. The clicked

proteins were loaded into SDS-PAGE and their fluorescence signals were visualized by fluorescence scanning. The same SDS gel was then stained by Coomassie blue after fluorescence scanning. The intensity of triptolide targets was enhanced with the concentration of triptolide probe increased, using 12% SDS-PAGE gel.

4.2.3 Pull down and iTRAQ labeling

The targets of triptolide were enriched by pull down approach. However, the non-specific binding proteins or endogenously biotinylated proteins may also be pulled down by this approach. To deal with this problem, iTRAQ could be introduced for ruling out non-specific targets by comparing the protein profile of probe-treated samples with that of the control sample. The workflow of the cell-based proteome profiling approach followed by iTRAQ labeling and LC-MS/MS for identification of potential cellular targets of triptolide was depicted in Figure 4.4.

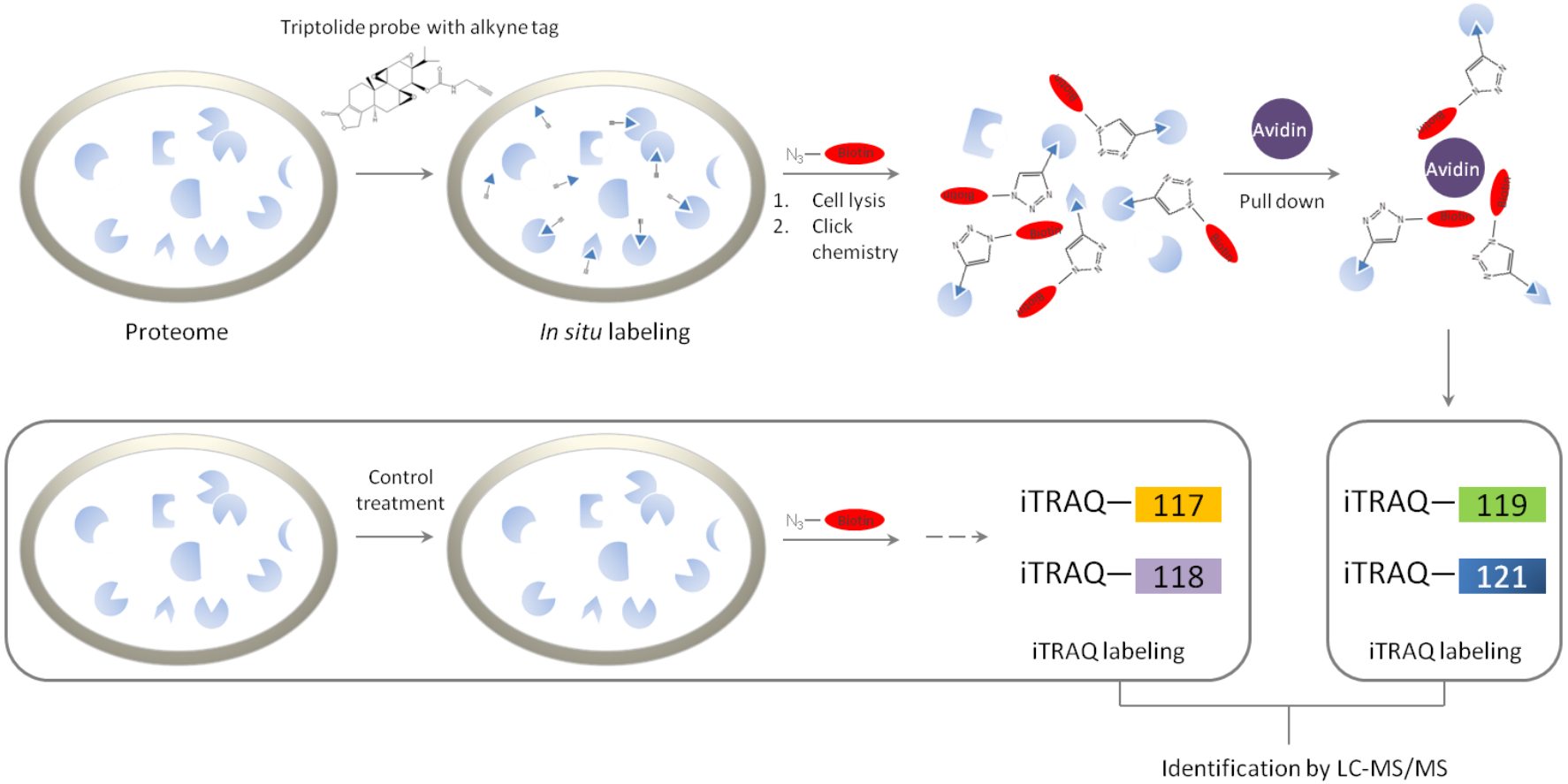

Figure 4.4 The workflow of identification of triptolide targets by combination of ABPP and iTRAQ approaches. HCT 116 cells treated with triptolide probe were subjected to click chemistry and pull down approaches. Proteins from cell treated with DMSO were also pulled down by beads. Then the control samples were labeled with iTRAQ 117 and 118, in two biological replicates. Samples treated with probe were labeled iTRAQ 119 and 121, in two biological replicates. After mixing, the labeled peptides were applied to LC-MS/MS sequencing for identification.

Thus, a total of 1585 proteins were successfully identified. The comparison between four sets of protein lists (119:117, 121:117, 119:118, and 121:118) was evaluated. Then proteins with a ratio more than 1.3 or less than 0.77 of two replicates (either 118:117 or 121:119 more than 1.3 or less than 0.77) were removed. To get the targets with high confidence, a highly strict ratio of 2.25 was chosen as the cut-off value for discriminating the specific from non-specific binding targets. As a result, 237 proteins were identified as reliable target candidates of triptolide.

4.2.4 GO analysis

The list of binding targets of triptolide was analyzed *via* Gene Ontology (GO) studies. It classified these proteins as per their molecular function and cellular component (Figure 4.5). In the cellular component analysis, the detailed distribution of cellular location indicated targets ubiquitously presented in the whole cell, with the cytoplasm (23%) having the largest population. In the molecular function analysis, most targets exerted binding (51%) and catalytic activity (30%).

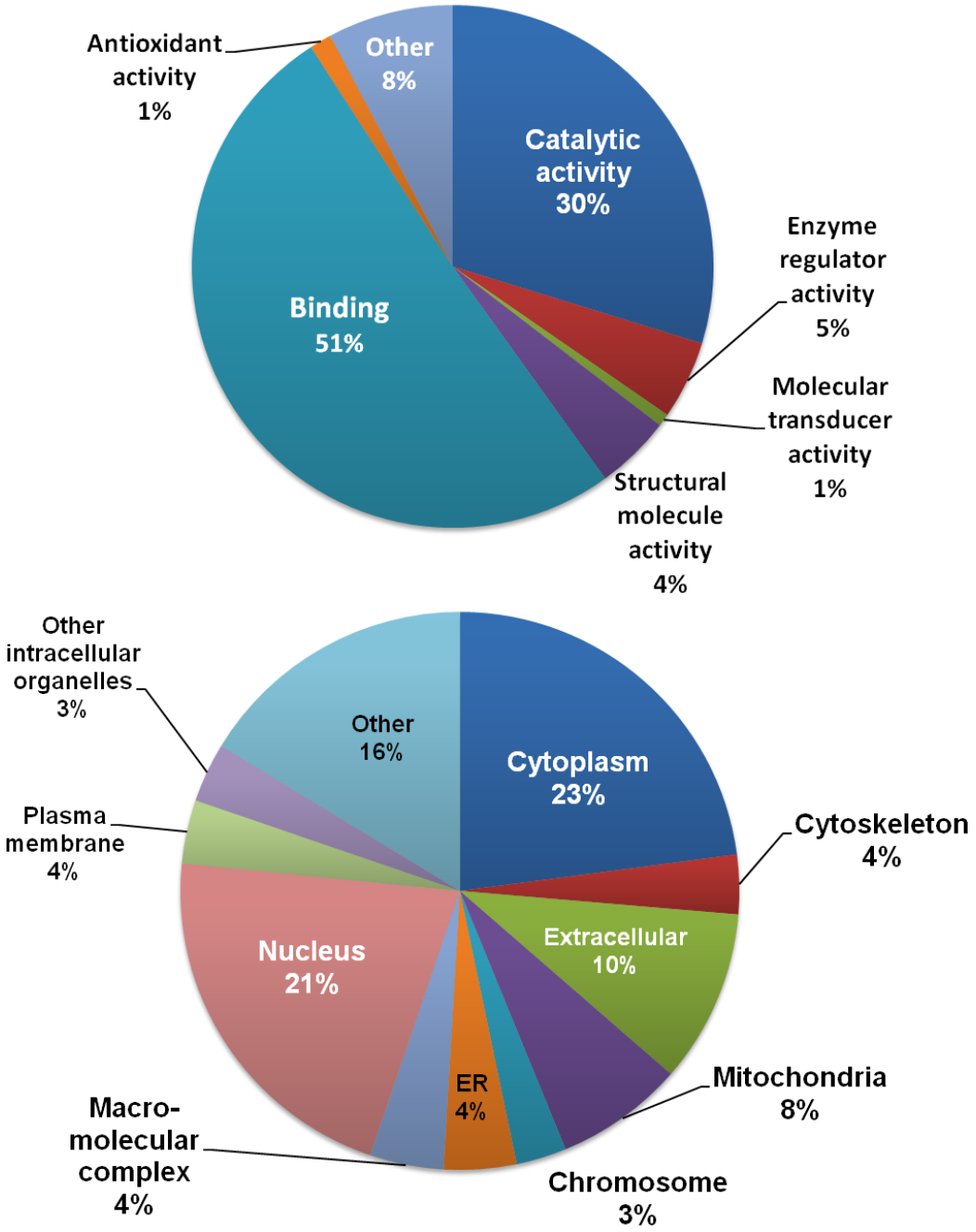

Figure 4.5 Molecular function (Upper) and cellular localization (Bottom) of binding targets of triptolide. The list of triptolide's targets were classified by GO analysis based on molecular function and cellular component. The majority of targets were mainly in the cytoplasm and nucleus; most of targets exert catalytic activity and binding activity.

4.2.5 Cellular immunofluorescence image

To examine the cellular distribution of triptolide targets, fluorescence cell images were obtained. HCT 116 cells were treated with 1% DMSO or 100 μM of triptolide probe for 12 hrs. Cellular binding targets of triptolide were incubated with click chemistry reagents with fluorophore and then detected by fluorescence scanning and photographed under 100-times microscope. As shown in Figure 4.6, there were no fluorescence signals in control sample but obvious signals in cells with triptolide probe's treatment. The fluorescence signals represent the targets of triptolide, suggesting that targets were ubiquitously distributed within the cells, which is in line with our GO analysis.

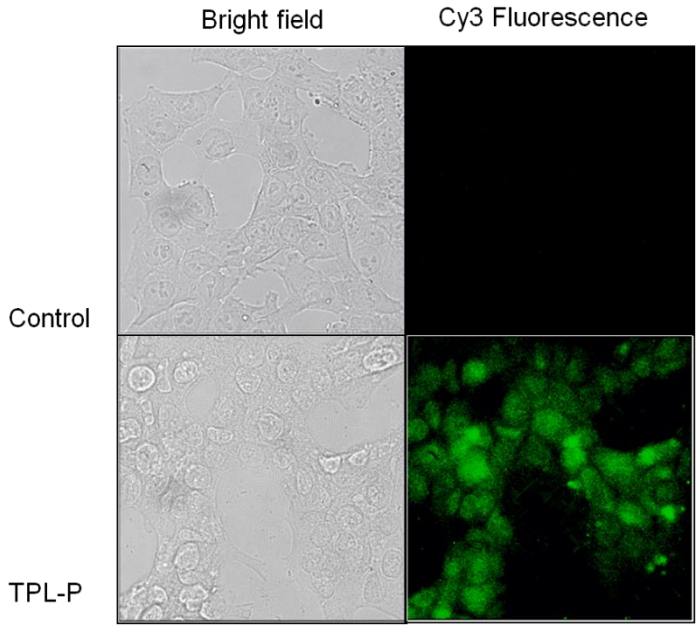

Figure 4.6 Quantitative cellular immunofluorescence images of triptolide targets. HCT 116 cells were treated with DMSO or 100 μM of triptolide probe for 12 hrs. Cells were washed, fixed and permeabilized. Triptolide cellular binding targets were labeled with click chemistry reagents with fluorophore and visualized by fluorescence scanning. The green fluorescence signals represented the binding targets of triptolide.

4.2.6 Network analysis by IPA

The list of triptolide's binding targets was then uploaded into IPA for network analysis. The functions and canonical pathways of these targets were summarized in Figure 4.7. The top functions of these proteins were determined to be *Cell Death and Survival*, followed by *Protein Synthesis* and *Cellular Growth and Proliferation*. These data demonstrated that the majority of triptolide's targets play important roles in the cell death and proliferation process, which is consistent with our previous findings. In addition, triptolide's targets were also shown to interfere with the protein synthesis.

The canonical pathways of triptolide's binding targets also demonstrated the importance of targets on the protein synthesis (Protein Ubiquitination Pathway, EIF2 Signaling and Regulation of eIF4 and p70S6K Signaling).

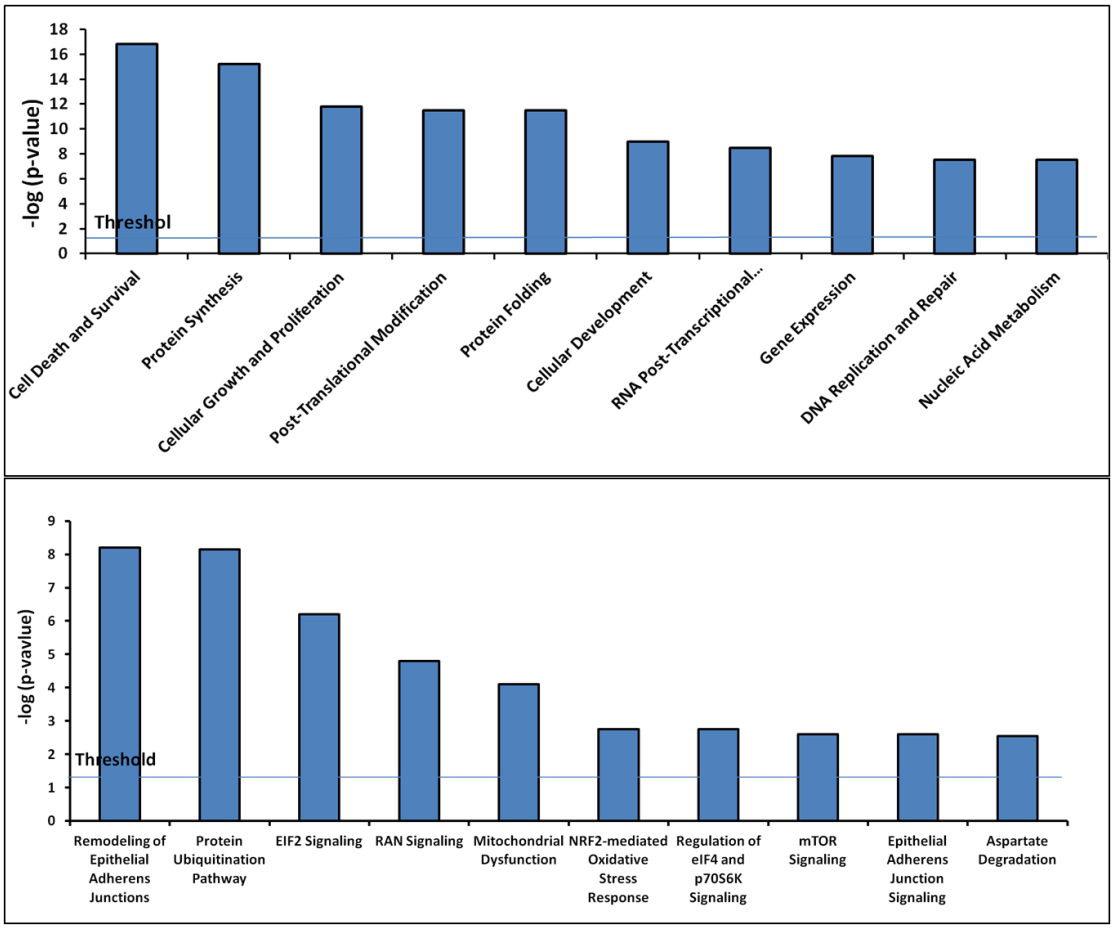

Figure 4.7 Functions (Upper) and canonical pathways (Bottom) analysis of triptolide's binding targets. The list of triptolide's binding targets was analyzed using IPA. The functions and canonical pathways were listed in the horizontal bar chart format.

Therefore, the rate of protein synthesis was measure based on L-azidohomoalanine (AHA) labeling method. The method was fully described in the previous study [144]. In the IPA network analysis, proteins synthesis ranked high and it plays critical roles in the development of cancers. The inhibitory activity of triptolide on protein synthesis was shown in Figure 4.8.

AHA is a surrogate for methionine. Therefore, it could be incorporated into

proteins during protein synthesis process. In addition, AHA contains an azide moiety so that click reaction could be applied to. Therefore, protein degradation and protein synthesis could be evaluated using fluorescence labeling. As shown in Figure 4.8, the fluorescence signals were significantly decreased with triptolide's treatment, which indicated that triptolide inhibited protein synthesis. This finding is consistent with our network analysis.

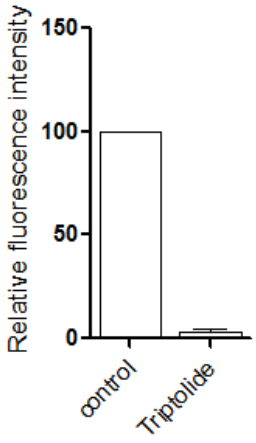

Figure 4.8 Triptolide was shown to interfere with protein synthesis. HCT 116 cells were labeled with 50 μM AHA with or without triptolide for 12 hrs. Then the cells were harvested for click reaction. The fluorescence intensity was analyzed by flow cytometry.

The top networks constituted with the identified targets were then depicted in Figure 4.9. It described the first and the second top networks, *Cell Death and Survival* and *Gene Expression and Protein Synthesis*, respectively. The green nodes in the network represent the target candidates of triptolide.

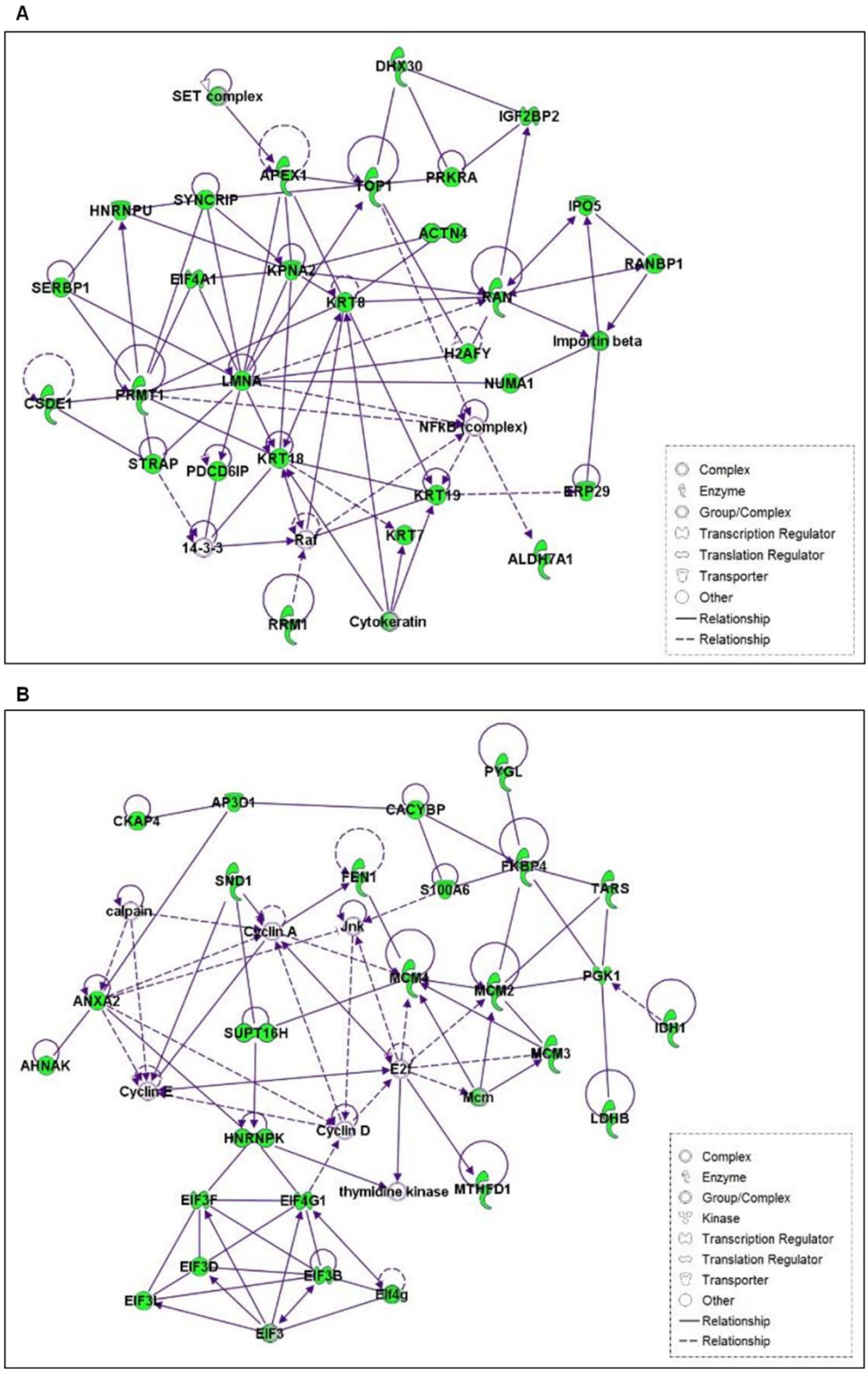

Figure 4.9 The top networks of binding targets were analyzed by Ingenuity Pathway Analysis (IPA). The list of binding targets of triptolide was uploaded into IPA for analysis. The networks "*Cell Death and Survival*" (A) and "*Gene Expression and Protein Synthesis*" (B) constituted with triptolide's binding targets were depicted.

4.2.7 Identification of binding targets *via* in-gel digestion and MS/MS

To narrow down the target list as well as to further validate our ABPP results, the pulled down proteins were loaded into SDS gel and visualized by silver staining (Figure 4.10A). By comparing the protein bands of treatment samples with control, five distinct bands were excised, in-gel digested and identified by MS/MS. The corresponding fluorescence bands, which represented the binding targets were labeled in Figure 4.10B and listed in Figure 4.10C. They were identified based on unused scores and molecular weight. Among these binding targets, Peroxiredoxin I and Annexin A1 attracted our attention because they were obviously absent in the control sample but found to be present in the treatment sample. In addition, they had relatively high unused scores and high percentage of coverage. Therefore, these proteins were chosen for the further validation.

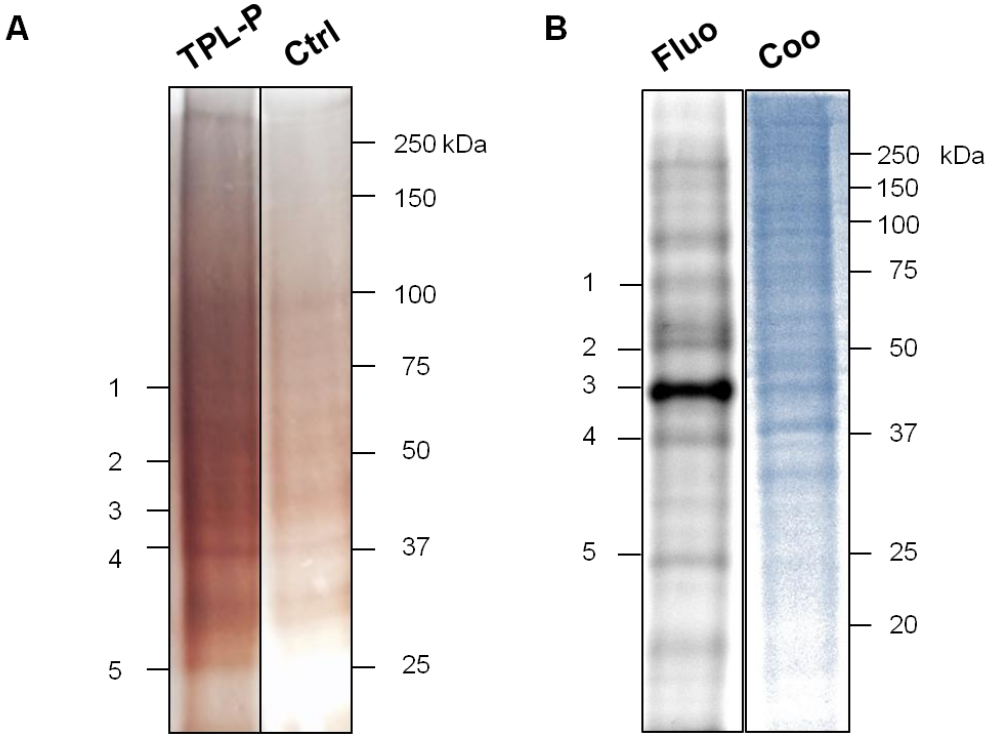

C

	ID	MW (kDa)	Unused score	% Cov
1	Asparagine synthetase	61	35.08	54
2	α-enolase	48	18.79	38.7
3	Actin	42	14.38	29.9
4	Annexin A1	35	23.97	45.1
5	Peroxiredoxin I	24	15.64	54.8

Figure 4.10 Identification of target bands by MS/MS. (A) The enriched proteins from HCT 116 cells with control and triptolide probe's treatment were loaded into SDS-PAGE gel and visualized by silver staining. By comparing the protein bands from probe-treated cells with control sample, five protein bands with significantly difference were excised and digested. The corresponding targets were labeled in the fluorescence labeling gel shown in (B). Subsequently, the protein bands were identified by MS/MS and listed in (C). (Fluo: Fluorescence, Coo: Coomassie blue)

4.2.8 Validation and functional analysis of triptolide's target – PRDX I

Peroxiredoxins (PRDXs) are a ubiquitous family of peroxidases that use a

conserved cysteine to reduce peroxide subtracts such as hydrogen peroxide [63, 80]. In mammals, PRDXs are thiol-dependent antioxidant proteins and therefore responsible for neutralizing reactive oxygen species (ROS) [145]. Based on the position or absence of peroxidatic cysteine (C_P), the mammalian PRDXs are divided into three subfamilies: typical 2-cys (PRDXs I-IV), atypical 2-cys (PRDX V) and 1-cys PRDX (PRDX VI). Typical 2-cys PRDXs contain an active site C_P that serves as the site of oxidation by peroxides to cysteine sulfenic acid (Cys-SOH). A resolving cysteine (C_R) of the other subunit then reacts with the C_P sulfonic acid to form a disulfide (head to tail), further reduced by Thioredoxin (Trx) [146, 147]. Much ongoing work is elucidating the important roles of PRDXs in antioxidant protection and cellular signaling pathways [148]. These studies demonstrated the potential of 2-cysteine PRDXs as therapeutic targets for major human diseases such as cancers and cardiovascular diseases [57-59, 145, 149, 150]. Recently, another diterpenoid isolated from the leaves of *Isodonadenanthus*, adenanthin, was shown to induce differentiation of leukemic cells by directly targeting PRDX I and PRDX II [147, 151].

4.2.8.1 Expression and purification of recombinant PRDX I

Human *PRDX I* gene was subcloned into pET28a vector. The specific primers used for amplifying *PRDX I* are:

Forward primer:	5’-CATGAATTCATGTCTTCAGGAAATGCT-3’

Reverse primer:	5’-TCACTCGAGTCACTTCTGCTTGGAGAA-3’

Therefore, the construct of 6×His-tagged fusion protein was generated. DNA sequence of construct of PRDX I was confirmed with 100% identities. Next, the construct was transformed into *E.coli* strain *BL21* for protein expression and purification. The protein was finally eluted and about 10 μl of the protein elution was then loaded into SDS gel for validation and quantitation.

4.2.8.2 Validation of triptolide-PRDX I binding using fluorescence labeling

After the protein PRDX I was expressed and purified, the binding activity of PRDX I with triptolide was analyzed. The purified PRDX I was incubated with triptolide probe and the complex was then incubated with click chemistry reagents with fluorophore. The binding of triptolide-PRDX I was validated by fluorescence labeling. Figure 4.11 showed that the purified PRDX I has the property of binding to triptolide and the specificity of binding activity will be further verified by competition assay.

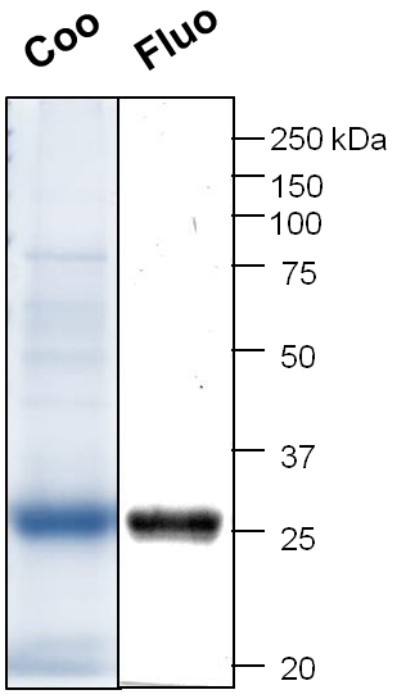

Figure 4.11 Validation of triptolide-PRDX I binding activity using fluorescence labeling. Equal amount of recombinant PRDX I was incubated with triptolide probe, followed by incubation with click chemistry reagents with fluorophore. Then the protein bands were visualized by fluorescence labeling. Coomassie blue staining shows the sample loading. (Fluo: Fluorescence, Coo: Coomassie blue)

4.2.8.3 Competition assay

As described above, PRDX I was found to be a potential cellular binding target of triptolide. To further validate this result, competition assay was carried out. Recombinant PRDX I was incubated with increasing concentrations of triptolide probe or pre-incubated with excess triptolide (10×triptolide). After click chemistry reaction, fluorescence signals were shown in Figure 4.12. The fluorescence signals with triptolide probe treatment verified that triptolide probe bound to PRDX I. With the concentration of triptolide probe increased, the fluorescence intensity was

enhanced. On the other hand, competition assay by pre-incubation of PRDX I with 10-fold of triptolide showed significantly diminished fluorescence signal, indicating that native triptolide might have occupied binding sites of PRDX I in the pre-treatment. This also confirmed that the binding between PRDX I and triptolide was specific, demonstrating the suitability of this probe in our study.

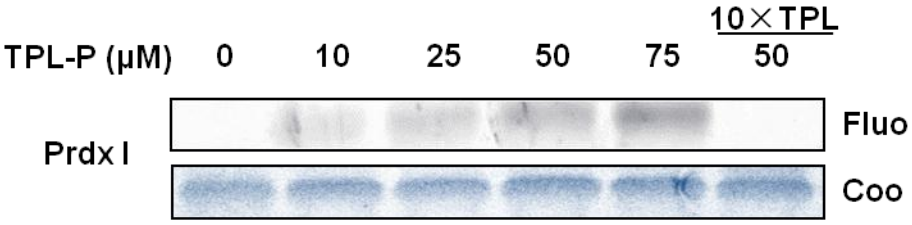

Figure 4.12 Validation of triptolide's target PRDX I by competition assay. PRDX I protein was incubated with increasing concentrations of triptolide probe or pre-incubated with 10 times concentration of triptolide (10 × triptolide). Click chemistry reaction was then performed and the fluorescence labeling was visualized by fluorescence scanning. PRDX I was concentration-dependently labeled by triptolide probe, while the 10-fold excess triptolide's pre-treatment reduced the fluorescence signals. Equal amount of protein loading was confirmed by Coomassie blue staining. (Fluo: Fluorescence, Coo: Coomassie blue)

4.2.8.4 Identification of binding sites

The triptolide-PRDX I complex was further validated and the exact binding sites of PRDX I were explored by using Mascot searching and MS/MS. PRDX I was incubated with DMSO or triptolide. The complex was then digested and analyzed by MS/MS. The mass spectra were converted into MGF for analysis. The modified residue mass difference 360.2 amu was used as the parameter for modification

searching. The spectra of peptide ^{169}HGEVCPAGWKPGSDTIKPDVQK^{190} of PRDX I incubated with DMSO or triptolide were depicted in Figure 4.13. The *b* and *y*-ions of this spectrum were analyzed. An *m/z* difference of 360.16 was detected in *b*-ion and *y*-ion of triptolide-PRDX I complex. There was a mass shift of around 360 Da, which corresponds to the molecular weight of triptolide, in *b5* ion and afterwards. These spectra indicated that peptide ^{169}HGEVCPAGWKPGSDTIKPDVQK^{190} was modified by triptolide by binding Cysteine 173 of PRDX I.

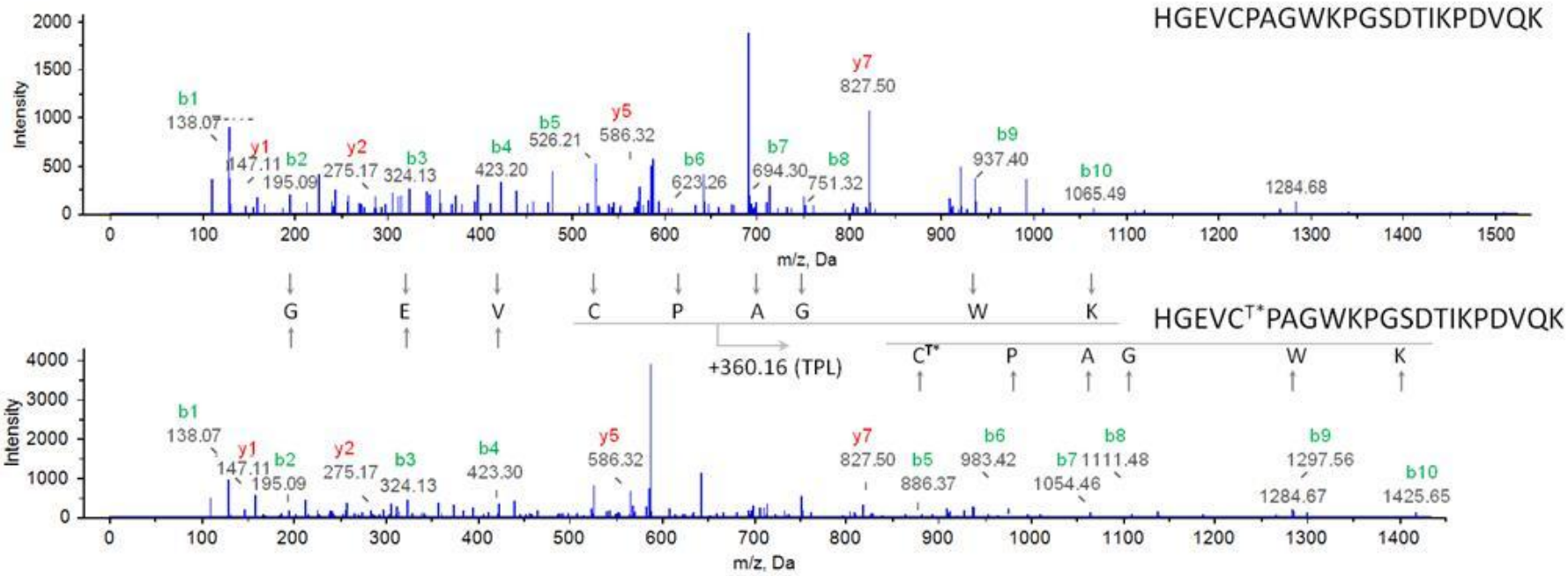

Figure 4.13 Identification of binding sites of protein PRDX I by MS/MS. PRDX I was incubated with DMSO (Upper) or triptolide (Bottom) for 2 hrs. The complex was digested and subjected to MS/MS sequencing for analysis. Molecular weight of triptolide was used as the parameter for modification search. The *b*- and *y*-ion analysis detected peaks with a mass difference of 360.16 Da compared to control. C^{T*} represented the triptolide-modified cysteine.

4.2.8.5 Molecular modeling

To further explore the triptolide-PRDX I binding model, the dimeric PRDX II (PDB: 1QMV) was used for Autodock simulation (Figure 4.14). The reason for choosing PRDX II is because PRDX I and PRDX II have 78% identities of sequence. In addition, all of PDB format of PRDX I have mutations in cysteines, which might not be suitable for our model. Triptolide was manually docked into the dimerization pocket and the conformation was optimized with lowest energy. In the modeled triptolide-PRDX II complex, triptolide has the Michael acceptor at C_4 forming a C-S bond with Cys172 (chain A) of PRDX II and the C_{14} hydroxyl group pointing toward the outside of the pocket. This result indicated that triptolide might render the enzyme inactive due to the disruption of both the Cys173-Cys52 disulfide bond and the dimeric conformation of the enzyme.

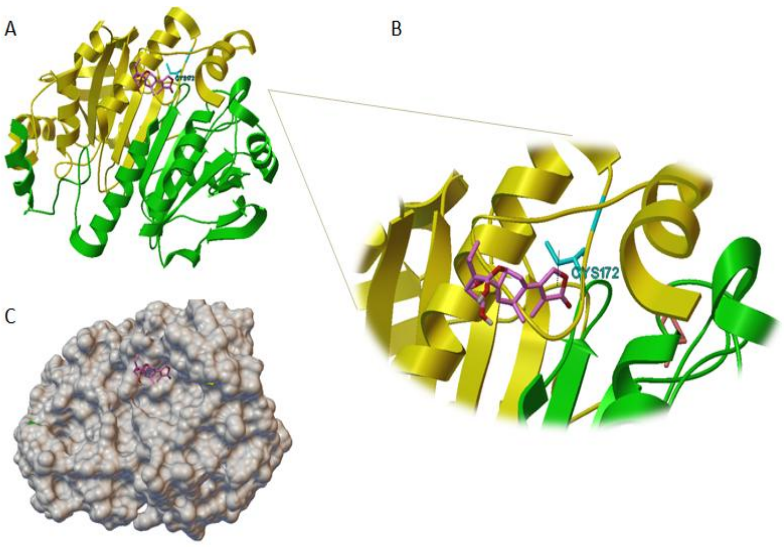

Figure 4.14 Docking simulation of triptolide-PRDX II complex. The PRDX II (PDB: 1QMV) dimer structure consists of two identical chains (yellow and green). The ligand triptolide (purple) was manually docked into PRDX II protein. This modeled triptolide-PRDX II complex contained the Michael acceptor at C_4 to form a C-S bond with Cys172 of PRDX II, as shown in the form of (A, B) Ribbon diagram and (C) Molecular surface diagram.

4.2.8.6 Inactivation of PRDX I induced by triptolide

To study whether triptolide exerted its function *via* inhibition of peroxidase activity of PRDX I, the peroxidase activity of recombinant PRDX I was measured. PRDX I was incubated with increasing concentrations of triptolide. It was then reacted with H_2O_2 substrate and fluorescent peroxidase substrate. The fluorescence intensities of PRDX I-triptolide complex was measured every 2 min (after 30 min, change to 5 min) until 60 min, which were shown in Figure 4.15A. Fluorescence intensity represented the amount of H_2O_2 reduced by PRDX I, proportional to their peroxidase activity. The amount of reduced H_2O_2 was determined according to the standard curve. Therefore, the peroxidase activities of PRDX I-DMSO, PRDX I-100 μM triptolide, PRDX I-500 μM triptolide and PRDX I-1 mM triptolide were determined to be 1.13, 1.02, 1.00 and 0.56 mU/L, respectively. This assay demonstrated that triptolide reduced the peroxidase activity of PRDX I significantly.

As PRDX I plays critical roles in ROS, the ROS level was evaluated and shown in Figure 4.15B. HCT 116 cells were treated with DMSO or triptolide, followed by

incubation with CM-H2DCFDA, a general oxidative stress indicator. The fluorescence intensity analyzed by flow cytometry suggested an increase in the ROS level in cells with triptolide treatment. This data demonstrated that triptolide increased the ROS in HCT 116 through decreasing the activity of PRDX I.

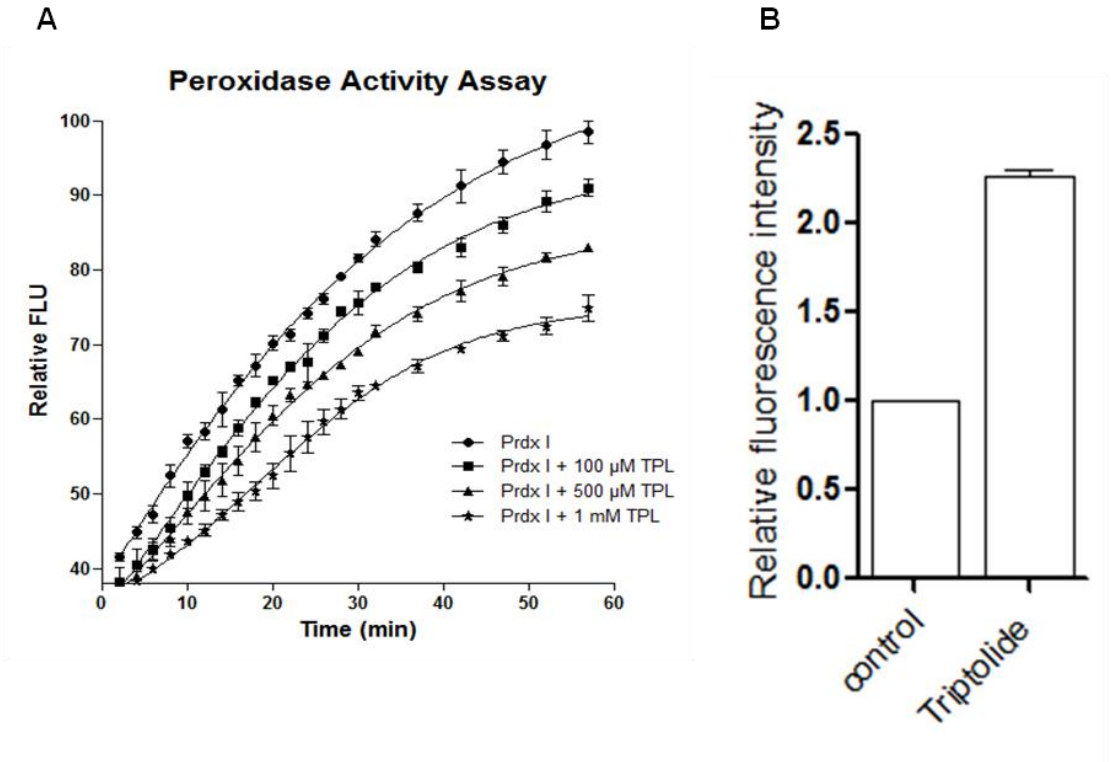

Figure 4.15 Peroxidase activity assay indicated the inhibitory activity of triptolide against peroxidase activity of PRDX I. (A) PRDX I was incubated with DMSO or increasing concentrations of triptolide. Fluorescence intensity which represented the amount of H_2O_2 reduced by PRDX I was measured every 2 min and then changed to 5 min after 30 min until 60 min. Peroxidase activities of peroxiredoxin I were reduced with the concentrations of triptolide increased. (B) ROS levels of control and treated cells were evaluated. HCT 116 cells were treated with DMSO or 100 nM of triptolide for 12 hrs, followed by incubation with CM-H2DCFDA. The fluorescence intensity was analyzed by flow cytometry.

4.2.9 Validation and functional analysis of triptolide target – Annexin A1

Annexins are a family of Ca^{2+}-regulated phospholipid-dependent proteins [152].

They are composed of a conserved core, which contains four repeats (six repeats in Annexin 6) of 70-80 amino acids folded into five α-helices [153] [154]. Annexins regulate the actin cytoskeleton, which plays important roles in cell morphology and cell migration [154] [155]. One of the subfamilies, Annexin A1 (ANXA1), shows tumor type-specific patterns of expression [156]. Specifically in colorectal cancer, ANXA1 was shown to promote progression, invasion and metastasis of colorectal cancer through activating the *N*-formyl peptide receptors (FPR) [157] [158] [159]. It was shown to be involved in different cell processes such as cell survival, proliferation, differentiation and migration [160] [161]. ANXA1 was also found to be over-expressed in primary tumors compared to normal colon [162]. As a result, Annexin A1 was regarded as a putative tumor biomarker and potential therapeutic target in colorectal cancers [162] [156].

Human Annexin A1 full-length protein (ab92966) from Abcam was incubated with excess triptolide using the same method described above. The triptolide-Annexin A1 complex was then digested and the modification was analyzed by MS/MS and Mascot searching. As a result, Cys270 and Cys324 of Annexin A1 were shown to be modified by triptolide, with the unused score 44 and 72, respectively (Figure 4.16).

4.2.9.1 Identification of binding sites of ANXA1 by MS/MS

The triptolide-Annexin A1 complex was further validated and the binding sites of

Annexin A1 was analyzed using MS/MS. Similar to the study of binding sites of PRDX I, Annexin A1 was incubated with DMSO or triptolide. After digestion, the mass spectra were converted to MGF for analysis. As shown in Figure 4.16, the spectra showed that the peptide ^{318}MYGISLCQAILDETK^{332} of Annexin A1 was modified with triptolide. An *m/z* difference of 360.16 was detected in *b*-ion and *y*-ion of triptolide-Annexin A1 complex that contains Cysteine 324. This shift with the mass difference ˜360 Da is consistent with the molecular weight of native triptolide, indicating that triptolide binds to the Cysteine 324 of Annexin A1.

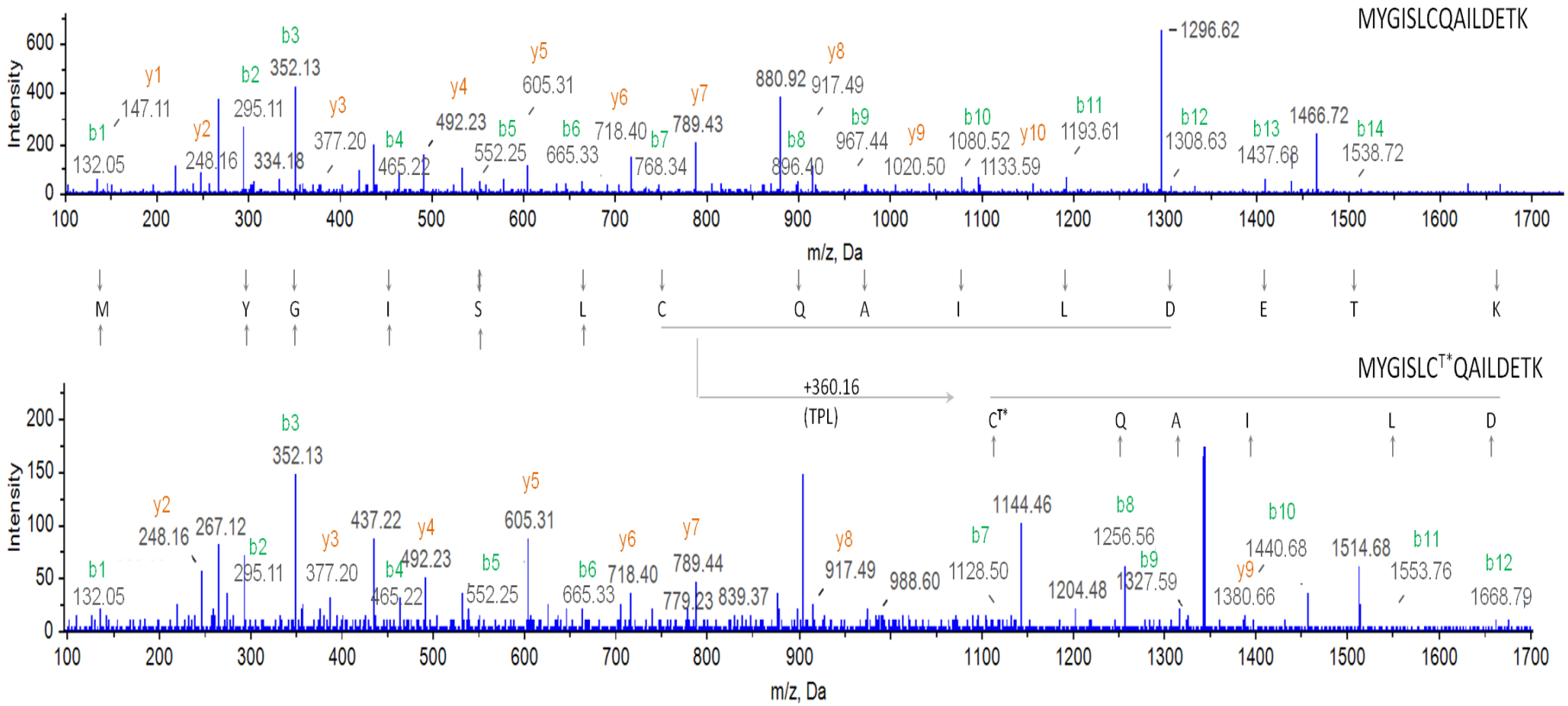

Figure 4.16 Identification of binding sites of ANXA1 with triptolide, using MS/MS analysis. Annexin A1 was incubated with DMSO (Upper) and triptolide (Bottom). After digestion, the peptides spectra were then converted to MGF for analysis. By analyzing the *b*- and *y*-ions of the spectra, a shift of 360.16 Da has be found between the triptolide-incubated and DMSO-incubated samples, which corresponds to the molecular weight of the native triptolide.

4.2.9.2 Docking simulation model of ANXA1-triptolide complex

To simulate the interaction between Annexin A1 and triptolide, the docking simulation was then carried out. Full-length Annexin A1 (PDB: 1MCX, Annexin A1 in the presence of calcium) was chosen to be input into the AutoDockTools for autodock simulation. The reason to select this structure is that other structures (like 1HM6) do not represent a typical core fold, neither to be full-length [152]. 1AIN was also considered. However, only the molecular surface diagram of 1AIN could be obtained, which cannot provide the detailed binding sites of protein-ligand compound. The structural alignment of protein Annexin A1 (PDB IDs: IMCX and 1AIN) was performed using PyMOL software. The result obtained showed that the RMS (Root Mean Square) Deviation is 0.475 between the two proteins which means that the proteins have very high structural similarity (Higher structural similarity is denoted by lower RMS values i.e., 100% structural similarity = 0.0 RMS value). In addition, 1MCX has the 89% sequence similarity with native Annexin A1. Due to above reasons, 1MCX was chosen for docking.

As shown in Figure 4.17, triptolide was manually docked into the pocket of Annexin A1. The conformation was optimized with lowest energy. C_4 of triptolide and Cys270 of Annexin A1 formed a C-S bond, leading to the bond breakage in the 5-membered unsaturated lactone ring.

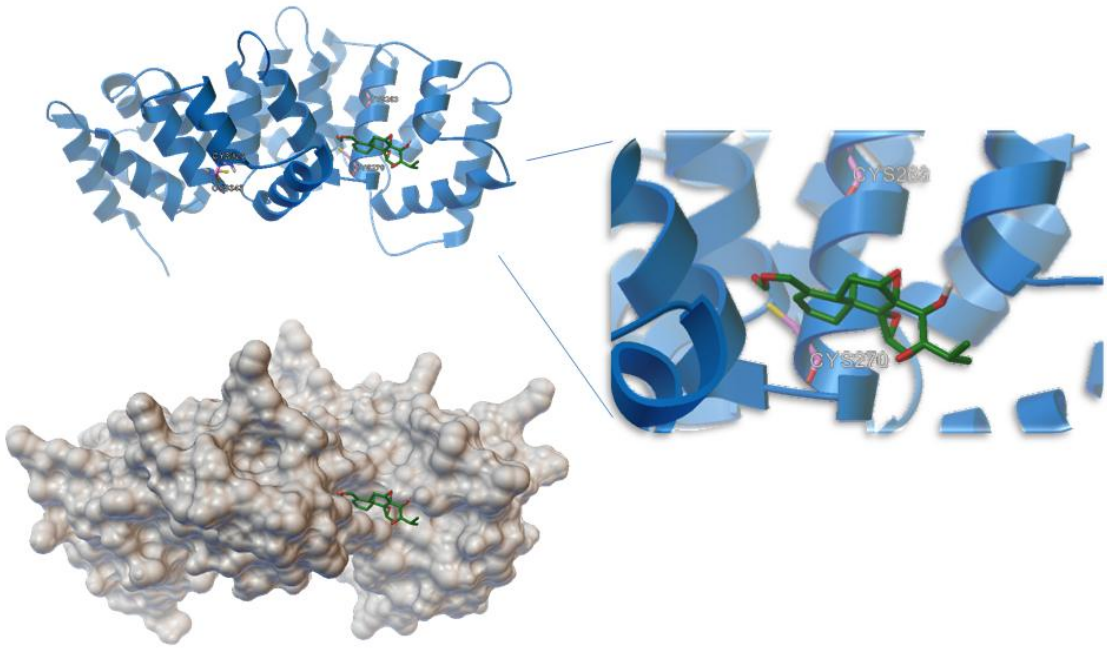

Figure 4.17 Docking simulation of triptolide-ANXA1 complex. Full-length Annexin A1 (PDB: 1MCX) was input into the AutoDockTools software. The ligand triptolide (green) was manually docked into Annexin A1 (blue). This complex was illustrated in the form of Ribbon diagram (Left upper and bottom) and Molecular surface diagram format (Right).

4.3 Discussion

As drugs exert pharmacological functions by binding their targets and inhibiting their activities, a comprehensive identification of the specific targets of a drug is important for unraveling its mechanisms and functions. Hydrolytic and proteolytic enzymes have been demonstrated to be up-regulated in many tumor cells [47]. As enzymes regulated essential cellular processes, they have become vital therapeutic targets for many human diseases [107]. However, it is difficult to investigate the functional roles of enzymes in cancer progression by traditional proteomics because

these technologies do not provide functional understanding of native proteins in the physiologically relevant environment *in vivo* [47]. Moreover, protein abundance does not truly reflect activity because most enzymes are expressed as inactive zymogens or reside in complex with their endogenous inhibitors [47].

So far, there are only five proteins identified as the direct binding targets of triptolide, indicating that there may be more binding targets with low abundance. However, all of their methods found the targets of triptolide *in vitro*, which might not truly reflect the active proteins *in vivo*.

Generally, chemical proteomics method have been developed to reveal drug-target interaction [116]. The commonly used methods involve global proteomics approach, affinity chromatography approach and activity-based protein profiling method. With global proteomics method, cells are treated with small molecules followed by system-wide proteome analysis [163]. However, although it maintains the native drug unmodified and the result is unbiased, the lack of enrichment limit its wide application. Another classic method to identify the drug-target interaction is the drug affinity chromatography method. The noncritical sites of the drug will be attached to affinity tag and then incubated with proteome [164][165]. However, strict washing required for removing nonspecific target identification decreases the likelihood of identifying weakly bound proteins.

To circumvent these limitations, a chemical proteomic method ABPP could be utilized to unravel the global target spectrum for covalent drugs [46]. Activity-based protein profiling (ABPP) combined with bio-orthogonal click chemistry is a novel functional proteomics technology to directly determine the functional state of enzymes both *in vitro* and *in vivo* [46, 47, 53, 108]. ABPP can only detect the functionally active form of target enzymes because most of the regulatory mechanisms for enzyme activity change the protein's active site. However, the results from this method may contain non-specific protein targets. The non-specific targets can be ruled out by comparison the protein profiles of probe-treated sample with the control. In our study, to discriminate specific protein targets from non-specific and endogenously biotinylated proteins, combination of ABPP and iTRAQ was introduced. The peptides labeled with different isobaric tags were pooled and fractionated by Liquid Chromatography (LC) and analyzed by tandem mass spectrometry (MS/MS), to be identified as a single MS peak (identical *m/z*). The quantification of the peptide abundance can be calculated from the relative areas of the reporter peaks.

In our study, triptolide probe was first designed to contain an alkyne and then subjected to ABPP. The triptolide-target complexes were visualized by fluorescence or enriched by pull down approach, followed by iTRAQ-LC-MS/MS identification.

For designing probe to contain an alkyne without changing the property of native triptolide, the activity sites of triptolide are explored according to structure-activity relationships (SAR). Due to triptolide's poor water solubility, medicinal chemists have synthesized several triptolide analogues for improving its properties for potential therapeutic uses. These modifications may occur on the C-14-hydroxyl group, epoxide groups, the lactone ring or the C5, 6-position. Many studies unravel functions of different sites of triptolide. Epoxy groups play different roles in determining biological activities. For example, modification of C-12,13-epoxide group and C-7,8-β-epoxide significantly affect triptolide's activity [78], while the C-9,11-β-epoxide group could be recognized as a potential modification site [166]. The investigations on the α, β-unsaturated-5-membered-lactone ring suggested that the D-ring with a five-membered unsaturated lactone or lactam ring is essential for its anti-cancer activity and the C18 carbonyl group may exert important roles on the interaction between triptolide and its targets [167]. However, the studies on C-14-hydroxyl group complex are complicated. Previous studies on the SAR of triptolide indicated that hydrogen-bonded C-14 of triptolide may account for its anti-tumor effect [168-171]. However, recent studies showed that substituting the C-14-hydroxyl group with fluoride or with a chiral epoxy group containing α oxygen configuration at the C-14 position retains the cytotoxicity of triptolide [171]. In addition, omtriptolide (PG-490-88Na, F60008) which was modified on C-14-hydroxyl

group has entered clinical trials for acute leukemia and advanced solid tumors due to its high water solubility [78]. These studies demonstrated that the modification of C14 did not change the main property of triptolide and improved water solubility. Therefore, in our study, the C-14-hydroxyl group was determined to be the modification site for probe to contain an alkyne. The triptolide probe reacted as the activity-based probe (ABP) that covalently binds to the catalytic site of specific target enzymes *in vivo*.

Next, for evaluating the property of triptolide probe, proliferation assay as well as fluorescence labeling were performed. The IC_{50} of triptolide probe was determined to be 2.2 μM, which is greater than the IC_{50} of native triptolide. However, previous study which successfully identified dCTPP1 as the binding targets of triptolide [111] utilized a probe with the IC_{50} of 168 μM. The proteome profiling assay also demonstrates that our triptolide probe is capable to profile the binding targets and it works well in click chemistry reaction. With the azide-modified cyanine 3 (Cy3) or azide-modified biotin, the binding targets of triptolide can be visualized or enriched, respectively.

With iTRAQ comparison of probe-enriched binding targets to the control, 237 proteins were identified as potential binding targets of triptolide. With GO and IPA

analysis, the cellular components, molecular functions and networks were visualized. Most of the targets were located in cytoplasm and nucleus. The distribution of triptolide binding targets was also detected with cellular immunofluorescence image, which further illustrates that the triptolide binding targets locate ubiquitously in different parts of the cell. ABPs covalently bind to active enzymes, thus permitting assignment of imaging signals to specific enzymes [47, 110]. As expected, the molecular function analysis showed that most of the targets have binding and catalytic activity, which is probably due to the nature of ABPP approaches. Identification of these enzymes also demonstrate that ABPP approach can provide us with a functional understanding of proteins in the complex process of tumorigenesis. The IPA analysis ranked the top network constituted by the enriched binding targets as "*Cell Death and Survival*", which is consistent with the anti-tumor property of native triptolide.

Among these 237 binding targets, dCTPP1 was also found in the list of enriched proteins, which is consistent with previous study [111]. Another two direct binding targets were found in our pull-down list but with cutoff less than our stringent cutoff value, 2.25. The stringent cutoff criterions aid to narrow down target candidates for the further validation study.

To narrow down the targets of interest as well as to further confirm our target list,

the enriched proteins from probe-treatment or control were visualized by silver staining after running SDS-PAGE gel. By comparing the intensity and abundance of bands, five bands were cut down followed by in-gel digestion and LC-MS/MS. These five bands were identified to be Asparagine synthetase, α-enolase, Actin, Annexin A1 and Peroxiredoxin I. These five proteins are also found in the list of 237 binding targets, further confirming the results of our proteomic approaches. Among them, Peroxiredoxin I and Annexin A1 were found to be obviously present in probe-treated sample but disappeared in control with high score and coverage. These proteins thus drew our attention and further validation experiments were conducted.

Peroxiredoxin I is a 22 kDa protein that belongs to peroxiredoxin family including six mammalian isoforms. All members in this family are conserved peroxidases due to the conserved peroxidase cysteine (C_P) and known for their antioxidant properties. The typical 2-cys PRDXs (PRDX I-IV) contain an additional conserved cysteine residue like Cys173 of PRDX I and Cys172 of PRDX II, which is also called resolving cysteine (C_R). Typical 2-cys PRDXs exert catalytic functions through oxidizing the C_P -SH to C_P-SOH, which reacts with C_R of the other subunit, forming a transient intermolecular disulfide. For example, Cys51 of PRDX II, the active site of peroxide reduction, is first oxidized to cysteine sulphinic acid by hydrogen peroxide and reacts with Cys172 (resolving cysteine), the second catalytic

cysteine residue [55].

To determine the specific residues of PRDX I that are modified by triptolide, the recombinant PRDX I protein was incubated with or without triptolide, followed by MS/MS. Peptides containing cysteine were evaluated because triptolide probably interacts as a Michael acceptor due to the α, β-unsaturated-5-membered-lactone ring. The molecular formula was used for modification searching. MS/MS analysis of both unmodified and modified peptide^{169}HGEVCPAGWKPGSDTIKPDVQK^{190} of PRDX I gave a partial series of *b*-ion fragments corresponding to the predicted sequence. Both MS/MS spectrums had the same mass from *b1* to *b4*, whereas the mass shifted 360.16 Da for modified fragment (from *b5* to *b22*). This result indicates that triptolide binds to the Cys173 of PRDX I. The *y*-ion fragments can also reveal the shift, which reflects triptolide modification. Cys173 of PRDX I is located near the C terminus at a disordered coil region that inserts into the pocket of another PRDX I monomer which contains Cys52 to form a dimmer [55, 172]. As the existing crystal structures of PRDX I are all mutants, the dimer structure of native PRDX II (PDB code: 1QMV) was used for a computation study. Triptolide molecule was manually docked into the dimerization pocket. This molecular modeling may provide some insights on the triptolide-PRDX I interaction at the atomic level. Therefore, triptolide modification may probably render the enzyme inactive due to the disruption of both the

Cys172-Cys51 disulfide bond and the dimeric conformation of the enzyme.

To test triptolide's inhibitory activity against PRDX I, the peroxidase activity of PRDX I incubated with or without triptolide was estimated. The peroxidase activity of PRDX I was decreased with the concentration of triptolide increased. Especially, when PRDX I was incubated with 1 mM of triptolide, the peroxidase activity was decreased around 50%. PRDXs are the third most abundant protein found in the erythrocyte [173] and ubiquitous in cells. PRDXs were shown to be upregulated in several human cancers [145, 149] and were proposed as potential targets for anticancer drugs. Many studies shows that PRDXs induce cell proliferation [58] and protect cancer cells from apoptosis [174, 175]. The mechanism for PRDX function may be due to its antioxidant property. High reactive oxygen species (ROS) level, which was demonstrated to increase in our experiment, can damage DNA and induce tumorigenesis [176, 177]. Therefore, the inhibitory activity of triptolide against PRDXs may have a significant impact in cancer treatment.

As the binding target PRDX I was reported last year, which is earlier than our proposed report, another protein, Annexin A1 also attracted our attention. Annexin A1's upregulation was involved in tumor invasion and lymph node metastasis of colorectal cancer. Its high expression level indicates that it might contribute to early

metastasis of colorectal cancer [178]. Therefore, Annexin A1 is a potential biomarker for predicting colorectal cancer malignant potential. In addition, according to the previous work, Annexin A1 was significantly down-regulated in HCT 116-transplanted nude mice treated with indomethacin (a kind of nonsteroidal anti-inflammatory drug) by the proteomics method [179], solidifying the importance of Annexin A1 as the potential drug target for colorectal cancers.

Similar to the study of PRDX I-triptolide complex, MS/MS analysis followed by Mascot modification searching as well as docking simulation of Annexin A1-triptolide complex were performed. In our study, Annexin A1 was found to bind to and interact with triptolide. Cys270 and Cys324 were identified as the binding sites of Annexin A1. Our study also demonstrated that triptolide might interfere with cell migration through inhibiting the activity of Annexin A1.

Therefore, our study profiled the targets of triptolide at a global level, which would shed some lights on the detailed mechanism of its biological activities. The regulated proteins could also serve as candidate targets for the therapeutic action of triptolide. Furthermore, construction of important protein networks might offer fruitful information for future research on colorectal cancer treatment. Profiling the targets of triptolide and exploring the signaling pathways are mutual promotional to

unravel its mechanism of action. Revealing the direct targets of triptolide will aid to design derivatives that might be less toxic with fewer side effects, but have similar inhibition effects with the native drug.

Chapter 5 Conclusion and Future Work

5.1 Discussion

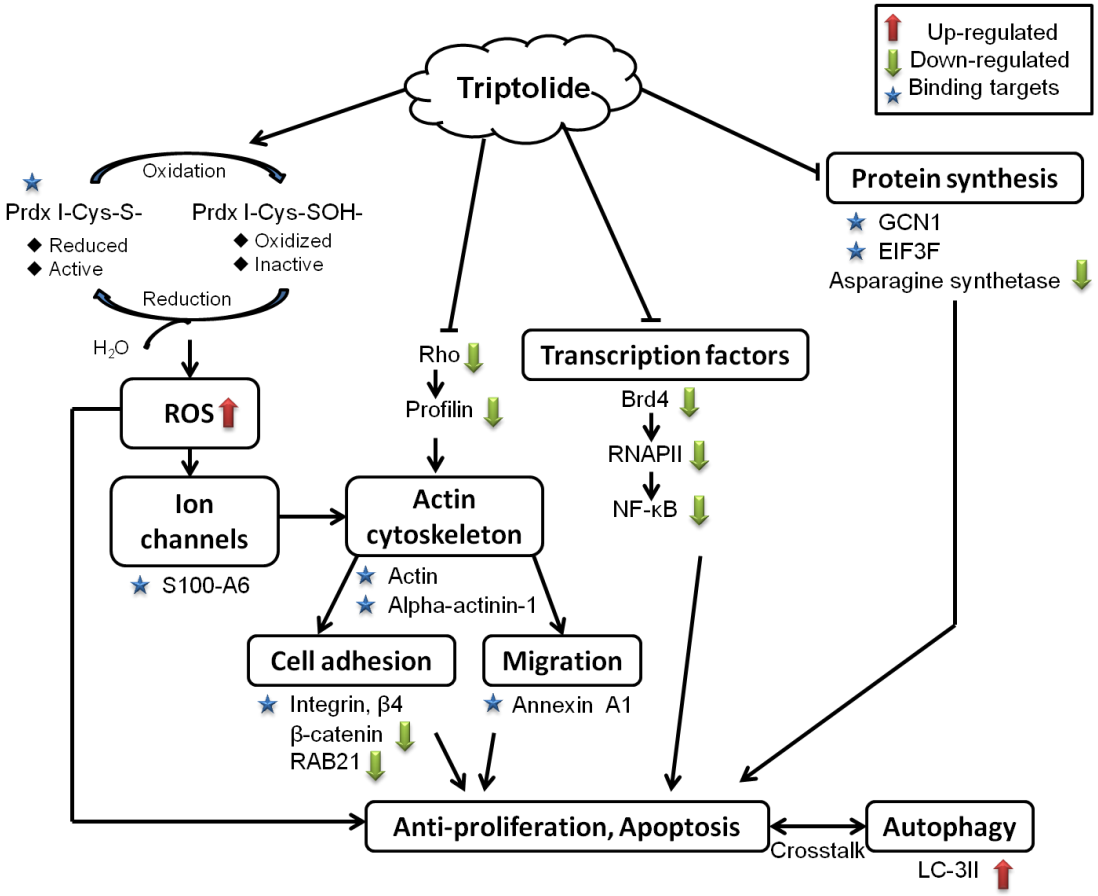

Figure 5.1 Overall proteome picture depicting activities of triptolide against colorectal cancer based on proteomics approaches. In our study, triptolide was shown to has strong anti-proliferative and pro-apoptotic activities against colorectal cancer cell line HCT 116 by increasing ROS level, interfering with actin cytoskeleton, protein synthesis and expression of transcription factors. Triptolide increases ROS level by blocking peroxidase activity of PRDX I. ROS is associated with ion channels and actin cytoskeleton, which play important roles in cancer growth. The overall picture includes network analysis by bioinformatics approaches and previous literature, molecular alteration by iTRAQ and proteomics approaches, and identification of binding targets of triptolide by chemical proteomics approaches. The up-and down-regulated proteins by triptolide were labeled with up arrow in red and down arrow in green, respectively. Direct binding targets of triptolide were labeled with blue stars.

Leigongteng was used in traditional Chinese medicine for more than two centuries for treatment of autoimmune and inflammatory diseases. In 1972, triptolide

was firstly extracted as the main component of *Leigongteng* and shown to have strong anti-tumor activities. Since then, various studies have explored its mechanism against tumor growth.

Triptolide possesses broad-spectrum anti-cancer activities. It was shown to induce apoptosis through increasing caspase 3, 8, 9 [66] and induce autophagy by increasing LC-3II [180]. It also inhibits expression of transcript factors such as NF-κB by down-regulating RNAPII [140]. However, the previous extensive studies did not provide us with the regulated targets at a global level. As tumors grow in multi-step and a complicated way, the detailed mechanism of action of the drug remains unclear. Therefore, in my study, proteomic approaches were utilized to provide a whole picture of the alteration of proteins from colorectal cancer cells treated by triptolide, as well as to study the direct binding targets of triptolide. These studies could shed some light on the mechanism of triptolide against colorectal cancer.

In my study, triptolide was demonstrated to induce ROS level elevation through directly binding to cysteines of Peroxiredoxin I (PRDX I) and inhibiting peroxidase activity of Peroxiredoxin I. PRDX I contains a peroxidatic cysteine (C_P), which could be oxidized by peroxides to cysteine sulfenic acid (Cys-SOH). Many ongoing studies have elucidated the importance of PRDX I in antioxidant protection [148]. As a result, 2-cysteine PRDXs were suggested to be therapeutic targets for cancers and

cardiovascular disease [147, 151]. ROS is toxic in cells due to the oxidative stress by their reaction with proteins and nucleic acids. Cellular response to ROS is essential to protect cells from oxidative damage [181]. The dysfunction of PRDX I by triptolide might induce oxidative stress and elevation of ROS level.

ROS also activate ion channels [182]. Oxidative stress induces Ca^{2+} cytoplasmic increase through calcium influx. The calcium influx might be due to the calcium release from ER [183]. H_2O_2 activates calcium and potassium channels. Although Ca^{2+} channels might be elevated by ROS, some Ca^{2+} binding proteins such as S100-A6 and Annexin A1 were shown to directly bind to triptolide according to our ABPP results. S100-A6 contributes to cellular calcium signaling and plays important roles in reorganizing actin cytoskeleton and in cell motility [184]. In addition, Annexin A1 was identified as the direct binding target of triptolide with ABPP approaches, followed by being validated by MS/MS approach. Annexins regulate the actin cytoskeleton, which plays important roles in cell morphology and cell migration. Cell migration was also found to be inhibited by triptolide, which implies that triptolide might interfere with cell migration via binding cysteines of Annexin A1 and inhibiting its functions.

Triptolide was also found to directly bind to Actin and α-actinin-1 according to our ABPP results. They play essential roles in actin cytoskeleton, which is relevant to

cell adhesion and cell mobility. Our iTRAQ results showed that actin cytoskeleton-related proteins, such as Rho guanine nucleotide exchange factor 2 (ARHGEF2) and Profilin -2 (PFN2) were significantly down-regulated by triptolide. ARHGEF2 activates Rho-GTPases by promoting the exchange of GDP for GTP. The activated Rho transduces various signals, including cytoskeleton reorganization, cellular invasion and cell proliferation. Profilin-2 binds to actin and affects the structure of the cytoskeleton. These results indicate that triptolide interferes with actin cytoskeleton, which might further affect the cell adhesion and cell migration.

Our observation under microscope as well as network analysis elucidated that triptolide interferes with cell adhesion. Integrin β4 was identified to be a direct binding target according to our ABPP results. It is a bridge for cell-cell and cell-extracellular matrix (ECM) interactions and plays multiple roles in cell adhesion, migration and tumor progression [185]. In addition, the relevant proteins, such as β-catenin and Ras-related protein Rab-21 were down-regulated, based on iTRAQ results.

In addition, triptolide also decreases expression of transcription factors. Transcription factors are commonly deregulated in cancer cells, making them as targets of cancer therapy [186]. Previous literature has demonstrated that triptolide induces p53 and Bcl2-associated X protein (Bax) [187]. It also inhibits STAT3 [187]

and XPB [151], exerting anti-proliferative activities against cancers. Pro-inflammatory gene, such as NF-κB, was shown to be down-regulated [121]. Next, the upstream regulator of NF-κB was examined. RNA Polymerase II , which regulates the expression of transcription factors such as NF-κB and STAT3 [140], was shown to be decreased in our iTRAQ result, which is consistent with the previous study [188]. BRD4 was demonstrated to phosphorylate CTD of RNA Polymerase II. BRD4 also restricts the release of paused RNAPII, serving as the rate-limiting step in the process of regulating transcription factors. Its high expression in cancers [189] makes it a biomarker for colorectal cancer. BRD4 was firstly reported to be down-regulated by triptolide in our study, providing a novel insight into the detailed mechanism of action of the drug.

In our study, triptolide was shown to interfere with protein synthesis, by estimating the protein synthesis rate with AHA treatment. Several proteins, such as eIF-2-α kinase activator GCN1 and Eukaryotic translation inhibition factor 3 subunit F (EIF3F) were identified as binding targets of triptolide. In addition, ASNS was down-regulated according to our iTRAQ result. ASNS is an enzyme that generates asparagine from aspartate. These results suggested that triptolide inhibits protein synthesis *via* binding several proteins like GCN1 and EIF3F and further down-regulating relevant proteins like ASNS.

In my study, triptolide has shown very strong anti-proliferation activity on colorectal cancer cell line HCT 116 in dose- and time-dependent manners. IC_{50} of triptolide on HCT 116 was determined to be 10 nM, which demonstrated a strong anti-tumor property of triptolide. The flow cytometry analysis also demonstrated that triptolide induces apoptosis of HCT 116. Our results indicated that several pathways, such as actin cytoskeleton, cell adhesion, migration, transcription factor expression and protein synthesis, contribute to the anti-proliferative and apoptosis activity of triptolide. Triptolide was also demonstrated to have multiple targets and exert many functions against colorectal cancer. Proteomics approaches provide us with an opportunity to study the alteration of proteins with triptolide's treatment at a global level, which aid to explore the mechanism of triptolide. The results of combination of ABPP and iTRAQ approaches provided a target list of triptolide, which could be a reference for the further study of interacting activity of triptolide and binding targets of triptolide.

5.2 Future Work

5.2.1 More cell models and other possible strategies

In the future study, some aspects could be improved. In our study, HCT 116 cells were used as model to study the mechanism of triptolide. Therefore, in the future work, different colorectal cancer cell lines and even other cancer cell lines could be

introduced for the mechanism study of triptolide. The comparison between different cell lines might provide insights into the identification of the targets as well as the signal pathways. Moreover, some *in vivo* colorectal cancer models with patient-derived primary tumor sample could also be introduced by using our proteomics approaches. This might provide more solid result. In addition, to further explore the mechanisms of triptolide on cancer cells, different functions of triptolide on normal and colorectal cancer cells would be studies. As shown in our experiment, proliferation of normal colorectal cell CCD 841 was not interfered by triptolide. To explore the reasons for that difference, in the future work, CCD 841 and HCT 116 cells will be treated with triptolide. The whole proteome from two samples will be extracted and labeled with iTRAQ reagents followed by MS/MS analysis. Network constituted by the significantly regulated proteins in normal cell samples will be analyzed, which might have much difference with the network of cancer cell samples. A comparison of protein profiling of cancer and normal cells could provide some insight into the study of the specific targets of triptolide in cancer cells, aiding to explore its application in clinic trials. As shown in our experiment, expression levels of BRD4 and β-catenin did not change in the normal cells. There might be more targets that are specifically interfered by triptolide in colorectal cancer cells. Identification of these specifically regulated proteins in cancer cells could aid to identify the targets of triptolide in cancer cells as well as to study the side effects of triptolide. These studies could also provide reference on the clinical trials of triptolide

and its derivatives.

In addition, other strategies for mechanism for study of pathways could be considered for the future study. Our work focused on analyzing the networks and pathways by profiling regulated proteins at a global level. The study focused mainly on proteomics and did not attempt to address either genomics or metabolomics. To provide supplemental information in facilitating data analysis, mRNA level change with triptolide treatment using a transcriptomics approach can be applied in the future. An additional advantage is that transcriptomics will also serve as supplementary datasets for mechanism analysis. In the future, data extracted by applying the proteomics approach and that acquired by applying the transcriptomics approach can be compared to validate and provide more solid result on the regulated molecular on both protein and mRNA level.

5.2.2 Function study of triptolide's binding targets

The future work will also include the validation of more direct binding targets and the study on the functional effects of triptolide on PRDX I and Annexin A1. In our ABPP results, Annexin A1 was identified as a direct binding target of triptolide. Although Annexin A1 promotes cell migration, which was interfered with triptolide's treatment, there is no direct evidence elucidating that triptolide reduces migration by inhibiting activity of Annexin A1. Therefore, the function of Annexin A1 will be

explored. The function of Annexin A1 or PRDX I could be interfered by introducing the mutations or siRNA of Annexin A1 or PRDX I in HCT 116 cells. By comparing the migration or other functions of the cells having WT Annexin A1 with those of cells with mutations or siRNA, we could study the functions of Annexin A1 in colorectal cancer. Similarly, by comparing the ROS level or other functions of the cells having WT PRDX I with those of cells with mutations or siRNA, the interfering function of triptolide on PRDX I will be established. In addition, the anti-tumor activity of triptolide on WT and mutation could be compared, which might provide some insight on the interference function of triptolide on its targets.

Our study has provided with a list of target candidates by using ABPP combined with iTRAQ approaches. Therefore, more binding targets of triptolide could also be validated based on the list. These studies might provide us with more comprehensive information about the mechanism of action of triptolide, which can help to unveil the mechanism of triptolide against colorectal cancer.

5.3 Conclusion

In summary, in our study, triptolide has been demonstrated to have strong anti-proliferative and pro-apoptotic activities against colorectal cancer cell line HCT 116. Several pathways interfered by triptolide, such as protein synthesis, ROS, actin

cytoskeleton, migration and the alterations of transcription factors contribute to triptolide's anti-tumor functions.

Triptolide has been demonstrated to induce ROS level elevation *via* inhibiting peroxidase activity of Peroxiredoxin I, which is abundant in cells and plays important roles in peroxidation. Several calcium-binding proteins, such as S100-A6 were shown to bind to triptolide directly. Actin-regulated proteins, such as α-actinin-1, integrin-β, and Annexin A1 were identified as direct binding targets of triptolide. They play important roles in actin cytoskeleton, cell migration and cell adhesion. Some relevant proteins, such as Rho, Profilin, β-catenin, RAB21 were also down-regulated by triptolide. Furthermore, triptolide has been demonstrated to inhibit protein synthesis. Several transcription factors, such as BRD4, RNA Polymerase II, and NF-κB involved in tumor proliferation were also verified to be down-regulated by triptolide. Among them, the down-regulation of BRD4 with triptolide treatment has never been reported before. These networks and expression alteration of proteins contribute to the anti-tumor activities of triptolide. Proteomics approaches allows the study of altered proteins by triptolide and binding targets of triptolide at a global level, which provides some insights on the mechanism of triptolide against colorectal cancer.

Reference

1. Siegel, R.L., K.D. Miller, and A. Jemal, *Cancer statistics, 2016.* CA: A cancer journal for clinicians, 2015.
2. Coussens, L.M. and Z. Werb, *Inflammation and cancer.* Nature, 2002. **420**(6917): p. 860-867.
3. Siegel, R.L., K.D. Miller, and A. Jemal, *Cancer statistics, 2016.* CA: a cancer journal for clinicians, 2016. **66**(1): p. 7-30.
4. Torre, L.A., et al., *Cancer statistics for Asian Americans, Native Hawaiians, and Pacific Islanders, 2016: Converging incidence in males and females.* CA: a cancer journal for clinicians, 2016.
5. Wu, S., et al., *Substantial contribution of extrinsic risk factors to cancer development.* Nature, 2016. **529**(7584): p. 43-47.
6. Hanahan, D. and R.A. Weinberg, *Hallmarks of cancer: the next generation.* cell, 2011. **144**(5): p. 646-674.
7. FEI, T.X., *Elucidating tumor suppressive function of Frataxin in colorectal cancer with a quantitative proteomics approach*. 2014.
8. Johnstone, R.W., A.A. Ruefli, and S.W. Lowe, *Apoptosis: a link between cancer genetics and chemotherapy.* Cell, 2002. **108**(2): p. 153-164.
9. Fernald, K. and M. Kurokawa, *Evading apoptosis in cancer.* Trends in cell biology, 2013. **23**(12): p. 620-633.
10. Chandel, N.S., et al., *Metabolic regulation of stem cell function in tissue homeostasis and organismal ageing.* Nature Cell Biology, 2016.
11. Pavlova, N.N. and C.B. Thompson, *The emerging hallmarks of cancer metabolism.* Cell metabolism, 2016. **23**(1): p. 27-47.
12. Strzyz, P., *Cancer biology: TGF [beta] and EMT as double agents.* Nature Reviews Molecular Cell Biology, 2016.
13. JINGJING, W., *The role of autocrine human growth hormone in colorectal cancer progression*. 2014.
14. Malkova, A. and G. Ira, *Break-induced replication: functions and molecular mechanism.* Current opinion in genetics & development, 2013. **23**(3): p. 271-279.
15. Xie, Z., et al., *Early telomerase inactivation accelerates aging independently of telomere length.* Cell, 2015. **160**(5): p. 928-939.
16. Elinav, E., et al., *Inflammation-induced cancer: crosstalk between tumours, immune cells and microorganisms.* Nature Reviews Cancer, 2013. **13**(11): p. 759-771.
17. Chaffer, C.L. and R.A. Weinberg, *A perspective on cancer cell metastasis.* Science, 2011. **331**(6024): p. 1559-1564.
18. Ridley, A.J., et al., *Cell migration: integrating signals from front to back.* Science, 2003. **302**(5651): p. 1704-1709.
19. Lee, H., et al., *Colorectal cancer and diet in an asian population—A case-control study among Singapore Chinese.* International journal of cancer, 1989. **43**(6): p. 1007-1016.
20. Sung, J.J., et al., *Increasing incidence of colorectal cancer in Asia: implications for screening.*

The lancet oncology, 2005. **6**(11): p. 871-876.

21. Fearon, E.R. and B. Vogelstein, *A genetic model for colorectal tumorigenesis.* Cell, 1990. **61**(5): p. 759-767.
22. Ohlsson, B., et al., *Follow-up after curative surgery for colorectal carcinoma.* Diseases of the colon & rectum, 1995. **38**(6): p. 619-626.
23. Miller, K.D., et al., *Cancer treatment and survivorship statistics, 2016.* CA: a cancer journal for clinicians, 2016.
24. GHOSH, D., *Proteomics based analysis identified CacyBP as a candidate biomarker for colorectal cancer metastasis*. 2012.
25. Lambertini, M., et al., *Ovarian suppression with triptorelin during adjuvant breast cancer chemotherapy and long-term ovarian function, pregnancies, and disease-free survival: a randomized clinical trial.* JAMA, 2015. **314**(24): p. 2632-2640.
26. Lauro, S., et al., *H39Genetic polymorphism can help physician choosing the best lung cancer chemotherapy.* Annals of Oncology, 2015. **26**(suppl 6): p. vi-vi.
27. Perroud, H.A., et al., *Metastatic breast cancer patients treated with low-dose metronomic chemotherapy with cyclophosphamide and celecoxib: clinical outcomes and biomarkers of response.* Cancer chemotherapy and pharmacology, 2016. **77**(2): p. 365-374.
28. Mann, J., *Natural products in cancer chemotherapy: past, present and future.* Nature Reviews Cancer, 2002. **2**(2): p. 143-148.
29. Chabner, B.A. and T.G. Roberts, *Chemotherapy and the war on cancer.* Nature Reviews Cancer, 2005. **5**(1): p. 65-72.
30. Lima, C.M.S.R., et al., *Abstract CT151: G1T28, a cyclin dependent kinase 4/6 inhibitor, in combination with etoposide and carboplatin for extensive stage small cell lung cancer (ES-SCLC): preliminary results.* Cancer Research, 2016. **76**(14 Supplement): p. CT151-CT151.
31. Liu, A.P., et al., *Refractory acute lymphoblastic leukemia in Chinese children: bridging to stem cell transplantation with clofarabine, cyclophosphamide and etoposide.* Annals of hematology, 2016. **95**(3): p. 501-507.
32. Ding, G., *Important Chinese herbal remedies.* Clinical therapeutics, 1986. **9**(4): p. 345-357.
33. Kupchan, S.M., et al., *Tumor inhibitors. LXXIII. Maytansine, a novel antileukemic ansa macrolide from Maytenus ovatus.* Journal of the American Chemical Society, 1972. **94**(4): p. 1354-1356.
34. Ling, D., et al., *pH-sensitive nanoformulated triptolide as a targeted therapeutic strategy for hepatocellular carcinoma.* ACS nano, 2014. **8**(8): p. 8027-8039.
35. Chan, E.W.-C., et al., *Triptolide induced cytotoxic effects on human promyelocytic leukemia, T cell lymphoma and human hepatocellular carcinoma cell lines.* Toxicology letters, 2001. **122**(1): p. 81-87.
36. Kim, M.J., et al., *Triptolide inactivates Akt and induces caspase-dependent death in cervical cancer cells via the mitochondrial pathway.* International journal of oncology, 2010. **37**(5): p. 1177-1185.
37. Chen, Z., et al., *Triptolide sensitizes pancreatic cancer cells to TRAIL-induced activation of the death receptor pathway.* Cancer letters, 2014. **348**(1): p. 156-166.

38. Wang, G., X.S. Xu, and Y. Zhang, *The role triptolide in sensitizing lung tumor cells to cisplatin-induced apoptosis.* Cancer Research, 2014. **74**(19 Supplement): p. 5110-5110.
39. Cragg, G.M., D.J. Newman, and K.M. Snader, *Natural products in drug discovery and development.* Journal of natural products, 1997. **60**(1): p. 52-60.
40. de Oliveira, A.M., et al., *Diterpenes: a therapeutic promise for cardiovascular diseases.* Recent patents on cardiovascular drug discovery, 2008. **3**(1): p. 1-8.
41. Tirapelli, C.R., et al., *Hypotensive action of naturally occurring diterpenes: a therapeutic promise for the treatment of hypertension.* Fitoterapia, 2010. **81**(7): p. 690-702.
42. Hanson, J.R., *Diterpenoids.* Natural Product Reports, 1998. **15**(1): p. 93-106.
43. Kong, L.-M., et al., *Identification and validation of p50 as the cellular target of eriocalyxin B.* Oncotarget, 2014. **5**(22): p. 11354.
44. Wang, J., et al., *A quantitative chemical proteomics approach to profile the specific cellular targets of andrographolide, a promising anticancer agent that suppresses tumor metastasis.* Molecular & Cellular Proteomics, 2014. **13**(3): p. 876-886.
45. Nguyen, V.S., et al., *Specificity and Inhibitory Mechanism of Andrographolide and Its Analogues as Antiasthma Agents on NF-κB p50.* Journal of natural products, 2015. **78**(2): p. 208-217.
46. Cheng, X., et al., *In situ proteome profiling of C75, a covalent bioactive compound with potential anticancer activities.* Organic letters, 2014. **16**(5): p. 1414-1417.
47. Paulick, M.G. and M. Bogyo, *Application of activity-based probes to the study of enzymes involved in cancer progression.* Current opinion in genetics & development, 2008. **18**(1): p. 97-106.
48. Butler, M.S., *Natural products to drugs: natural product derived compounds in clinical trials.* Nat Prod Rep, 2005. **22**(2): p. 162-95.
49. Li, Z., et al., *Design and synthesis of novel C14-hydroxyl substituted triptolide derivatives as potential selective antitumor agents.* J Med Chem, 2009. **52**(16): p. 5115-23.
50. Evans, M.J. and B.F. Cravatt, *Mechanism-based profiling of enzyme families.* Chemical reviews, 2006. **106**(8): p. 3279-3301.
51. Ghosh, D., et al., *iTRAQ Based Quantitative Proteomics Approach Validated the Role of Calcyclin Binding Protein (CacyBP) in Promoting Colorectal Cancer Metastasis*.* Molecular & Cellular Proteomics, 2013. **12**(7): p. 1865-1880.
52. Zhou, Z.L., et al., *Triptolide: structural modifications, structure-activity relationships, bioactivities, clinical development and mechanisms.* Nat Prod Rep, 2012. **29**(4): p. 457-75.
53. Nomura, D.K., M.M. Dix, and B.F. Cravatt, *Activity-based protein profiling for biochemical pathway discovery in cancer.* Nature Reviews Cancer, 2010. **10**(9): p. 630-638.
54. Zhou, B., et al., *Synthesis and biological evaluation of novel triptolide analogues for anticancer activity.* Bioorg Med Chem Lett, 2010. **20**(21): p. 6217-21.
55. Schröder, E., et al., *Crystal structure of decameric 2-Cys peroxiredoxin from human erythrocytes at 1.7 Å resolution.* Structure, 2000. **8**(6): p. 605-615.
56. Liu, Q., *Triptolide and its expanding multiple pharmacological functions.* Int Immunopharmacol, 2011. **11**(3): p. 377-83.
57. Barber, S.C., R.J. Mead, and P.J. Shaw, *Oxidative stress in ALS: a mechanism of*

neurodegeneration and a therapeutic target. Biochimica et Biophysica Acta (BBA)-Molecular Basis of Disease, 2006. **1762**(11): p. 1051-1067.

58. Butterfield, L.H., et al., *From cytoprotection to tumor suppression: the multifactorial role of peroxiredoxins.* Antioxidants & redox signaling, 1999. **1**(4): p. 385-402.
59. Zhao, W., et al., *Protection of peroxiredoxin II on oxidative stress-induced cardiomyocyte death and apoptosis.* Basic research in cardiology, 2009. **104**(4): p. 377-389.
60. Qiu, D., *Immunosuppressant PG490 (Triptolide) Inhibits T-cell Interleukin-2 Expression at the Level of Purine-box/Nuclear Factor of Activated T-cells and NF-kappa B Transcriptional Activation.* Journal of Biological Chemistry, 1999. **274**(19): p. 13443-13450.
61. Kim, J.-A., et al., *Activity assay of mammalian 2-cys peroxiredoxins using yeast thioredoxin reductase system.* Analytical biochemistry, 2005. **338**(2): p. 216-223.
62. Pan, J., *RNA polymerase - an important molecular target of triptolide in cancer cells.* Cancer Lett, 2010. **292**(2): p. 149-52.
63. Cox, A.G., et al., *The thioredoxin reductase inhibitor auranofin triggers apoptosis through a Bax/Bak-dependent process that involves peroxiredoxin 3 oxidation.* Biochemical pharmacology, 2008. **76**(9): p. 1097-1109.
64. Westerheide, S.D., et al., *Triptolide, an inhibitor of the human heat shock response that enhances stress-induced cell death.* J Biol Chem, 2006. **281**(14): p. 9616-22.
65. Wan, C.K., et al., *Triptolide induces Bcl-2 cleavage and mitochondria dependent apoptosis in p53-deficient HL-60 cells.* Cancer Lett, 2006. **241**(1): p. 31-41.
66. Choi, Y.-J., et al., *Immunosuppressant PG490 (triptolide) induces apoptosis through the activation of caspase-3 and down-regulation of XIAP in U937 cells.* Biochemical pharmacology, 2003. **66**(2): p. 273-280.
67. Chang, W.T., et al., *Triptolide and chemotherapy cooperate in tumor cell apoptosis. A role for the p53 pathway.* J Biol Chem, 2001. **276**(3): p. 2221-7.
68. Vispe, S., et al., *Triptolide is an inhibitor of RNA polymerase I and II-dependent transcription leading predominantly to down-regulation of short-lived mRNA.* Mol Cancer Ther, 2009. **8**(10): p. 2780-90.
69. Zhao, F., et al., *Triptolide alters histone H3K9 and H3K27 methylation state and induces G0/G1 arrest and caspase-dependent apoptosis in multiple myeloma in vitro.* Toxicology, 2010. **267**(1-3): p. 70-9.
70. Tai, C.J., et al., *The investigation of mitogen-activated protein kinase phosphatase-1 as a potential pharmacological target in non-small cell lung carcinomas, assisted by non-invasive molecular imaging.* BMC Cancer, 2010. **10**: p. 95.
71. Miyata, Y., T. Sato, and A. Ito, *Triptolide, a diterpenoid triepoxide, induces antitumor proliferation via activation of c-Jun NH2-terminal kinase 1 by decreasing phosphatidylinositol 3-kinase activity in human tumor cells.* Biochem Biophys Res Commun, 2005. **336**(4): p. 1081-6.
72. Xu, B., et al., *Triptolide simultaneously induces reactive oxygen species, inhibits NF-kappaB activity and sensitizes 5-fluorouracil in colorectal cancer cell lines.* Cancer Lett, 2010. **291**(2): p. 200-8.
73. Wang, W., et al., *Enhanced antitumor effect of combined triptolide and ionizing radiation.*

Clin Cancer Res, 2007. **13**(16): p. 4891-9.

74. Li, C.J., et al., *Synergistic anticancer activity of triptolide combined with cisplatin enhances apoptosis in gastric cancer in vitro and in vivo.* Cancer Lett, 2012. **319**(2): p. 203-13.
75. Lipsky, P.E. and X.-L. Tao. *A potential new treatment for rheumatoid arthritis: thunder god vine*. in *Seminars in arthritis and rheumatism*. 1997. Elsevier.
76. S., D.G., *Ding G S. Important Chinese herbal remedies[J]. Clinical therapeutics, 1986, 9(4): 345-357.* 1986. **9**(4).
77. Leuenroth, S.J., et al., *Triptolide is a traditional Chinese medicine-derived inhibitor of polycystic kidney disease.* Proc Natl Acad Sci U S A, 2007. **104**(11): p. 4389-94.
78. Zhou, Z.-L., et al., *Triptolide: structural modifications, structure–activity relationships, bioactivities, clinical development and mechanisms.* Natural product reports, 2012. **29**(4): p. 457-475.
79. Kiviharju, T.M., et al., *Antiproliferative and proapoptotic activities of triptolide (PG490), a natural product entering clinical trials, on primary cultures of human prostatic epithelial cells.* Clinical Cancer Research, 2002. **8**(8): p. 2666-2674.
80. Hall, A., et al., *Structure-based insights into the catalytic power and conformational dexterity of peroxiredoxins.* Antioxidants & redox signaling, 2011. **15**(3): p. 795-815.
81. Ziaei, S. and R. Halaby, *Immunosuppressive, anti-inflammatory and anti-cancer properties of triptolide: A mini review.* Avicenna Journal of Phytomedicine, 2016. **6**(2): p. 149.
82. Qi, X., et al., *Dephosphorylation of Tak1 at Ser412 greatly contributes to the spermatocyte-specific testis toxicity induced by (5R)-5-hydroxytriptolide in C57BL/6 mice.* Toxicology Research, 2016. **5**(2): p. 594-601.
83. Krishna, G., et al., *PG490-88, a derivative of triptolide, blocks bleomycin-induced lung fibrosis.* The American journal of pathology, 2001. **158**(3): p. 997-1004.
84. Han, R., et al., *Triptolide in the treatment of psoriasis and other immune-mediated inflammatory diseases.* British journal of clinical pharmacology, 2012. **74**(3): p. 424-436.
85. Wang, L., et al., *(5R)-5-hydroxytriptolide (LLDT-8), a novel immunosuppressant in clinical trials, exhibits potent antitumor activity via transcription inhibition.* Cancer letters, 2012. **324**(1): p. 75-82.
86. Zhou, R., et al., *Preventive effects of (5R)-5-hydroxytriptolide on concanavalin A-induced hepatitis.* Eur J Pharmacol, 2006. **537**(1-3): p. 181-9.
87. Liu, J., et al., *Derivatization of (5R)-hydroxytriptolide from benzylamine to enhance mass spectrometric detection: application to a Phase I pharmacokinetic study in humans.* Anal Chim Acta, 2011. **689**(1): p. 69-76.
88. Schenone, M., et al., *Target identification and mechanism of action in chemical biology and drug discovery.* Nature chemical biology, 2013. **9**(4): p. 232-240.
89. KAI, L., *Developing Chemical Proteomic Tools Connecting Proteins and Small Molecules*. 2011.
90. Burley, S.K., et al., *Structural genomics: beyond the human genome project.* Nature genetics, 1999. **23**(2): p. 151-157.
91. Daly, S.J., et al., *Production and analytical applications of scFv antibody fragments.* Analytical letters, 2001. **34**(11): p. 1799-1827.

92. Blackstock, W.P. and M.P. Weir, *Proteomics: quantitative and physical mapping of cellular proteins.* Trends in biotechnology, 1999. **17**(3): p. 121-127.
93. JIGANG, W., *Quantitative chemical proteomics investigations of targets of andrographolide and proteolysis of autophagy.* 2013.
94. Yates, J.R., C.I. Ruse, and A. Nakorchevsky, *Proteomics by mass spectrometry: approaches, advances, and applications.* Annual review of biomedical engineering, 2009. **11**: p. 49-79.
95. Glish, G.L. and R.W. Vachet, *The basics of mass spectrometry in the twenty-first century.* Nature Reviews Drug Discovery, 2003. **2**(2): p. 140-150.
96. HAIBIN, S., *Developing High-Throughput Chemical Approaches For Proteomic Profiling Of Aspartic Proteases And Protein Kinases*. 2011.
97. Duncan, P.J.G.M.W. and A.L. Yergey, *Quantifying Proteins by Mass Spectrometry.* Spectroscopy, 2015. **30**(10).
98. Zhao, Z., et al., *Functional proteomics of Arabidopsis thaliana guard cells uncovers new stomatal signaling pathways.* The Plant Cell, 2008. **20**(12): p. 3210-3226.
99. Friedman, D.B., et al., *Proteome analysis of human colon cancer by two-dimensional difference gel electrophoresis and mass spectrometry.* Proteomics, 2004. **4**(3): p. 793-811.
100. Alban, A., et al., *A novel experimental design for comparative two-dimensional gel analysis: Two-dimensional difference gel electrophoresis incorporating a pooled internal standard.* Proteomics, 2003. **3**(1): p. 36-44.
101. Issaq, H.J., et al., *Multidimensional separation of peptides for effective proteomic analysis.* Journal of Chromatography B, 2005. **817**(1): p. 35-47.
102. Shi, Y., et al., *The role of liquid chromatography in proteomics.* Journal of Chromatography A, 2004. **1053**(1): p. 27-36.
103. Han, C.-L., et al., *Membrane Proteomics for the Opportunity of Cancer Biomarker and Drug Target Discovery*, in *Systems Biology: Applications in Cancer-Related Research*. 2012. p. 259-286.
104. Langley, S.R., et al., *Proteomics: from single molecules to biological pathways.* Cardiovascular research, 2013. **97**(4): p. 612-622.
105. Savino, R., et al., *The proteomics big challenge for biomarkers and new drug-targets discovery.* International journal of molecular sciences, 2012. **13**(11): p. 13926-13948.
106. Guo, S., J. Zou, and G. Wang, *Advances in the proteomic discovery of novel therapeutic targets in cancer.* Drug design, development and therapy, 2013. **7**: p. 1259.
107. Cheng, X., et al., *A tuned affinity-based staurosporine probe for in situ profiling of protein kinases.* Chem. Commun., 2014. **50**(22): p. 2851-2853.
108. Yang, P.-Y., et al., *Activity-based proteome profiling of potential cellular targets of orlistat−an FDA-approved drug with anti-tumor activities.* Journal of the American Chemical Society, 2009. **132**(2): p. 656-666.
109. Leuenroth, S.J., et al., *Triptolide is a traditional Chinese medicine-derived inhibitor of polycystic kidney disease.* Proceedings of the National Academy of Sciences, 2007. **104**(11): p. 4389-4394.
110. Fonovic, M. and M. Bogyo, *Activity based probes for proteases: applications to biomarker discovery, molecular imaging and drug screening.* Current pharmaceutical design, 2007. **13**(3):

p. 253-261.

111. Corson, T.W., et al., *Triptolide directly inhibits dCTP pyrophosphatase.* ChemBioChem, 2011. **12**(11): p. 1767-1773.

112. Titov, D.V., et al., *XPB, a subunit of TFIIH, is a target of the natural product triptolide.* Nature chemical biology, 2011. **7**(3): p. 182-188.

113. He, Q.L., et al., *Covalent Modification of a Cysteine Residue in the XPB Subunit of the General Transcription Factor TFIIH Through Single Epoxide Cleavage of the Transcription Inhibitor Triptolide.* Angewandte Chemie International Edition, 2015. **54**(6): p. 1859-1863.

114. Vispé, S., et al., *Triptolide is an inhibitor of RNA polymerase I and II–dependent transcription leading predominantly to down-regulation of short-lived mRNA.* Molecular cancer therapeutics, 2009. **8**(10): p. 2780-2790.

115. Verhelst, S. and M. Bogyo, *Chemical proteomics applied to target identification and drug discovery.* Biotechniques, 2005. **38**(2): p. 175-177.

116. Rix, U. and G. Superti-Furga, *Target profiling of small molecules by chemical proteomics.* Nature chemical biology, 2009. **5**(9): p. 616-624.

117. Pawson, A.J., et al., *The IUPHAR/BPS Guide to PHARMACOLOGY: an expert-driven knowledgebase of drug targets and their ligands.* Nucleic Acids Research, 2014. **42**(D1): p. D1098-D1106.

118. Zhou, Y., W. Li, and Y. Xiao, *Profiling of Multiple Targets of Artemisinin Activated by Hemin in Cancer Cell Proteome.* ACS chemical biology, 2016. **11**(4): p. 882-888.

119. Fidler, J.M., et al., *Preclinical antileukemic activity, toxicology, toxicokinetics and formulation development of triptolide derivative MRx102.* Cancer chemotherapy and pharmacology, 2014. **73**(5): p. 961-974.

120. Wai-Ching Chan, E., et al., *Triptolide induced cytotoxic effects on human promyelocytic leukemia, T cell lymphoma and human hepatocellular carcinoma cell lines.* Toxicology letters, 2001. **122**(1): p. 81-87.

121. YinJun, L., J. Jie, and W. YunGui, *Triptolide inhibits transcription factor NF-kappaB and induces apoptosis of multiple myeloma cells.* Leukemia research, 2005. **29**(1): p. 99-105.

122. Zhao, F., et al., *Triptolide alters histone H3K9 and H3K27 methylation state and induces G0/G1 arrest and caspase-dependent apoptosis in multiple myeloma in vitro.* Toxicology, 2010. **267**(1): p. 70-79.

123. Gan, C.S., et al., *Technical, experimental, and biological variations in isobaric tags for relative and absolute quantitation (iTRAQ).* Journal of proteome research, 2007. **6**(2): p. 821-827.

124. Ghosh, D., et al., *Identification of key players for colorectal cancer metastasis by iTRAQ quantitative proteomics profiling of isogenic SW480 and SW620 cell lines.* Journal of proteome research, 2011. **10**(10): p. 4373-4387.

125. Dey, A., et al., *A bromodomain protein, MCAP, associates with mitotic chromosomes and affects G2-to-M transition.* Molecular and cellular biology, 2000. **20**(17): p. 6537-6549.

126. Wu, S.-Y. and C.-M. Chiang, *The double bromodomain-containing chromatin adaptor Brd4 and transcriptional regulation.* Journal of Biological Chemistry, 2007. **282**(18): p. 13141-13145.

127. Yang, Z., et al., *Recruitment of P-TEFb for stimulation of transcriptional elongation by the bromodomain protein Brd4.* Molecular cell, 2005. **19**(4): p. 535-545.
128. Devaiah, B.N., et al., *BRD4 is an atypical kinase that phosphorylates serine2 of the RNA polymerase II carboxy-terminal domain.* Proceedings of the National Academy of Sciences, 2012. **109**(18): p. 6927-6932.
129. Zuber, J., et al., *RNAi screen identifies Brd4 as a therapeutic target in acute myeloid leukaemia.* Nature, 2011. **478**(7370): p. 524-528.
130. Delmore, J.E., et al., *BET bromodomain inhibition as a therapeutic strategy to target c-Myc.* Cell, 2011. **146**(6): p. 904-917.
131. Kemler, R., *From cadherins to catenins: cytoplasmic protein interactions and regulation of cell adhesion.* Trends in Genetics, 1993. **9**(9): p. 317-321.
132. Bienz, M., *β-Catenin: a pivot between cell adhesion and Wnt signalling.* Current Biology, 2005. **15**(2): p. R64-R67.
133. Conacci-Sorrell, M., J. Zhurinsky, and A. Ben-Ze'ev, *The cadherin-catenin adhesion system in signaling and cancer.* The Journal of clinical investigation, 2002. **109**(8): p. 987-991.
134. Munemitsu, S., et al., *Regulation of intracellular beta-catenin levels by the adenomatous polyposis coli (APC) tumor-suppressor protein.* Proceedings of the National Academy of Sciences, 1995. **92**(7): p. 3046-3050.
135. Brembeck, F.H., M. Rosário, and W. Birchmeier, *Balancing cell adhesion and Wnt signaling, the key role of β-catenin.* Current opinion in genetics & development, 2006. **16**(1): p. 51-59.
136. Siegel, R.L., K.D. Miller, and A. Jemal, *Cancer statistics, 2015.* CA: a cancer journal for clinicians, 2015. **65**(1): p. 5-29.
137. Martín, M.A., L. Goya, and S. Ramos, *Preventive effects of cocoa and cocoa antioxidants in colon cancer.* Diseases, 2016. **4**(1): p. 6.
138. Shanmugam, M.K., et al. *Cancer prevention and therapy through the modulation of transcription factors by bioactive natural compounds*. in *Seminars in cancer biology*. 2016. Elsevier.
139. Lu, Y., et al., *TAB1: a target of triptolide in macrophages.* Chemistry & biology, 2014. **21**(2): p. 246-256.
140. Pan, J., *RNA polymerase–an important molecular target of triptolide in cancer cells.* Cancer letters, 2010. **292**(2): p. 149-152.
141. Bywater, M.J., et al., *Dysregulation of the basal RNA polymerase transcription apparatus in cancer.* Nature Reviews Cancer, 2013. **13**(5): p. 299-314.
142. Kellner, W.A., et al., *Distinct isoforms of the Drosophila Brd4 homologue are present at enhancers, promoters and insulator sites.* Nucleic acids research, 2013. **41**(20): p. 9274-9283.
143. Zhao, Q., et al., *Natural products triptolide, celastrol, and withaferin A inhibit the chaperone activity of peroxiredoxin I.* Chemical Science, 2015. **6**(7): p. 4124-4130.
144. Zhang, J., et al., *Development of a novel method for quantification of autophagic protein degradation by AHA labeling.* Autophagy, 2014. **10**(5): p. 901-912.
145. Lu, W., et al., *Peroxiredoxin 2 is upregulated in colorectal cancer and contributes to colorectal cancer cells' survival by protecting cells from oxidative stress.* Molecular and cellular biochemistry, 2014. **387**(1-2): p. 261-270.

146. Rhee, S.G., et al., *Peroxiredoxin functions as a peroxidase and a regulator and sensor of local peroxides.* Journal of Biological Chemistry, 2012. **287**(7): p. 4403-4410.
147. Muchowicz, A., et al., *Adenanthin targets proteins involved in the regulation of disulphide bonds.* Biochemical pharmacology, 2014. **89**(2): p. 210-216.
148. Winterbourn, C.C., *Reconciling the chemistry and biology of reactive oxygen species.* Nature chemical biology, 2008. **4**(5): p. 278-286.
149. Kang, S.W., et al., *2-Cys peroxiredoxin function in intracellular signal transduction: therapeutic implications.* Trends in molecular medicine, 2005. **11**(12): p. 571-578.
150. Stresing, V., et al., *Peroxiredoxin 2 specifically regulates the oxidative and metabolic stress response of human metastatic breast cancer cells in lungs.* Oncogene, 2013. **32**(6): p. 724-735.
151. Liu, C.-X., et al., *Adenanthin targets peroxiredoxin I and II to induce differentiation of leukemic cells.* Nature chemical biology, 2012. **8**(5): p. 486-493.
152. Rosengarth, A. and H. Luecke, *A calcium-driven conformational switch of the N-terminal and core domains of annexin A1.* Journal of molecular biology, 2003. **326**(5): p. 1317-1325.
153. Benz, J. and A. Hofmann, *Annexins: from structure to function.* Biological chemistry, 1996. **378**(3-4): p. 177-183.
154. Hayes, M.J., et al., *Annexin–actin interactions.* Traffic, 2004. **5**(8): p. 571-576.
155. Revenu, C., et al., *The co-workers of actin filaments: from cell structures to signals.* Nature reviews Molecular cell biology, 2004. **5**(8): p. 635-646.
156. Guo, C., S. Liu, and M.-Z. Sun, *Potential role of Anxa1 in cancer.* Future oncology, 2013. **9**(11): p. 1773-1793.
157. Guzmán-Aránguez, A., et al., *Differentiation of human colon adenocarcinoma cells alters the expression and intracellular localization of annexins A1, A2, and A5.* Journal of cellular biochemistry, 2005. **94**(1): p. 178-193.
158. Lecona, E., et al., *Upregulation of annexin A1 expression by butyrate in human colon adenocarcinoma cells: role of p53, NF-Y, and p38 mitogen-activated protein kinase.* Molecular and cellular biology, 2008. **28**(15): p. 4665-4674.
159. Bizzarro, V., et al., *Annexin A1 induces skeletal muscle cell migration acting through formyl peptide receptors.* PloS one, 2012. **7**(10): p. e48246.
160. Lim, L.H. and S. Pervaiz, *Annexin 1: the new face of an old molecule.* The FASEB Journal, 2007. **21**(4): p. 968-975.
161. Boudhraa, Z., et al., *Annexin A1 localization and its relevance to cancer.* Clinical Science, 2016. **130**(4): p. 205-220.
162. Duncan, R., et al., *Characterisation and protein expression profiling of annexins in colorectal cancer.* British journal of cancer, 2008. **98**(2): p. 426-433.
163. García, Á., et al., *A global proteomics approach identifies novel phosphorylated signaling proteins in GPVI-activated platelets: Involvement of G6f, a novel platelet Grb2-binding membrane adapter.* Proteomics, 2006. **6**(19): p. 5332-5343.
164. Lomenick, B., et al., *Target identification using drug affinity responsive target stability (DARTS).* Proceedings of the National Academy of Sciences, 2009. **106**(51): p. 21984-21989.
165. Bertucci, C., et al., *Drug affinity to immobilized target bio-polymers by high-performance liquid chromatography and capillary electrophoresis.* Journal of Chromatography B, 2003.

797(1): p. 111-129.

166. Zhou, B., et al., *Synthesis and biological evaluation of novel triptolide analogues for anticancer activity.* Bioorganic & medicinal chemistry letters, 2010. **20**(21): p. 6217-6221.
167. Yuan, H., J.H. Musser, and D. Dai, *Triptolide lactone ring derivatives as immunomodulators and anticancer agents*. 2013, Google Patents.
168. Kupchan, S.M. and R.M. Schubert, *Selective alkylation: a biomimetic reaction of the antileukemic triptolides?* Science, 1974. **185**(4153): p. 791-793.
169. Dai, D., J.M. Fidler, and J.H. Musser, *Amino acid derivatives of triptolide compounds as immune modulators and anticancer agents*. 2003, Google Patents.
170. Butler, M.S., *Natural products to drugs: natural product-derived compounds in clinical trials.* Natural product reports, 2008. **25**(3): p. 475-516.
171. Li, Z., et al., *Design and synthesis of novel C14-hydroxyl substituted triptolide derivatives as potential selective antitumor agents.* Journal of medicinal chemistry, 2009. **52**(16): p. 5115-5123.
172. Hirotsu, S., et al., *Crystal structure of a multifunctional 2-Cys peroxiredoxin heme-binding protein 23 kDa/proliferation-associated gene product.* Proceedings of the National Academy of Sciences, 1999. **96**(22): p. 12333-12338.
173. Moore, R.B., et al., *Reconstitution of Ca (2+)-dependent K+ transport in erythrocyte membrane vesicles requires a cytoplasmic protein.* Journal of Biological Chemistry, 1991. **266**(28): p. 18964-18968.
174. Zhang, P., et al., *Thioredoxin peroxidase is a novel inhibitor of apoptosis with a mechanism distinct from that of Bcl-2.* Journal of Biological Chemistry, 1997. **272**(49): p. 30615-30618.
175. Park, S.-H., et al., *Antisense of human peroxiredoxin II enhances radiation-induced cell death.* Clinical cancer research, 2000. **6**(12): p. 4915-4920.
176. Trachootham, D., et al., *Redox regulation of cell survival.* Antioxidants & redox signaling, 2008. **10**(8): p. 1343-1374.
177. Ruckenstuhl, C., et al., *The Warburg effect suppresses oxidative stress induced apoptosis in a yeast model for cancer.* PloS one, 2009. **4**(2): p. e4592.
178. He, Z.-Y., et al., *Up-regulation of hnRNP A1, Ezrin, tubulin β-2C and Annexin A1 in sentinel lymph nodes of colorectal cancer.* World J Gastroenterol, 2010. **16**(37): p. 4670-4676.
179. Wang, Y.-J., et al., *Preliminary proteomic analysis of indomethacin's effect on tumor transplanted with colorectal cancer cell in nude mice.* BMB Reports, 2006. **39**(2): p. 171-177.
180. Mujumdar, N., et al., *Triptolide induces cell death in pancreatic cancer cells by apoptotic and autophagic pathways.* Gastroenterology, 2010. **139**(2): p. 598-608.
181. Schieffer, B., et al., *Role of NAD (P) H oxidase in angiotensin II–induced JAK/STAT signaling and cytokine induction.* Circulation Research, 2000. **87**(12): p. 1195-1201.
182. Annunziato, L., et al., *Modulation of ion channels by reactive oxygen and nitrogen species: a pathophysiological role in brain aging?* Neurobiology of aging, 2002. **23**(5): p. 819-834.
183. Ram ́ez, A., et al., *Ion Channels and Oxidative Stress as a Potential Link for the Diagnosis or Treatment of Liver Diseases.* Oxidative medicine and cellular longevity, 2016. **2016**.
184. Duan, L., et al., *S100A6 stimulates proliferation and migration of colorectal carcinoma cells through activation of the MAPK pathways.* International journal of oncology, 2014. **44**(3): p.

781-790.

185. Wang, L., et al., *The roles of integrin β4 in vascular endothelial cells.* Journal of cellular physiology, 2012. **227**(2): p. 474-478.

186. Havens, C.G., et al., *Regulation of late G1/S phase transition and APCCdh1 by reactive oxygen species.* Molecular and Cellular Biology, 2006. **26**(12): p. 4701-4711.

187. Chang, W.-T., et al., *Triptolide and chemotherapy cooperate in tumor cell apoptosis A role for the p53 pathway.* Journal of Biological Chemistry, 2001. **276**(3): p. 2221-2227.

188. Manzo, S.G., et al., *Natural product triptolide mediates cancer cell death by triggering CDK7-dependent degradation of RNA polymerase II.* Cancer research, 2012. **72**(20): p. 5363-5373.

189. Venkataraman, S., et al., *Inhibition of BRD4 attenuates tumor cell self-renewal and suppresses stem cell signaling in MYC driven medulloblastoma.* Oncotarget, 2014. **5**(9): p. 2355-2371.

Appendices I: Significantly regulated proteins by triptolide with 6 hrs of treatment

N	Unused	Total	% Cov	Accession #	Protein ID	Peptides (95%)	114:113	118:113	114:117	118:117	Geometric Mean
1	5.88	5.94	43.5	Q8IZ73	RNA pseudouridylate synthase domain-containing protein 2	3	0.8889	0.6453	0.4161	0.3022	0.518234936
2	2.04	2.06	24.9	Q3ZCQ8	Mitochondrial import inner membrane translocase subunit TIM50	1	0.5741	0.4644	0.6994	0.566	0.569974537
3	**2.05**	**2.14**	**48**	**Q9UL25**	**Ras-related protein Rab-21**	**2**	**0.5654**	**0.5481**	**0.6494**	**0.6298**	**0.596667849**
4	2.17	4.51	34.5	Q9Y4I1	Unconventional myosin-Va	2	0.7163	0.7205	0.5387	0.5355	0.621167674
5	4.21	4.81	34.9	Q8WVB6	Chromosome transmission fidelity protein 18 homolog	2	0.5547	0.8994	0.4371	0.7091	0.627082723
6	1.49	1.71	44.4	P49720	Proteasome subunit beta type-3	1	0.5338	0.4026	0.9884	0.7458	0.630887415
7	2	2.05	18.4	P23511	Nuclear transcription factor Y subunit alpha	1	0.6126	0.6426	0.6207	0.6513	0.631604382
8	2	2	37.1	Q14657	EKC/KEOPS complex subunit LAGE3	1	0.474	0.5489	0.7495	0.8683	0.64147281
9	2.02	2.16	20.7	Q969X6	Cirhin	2	0.8512	0.636	0.7146	0.5341	0.674207501
10	2.03	7.01	45.1	P48735	Isocitrate dehydrogenase [NADP], mitochondrial	4	0.653	0.6704	0.6925	0.7113	0.681443641
11	0.91	1.07	37.8	Q9HBL8	NmrA-like family domain-containing protein 1	1	0.8093	0.7309	0.6528	0.5898	0.690817139
12	2.1	2.53	46.2	Q9BZL4	Protein phosphatase 1 regulatory subunit 12C	1	1.0717	0.6249	0.7863	0.445	0.695757683
13	1.46	1.47	20.2	Q96RF0	Sorting nexin-18	1	0.7211	0.8565	0.5642	0.68	0.69769597
14	2	2.16	34	Q96C57	Uncharacterized protein C12orf43	1	0.6217	0.6368	0.7672	0.7862	0.69904702
15	4.03	4.47	56.6	Q9Y2Q3	Glutathione S-transferase kappa 1	2	0.4663	0.6322	0.7804	1.0586	0.702493426
16	1.09	1.15	54.2	Q9NP97	Dynein light chain roadblock-type 1	1	0.7304	1.0546	0.4714	0.6809	0.705148134
17	1.14	1.17	19.5	Q96N66	Lysophospholipid acyltransferase 7	1	0.5777	0.7694	0.6486	0.8642	0.706498817
18	2.01	2.35	28.8	Q643R3	Lysophospholipid acyltransferase LPCAT4	1	0.8002	0.5424	0.9287	0.6297	0.709793212
19	2.02	2.24	28.4	Q96G23	Ceramide synthase 2	1	0.6525	0.7074	0.7215	0.784	0.714824604

20	2.08	2.25	16.4	Q8N5C8	TGF-beta-activated kinase 1 and MAP3K7-binding protein 3	1	0.6535	0.7081	0.7251	0.7807	0.715410925
21	2.1	3.35	34.5	O60343	TBC1 domain family member 4	2	0.8401	0.9744	0.5392	0.627	0.725306252
22	1.24	1.65	26.9	Q9UI17	Dimethylglycine dehydrogenase, mitochondrial	1	0.8027	0.5612	0.95	0.6645	0.730251368
23	2.03	2.07	45.8	Q9NS69	Mitochondrial import receptor subunit TOM22 homolog	1	0.8418	0.648	0.8606	0.6627	0.746836543
24	2.01	2.48	35.7	Q9UBB9	Tuftelin-interacting protein 11	1	0.7696	0.7037	0.8105	0.74	0.754934612
25	1.79	2.69	37.5	Q8TD16	Protein bicaudal D homolog 2	1	0.8568	0.8403	0.6919	0.6788	0.762561274
26	4	4.05	27.1	O15127	Secretory carrier-associated membrane protein 2	2	0.8483	0.7125	0.8098	0.7088	0.767465664
27	1.01	1.24	48.4	O43427	Acidic fibroblast growth factor intracellular-binding protein	1	0.9037	0.7387	0.8039	0.6574	0.770692313
28	7.52	7.54	59	Q15287	RNA-binding protein with serine-rich domain 1	7	0.7128	0.6574	0.9266	0.8455	0.778396411
29	2	2.15	33.7	P23786	Carnitine O-palmitoyltransferase 2, mitochondrial	2	0.8638	0.7553	0.8054	0.7045	0.780021057
30	4	4.09	46.6	P37235	Hippocalcin-like protein 1	2	0.827	0.9724	0.6327	0.7442	0.784439565
31	2.04	3.12	33.7	P46100	Transcriptional regulator ATRX	1	0.6299	0.7939	0.7823	0.9822	0.787322509
32	2.01	4.86	29.7	O15357	Phosphatidylinositol 3,4,5-trisphosphate 5-phosphatase 2	2	0.7088	0.8396	0.7419	0.8792	0.789327615
33	5.52	6.54	37.1	Q9UKE5	TRAF2 and NCK-interacting protein kinase	3	0.7532	0.601	1.0392	0.8295	0.790360228
34	4.29	4.57	32.1	Q08J23	tRNA (cytosine(34)-C(5))-methyltransferase	3	0.7543	0.7995	0.7824	0.8323	0.791621951
35	2	2.07	16.4	O95365	Zinc finger and BTB domain-containing protein 7A	1	0.6824	0.79	0.7979	0.9241	0.794023555
36	2.08	2.55	46.8	Q9NRP2	COX assembly mitochondrial protein 2 homolog	1	0.6997	0.798	0.7937	0.9061	0.796043534
37	1.52	1.62	47.2	Q03135	Caveolin-1	2	0.6692	0.769	0.8513	0.9787	0.809195806
38	2.34	2.45	30.5	Q96DV4	39S ribosomal protein L38, mitochondrial	1	0.9013	0.8173	0.8042	0.7267	0.810013999
39	2.44	2.66	32.8	Q8IY37	Probable ATP-dependent RNA helicase DHX37	1	0.8193	0.9392	0.7043	0.8081	0.813497005
40	1.92	2.04	35.4	Q9HCC0	Methylcrotonoyl-CoA carboxylase beta chain, mitochondrial	1	0.7782	0.7943	0.8398	0.8575	0.816810754
41	2.06	2.55	49.1	Q9NUL3	Double-stranded RNA-binding protein Staufen homolog 2	1	0.7673	0.835	0.8133	0.8855	0.824181293
42	1.39	1.57	23.5	Q15165	Serum paraoxonase/arylesterase 2	1	0.8327	0.7952	0.8541	0.816	0.824215835
43	3.43	3.69	42.3	P82675	28S ribosomal protein S5, mitochondrial	3	0.8245	0.9029	0.7684	0.8418	0.833022338

44	2.01	2.25	20.9	Q8TDN4	CDK5 and ABL1 enzyme substrate 1	1	0.6406	0.8314	0.8477	1.1006	0.839589815
45	0.83	0.9	22	Q6UWP7	Lysocardiolipin acyltransferase 1	2	1.1766	1.1108	1.2534	1.1838	1.180071129
46	2.03	7.41	63.1	P12235	ADP/ATP translocase 1	9	1.2137	1.1878	1.1761	1.1509	1.181909241
47	4.32	5.78	53.9	P53367	Arfaptin-1	4	1.1058	1.1753	1.1899	1.2641	1.182440522
48	2.44	2.54	47.3	P49914	5-formyltetrahydrofolate cyclo-ligase	1	1.174	1.4003	1.0012	1.1948	1.184203418
49	4.38	5.48	33.2	Q15003	Condensin complex subunit 2	3	1.1785	1.1134	1.2706	1.2009	1.189526509
50	2.03	2.35	31.1	O95260	Arginyl-tRNA--protein transferase 1	1	1.2338	1.3227	1.066	1.1801	1.197003812
51	1.39	3.69	53	O43583	Density-regulated protein	2	1.0967	1.1777	1.2408	1.334	1.209191354
52	2.99	3.15	31.8	Q8TBF2	Prostamide/prostaglandin F synthase	2	1.1326	1.2111	1.2276	1.3125	1.219279265
53	2.11	4.87	44.2	Q9H0B6	Kinesin light chain 2	2	1.4322	1.265	1.1792	1.046	1.222653337
54	6.02	6.22	21.6	Q9BQA1	Methylosome protein 50	3	1.2756	1.3092	1.1462	1.1757	1.224811788
55	2.07	2.77	30.4	Q92576	PHD finger protein 3	1	1.2778	1.2516	1.2085	1.1842	1.22998563
56	0.81	1.19	30.5	Q96DN5	TBC1 domain family member 31	2	1.1767	1.552	0.9744	1.2915	1.231252964
57	2.71	3.07	17.1	Q9BV38	WD repeat-containing protein 18	2	1.2538	1.3543	1.1342	1.218	1.2375707
58	2.05	2.86	39.8	Q96T58	Msx2-interacting protein	1	1.1769	1.413	1.092	1.3112	1.242205151
59	7.61	7.89	39.1	P04844	Dolichyl-diphosphooligosaccharide--protein glycosyltransferase subunit 2	7	1.3118	1.2897	1.2068	1.1772	1.245117882
60	2.01	2.06	70.1	Q9NYJ1	Cytochrome c oxidase assembly factor 4 homolog	1	0.9875	1.3194	1.1797	1.5769	1.247734918
61	2	2	49.5	P07311	Acylphosphatase-1	1	1.3157	1.5866	0.9915	1.1961	1.25435693
62	4	4.05	40.1	Q7Z6J9	tRNA-splicing endonuclease subunit Sen54	2	1.2558	1.6058	0.9855	1.2607	1.258114241
63	2	2.08	32.1	Q14232	Translation initiation factor eIF-2B subunit alpha	1	1.272	1.1869	1.3474	1.2578	1.264743173
64	5.78	6.96	34.9	Q5JRA6	Melanoma inhibitory activity protein 3	3	1.3028	1.5837	1.0108	1.2284	1.26514099
65	1.36	1.48	21.7	A8CG34	Nuclear envelope pore membrane protein POM 121C	1	1.3548	1.6958	0.946	1.1846	1.266712835
66	4.57	4.75	32.2	P30566	Adenylosuccinate lyase	3	1.2093	1.4196	1.1501	1.3377	1.274819193

67	2	2.08	29.1	P62306	Small nuclear ribonucleoprotein F	2	1.0202	1.3411	1.2367	1.6264	1.287981283
68	2	2.14	33.9	Q7Z7F0	UPF0469 protein KIAA0907	1	1.2582	1.2973	1.2793	1.3196	1.28840144
69	1.51	1.69	38.8	O75521	Enoyl-CoA delta isomerase 2, mitochondrial	1	1.5508	1.331	1.1765	1.1519	1.293257898
70	2	2.08	28	Q9Y5P4	Collagen type IV alpha-3-binding protein	1	1.4563	1.2925	1.3004	1.1546	1.296574508
71	2.02	2.03	52.3	O60783	28S ribosomal protein S14, mitochondrial	1	1.4756	1.2886	1.324	1.1567	1.306317887
72	2.01	5.33	27.5	O14787	Transportin-2	2	1.106	1.2895	1.3265	1.5473	1.308020539
73	1.03	3.09	31.4	P38432	Coilin	2	1.8665	1.3157	1.301	0.9175	1.308479912
74	4.19	4.45	28.4	Q8WTS6	Histone-lysine N-methyltransferase SETD7	2	1.1186	1.2423	1.3846	1.5383	1.311646084
75	6.09	6.14	33	Q10713	Mitochondrial-processing peptidase subunit alpha	3	1.2982	1.3639	1.2722	1.3372	1.317403987
76	4.51	5.12	66.5	P61289	Proteasome activator complex subunit 3	2	1.5942	1.2356	1.4124	1.0951	1.321168006
77	0.87	1.09	39.7	Q9UL03	Integrator complex subunit 6	1	1.4899	1.2687	1.3787	1.1744	1.322666852
78	6.7	8.15	46	O43795	Unconventional myosin-Ib	5	1.2389	1.1944	1.8665	1.1198	1.326137714
79	2.21	2.87	29.7	Q96N67	Dedicator of cytokinesis protein 7	1	1.5934	1.496	1.1804	1.1087	1.328999794
80	2.04	2.15	55.7	Q5HYK3	2-methoxy-6-polyprenyl-1,4-benzoquinol methylase	1	1.4744	1.1125	1.5896	1.2	1.329983063
81	2.43	3.07	28	P35568	Insulin receptor substrate 1	4	1.3685	1.1572	1.5388	1.3017	1.334555309
82	0.81	0.87	27.1	Q9GZT8	Putative GTP cyclohydrolase 1 type 2 NIF3L1	1	1.1291	1.3553	1.34	1.6091	1.347764211
83	0.81	1.32	39.8	O75335	Liprin-alpha-4	1	1.5417	1.5785	1.1509	1.1788	1.347970984
84	2	2.01	20.6	Q9BV86	N-terminal Xaa-Pro-Lys N-methyltransferase 1	1	1.668	1.5522	1.1836	1.1018	1.355541639
85	2.01	2.09	47.9	Q9NRN7	L-aminoadipate-semialdehyde dehydrogenase-phosphopantetheinyl transferase	1	1.0395	1.3138	1.4055	1.777	1.358995464
86	0.83	2.34	25	Q8IYQ7	Threonine synthase-like 1	2	1.4592	1.7071	1.0914	1.2774	1.365121043
87	2.01	2.08	31.7	P54105	Methylosome subunit pICln	1	1.4891	1.4672	1.2711	1.2529	1.365769241
88	5.6	6.26	37.9	P22033	Methylmalonyl-CoA mutase, mitochondrial	4	1.3729	1.2018	1.6103	1.4228	1.394377732
89	2.02	3.72	25.3	Q8TCU6	Phosphatidylinositol 3,4,5-trisphosphate-dependent Rac	2	1.0651	1.2473	1.5981	1.8723	1.412001552

					exchanger 1 protein						
90	5.87	6.6	23.7	P50851	Lipopolysaccharide-responsive and beige-like anchor protein	3	1.434	1.4176	1.4225	1.4068	1.420191381
91	2	2.15	24.1	Q9HBU6	Ethanolamine kinase 1	1	1.2945	1.0813	1.878	1.5693	1.425156163
92	2.02	2.16	29.3	Q96BN8	Ubiquitin thioesterase otulin	1	1.9127	1.6111	1.2635	1.0647	1.426898114
93	1.27	1.77	28.7	P55196	Afadin	1	1.348	1.9482	1.0697	1.5467	1.44376955
94	2.05	2.99	31.3	P52306	Rap1 GTPase-GDP dissociation stimulator 1	2	2.2211	1.4517	1.556	1.0174	1.503095514
95	1.71	1.83	31.7	Q00577	Transcriptional activator protein Pur-alpha	1	1.445	1.3698	1.7347	1.6451	1.541648705
96	2.02	2.31	19.5	P54802	Alpha-N-acetylglucosaminidase	1	1.836	2.0465	1.2172	1.3572	1.578419927
97	2.01	2.2	19.4	Q8NE86	Calcium uniporter protein, mitochondrial	1	1.8466	0.9031	2.7659	1.3532	1.580617494
98	2.12	2.73	40.3	O75746	Calcium-binding mitochondrial carrier protein Aralar1	1	1.3355	1.6134	1.5631	1.8892	1.588227316
99	2.04	4.47	34.5	Q10570	Cleavage and polyadenylation specificity factor subunit 1	2	1.701	2.1374	1.194	1.5009	1.597668052
100	1.08	1.1	61.2	O15145	Actin-related protein 2/3 complex subunit 3	1	1.5386	1.4174	1.8238	1.6808	1.607969667
101	3.06	3.13	32.2	Q9Y639	Neuroplastin	2	1.3418	1.3315	2.2059	2.1899	1.713995848
102	2.85	3.82	32.5	O95834	Echinoderm microtubule-associated protein-like 2	3	1.6602	2.2618	1.3354	1.8201	1.738122204
103	6.13	15.1	40.9	P13645	Keratin, type I cytoskeletal 10	9	2.5131	0.9875	3.0897	1.216	1.747427598
104	2.01	2.35	34.5	Q9BYM8	RanBP-type and C3HC4-type zinc finger-containing protein 1	1	1.3464	1.02	3.3829	2.5638	1.857748394
105	2.04	2.47	22.2	Q8N612	FTS and Hook-interacting protein	1	4.4072	1.8706	2.5641	1.0888	2.190315568

Appendices II: Significantly regulated proteins by triptolide with 48 hrs of treatment

N	Unused	Total	% Cov	Accession #	Protein ID	Peptides (95%)	114:113	118:113	114:117	118:117	Geometric Mean
1	1.42	1.62	28.9	Q8N806	Putative E3 ubiquitin-protein ligase UBR7	1	0.7761	0.9133	0.01	0.0117	0.095428753
2	2.04	2.47	22.2	Q8N612	FTS and Hook-interacting protein	1	0.5258	0.7641	0.0963	0.1417	0.272108263
3	0.79	1.1	50.3	Q8N998	Coiled-coil domain-containing protein 89	1	0.3728	1.0384	0.0862	0.2431	0.30011189
4	2.02	2.31	19.5	P54802	Alpha-N-acetylglucosaminidase	1	0.391	0.5643	0.2791	0.4079	0.398107251
5	2	2.15	24.1	Q9HBU6	Ethanolamine kinase 1	1	0.5504	0.9944	0.1871	0.3423	0.432693187
6	2.01	2.01	16.1	Q9UHY7	Enolase-phosphatase E1	1	0.5985	0.5046	0.4156	0.3548	0.459375298
7	1.4	1.4	19.9	A6NDG6	Phosphoglycolate phosphatase	1	0.3097	0.6853	0.3379	0.7572	0.482730994
8	1	3.72	32.1	Q8WXE1	ATR-interacting protein	2	0.6479	0.4825	0.5029	0.3792	0.494127262
9	1.49	1.75	57.9	P57076	UPF0769 protein C21orf59	1	0.2597	0.3952	0.6294	0.97	0.50031882
10	2	4.35	23.3	Q9NQH7	Probable Xaa-Pro aminopeptidase 3	3	0.295	0.6817	0.4388	1.0272	0.548699084
11	**1.9**	**4.95**	**26.2**	**O60885**	**Bromodomain-containing protein 4**	**2**	**0.3136**	**0.9782**	**0.3862**	**0.7774**	**0.550890305**
12	2.12	2.73	40.3	O75746	Calcium-binding mitochondrial carrier protein Aralar1	1	0.4143	1.1764	0.2677	0.77	0.562992049
13	1.24	1.65	26.9	Q9UI17	Dimethylglycine dehydrogenase, mitochondrial	1	0.768	0.7614	0.4552	0.457	0.590572386
14	2.18	2.66	24.7	Q14202	Zinc finger MYM-type protein 3	1	0.501	0.8416	0.4119	0.7007	0.59063182
15	2.09	2.28	46.4	Q14554	Protein disulfide-isomerase A5	2	0.6887	0.6918	0.5144	0.5207	0.597688355
16	**2.07**	**4.13**	**35.7**	**Q92974**	**Rho guanine nucleotide exchange factor 2**	**2**	**0.381**	**0.5412**	**0.694**	**0.9984**	**0.614804024**
17	0.83	0.93	25.1	Q99720	Sigma non-opioid intracellular receptor 1	1	0.4894	0.704	0.5359	0.7807	0.616170838
18	2.11	3.21	34.5	O95425	Supervillin	1	0.548	0.9145	0.424	0.7166	0.624671558
19	2.4	3.68	28.2	Q9UKK3	Poly [ADP-ribose] polymerase 4	2	0.3412	0.7111	0.5609	1.184	0.633569425
20	2.03	2.51	24	Q16706	Alpha-mannosidase 2	1	0.5899	0.8873	0.4671	0.7116	0.645838114

21	2.02	2.04	32.7	P12955	Xaa-Pro dipeptidase	1	0.6719	0.9059	0.4742	0.6475	0.657501209
22	**5.56**	**5.56**	**57.1**	**P35080**	**Profilin-2**	**4**	**0.6412**	**0.8511**	**0.512**	**0.677**	**0.659489953**
23	2	2.07	20.4	Q86U90	YrdC domain-containing protein, mitochondrial	1	0.8028	1	0.435	0.5487	0.661618888
24	2.11	4.87	44.2	Q9H0B6	Kinesin light chain 2	2	0.6901	0.6597	0.6585	0.6498	0.664352387
25	2.04	4.47	34.5	Q10570	Cleavage and polyadenylation specificity factor subunit 1	2	0.3946	0.6148	0.7145	1.1277	0.664923509
26	2.01	5.33	27.5	O14787	Transportin-2	2	0.4358	0.7847	0.5784	1.0548	0.675845336
27	1.99	2.22	51.1	Q86Y82	Syntaxin-12	2	0.6865	0.5066	0.9201	0.6876	0.684887368
28	1.82	2.12	30	Q15054	DNA polymerase delta subunit 3	1	0.5404	0.7378	0.6398	0.8848	0.68926438
29	1.81	1.86	27.2	O94888	UBX domain-containing protein 7	2	0.6687	0.4834	0.9836	0.7201	0.691731137
30	2.04	2.18	50	Q9BRT2	Ubiquinol-cytochrome-c reductase complex assembly factor 2	1	0.435	0.8123	0.5874	1.1109	0.692952801
31	10.11	11.1	43.9	O75150	E3 ubiquitin-protein ligase BRE1B	6	0.6241	0.6992	0.6866	0.7789	0.695040763
32	2	2	32.7	Q96C90	Protein phosphatase 1 regulatory subunit 14B	1	0.6325	0.7888	0.6135	0.7749	0.697865799
33	3.24	4.21	44.2	Q6WCQ1	Myosin phosphatase Rho-interacting protein	2	0.5869	0.7121	0.6797	0.8352	0.697916093
34	4.09	4.58	43.8	Q9Y5K5	Ubiquitin carboxyl-terminal hydrolase isozyme L5	3	0.5133	0.7494	0.6573	0.9718	0.704054648
35	6.14	6.41	62.1	P63162	Small nuclear ribonucleoprotein-associated protein N	5	0.756	0.7527	0.653	0.6682	0.705896195
36	15.47	15.47	20.8	P16070	CD44 antigen	12	0.6772	0.7051	0.7073	0.7503	0.70949864
37	**1.38**	**1.62**	**27.6**	**P19388**	**DNA-directed RNA polymerases I, II, and III subunit RPABC1**	**4**	**0.6928**	**0.7135**	**0.7041**	**0.7502**	**0.714830896**
38	4.04	4.19	38.7	Q96A33	Coiled-coil domain-containing protein 47	2	0.7827	0.6842	0.7535	0.6659	0.719975418
39	2.01	2.07	24.4	Q96AB3	Isochorismatase domain-containing protein 2	1	0.6836	0.7645	0.6748	0.7644	0.7205578
40	2.9	3.2	25.4	Q06587	E3 ubiquitin-protein ligase RING1	2	0.7359	0.6674	0.7774	0.7176	0.723490767
41	1.98	2.31	47.3	P53004	Biliverdin reductase A	1	0.8144	0.8382	0.6208	0.6471	0.72364761
42	0.97	1.02	36.4	Q6ZSJ8	Uncharacterized protein C1orf122	1	0.4765	0.7618	0.6865	1.1114	0.725443681

43	1.36	1.77	28.2	Q9Y2L9	Leucine-rich repeat and calponin homology domain-containing protein 1	1	0.5285	0.6973	0.7615	1.0174	0.730981818
44	4.48	5.57	44.8	Q9H2G2	STE20-like serine/threonine-protein kinase	2	0.7068	1.0141	0.5246	0.7741	0.734515
45	0.9	0.94	26.5	A6NJ78	Probable methyltransferase-like protein 15	1	0.7517	0.7237	0.7453	0.7267	0.736753743
46	2.04	2.06	24.9	Q3ZCQ8	Mitochondrial import inner membrane translocase subunit TIM50	1	0.8048	0.7501	0.7245	0.6838	0.739509325
47	2	2	37.1	Q14657	EKC/KEOPS complex subunit LAGE3	1	0.7086	0.8904	0.6132	0.7804	0.741270004
48	2	2.08	32.4	Q9UNL2	Translocon-associated protein subunit gamma	1	0.5257	0.7136	0.7664	1.0537	0.741893086
49	2.02	2.14	26.6	Q9Y2Z4	Tyrosine--tRNA ligase, mitochondrial	1	0.6182	0.7722	0.708	0.8964	0.741905304
50	1.49	1.71	44.4	P49720	Proteasome subunit beta type-3	1	0.8182	0.6287	0.8701	0.6772	0.741988652
51	3.63	4.48	41.8	P52756	RNA-binding protein 5	3	0.7899	0.7195	0.7814	0.7168	0.751136003
52	21.83	22.66	36.1	P28290	Sperm-specific antigen 2	15	0.7084	0.7865	0.7158	0.805	0.752733446
53	2.06	2.25	21.1	Q15334	Lethal(2) giant larvae protein homolog 1	1	0.6827	0.7319	0.7933	0.8613	0.764395969
54	2.47	2.71	44.8	Q9GZT9	Egl nine homolog 1	1	0.7014	0.8026	0.7267	0.8387	0.765343997
55	3.74	6.13	48	Q9UDT6	CAP-Gly domain-containing linker protein 2	3	0.6731	0.7108	0.8171	0.8809	0.76605016
56	2.02	2.13	18.5	Q00613	Heat shock factor protein 1	1	0.8833	0.8056	0.7314	0.6687	0.768074756
57	1.76	1.9	35.8	Q8TB36	Ganglioside-induced differentiation-associated protein 1	1	0.731	0.8617	0.6847	0.8175	0.770575842
58	2	4.77	55.8	Q9NQ29	Putative RNA-binding protein Luc7-like 1	3	0.5996	0.7744	0.7633	0.9984	0.771270465
59	**16.54**	**16.81**	**45.3**	**P08243**	**Asparagine synthetase [glutamine-hydrolyzing]**	**11**	**0.7454**	**0.8266**	**0.7224**	**0.8116**	**0.77526672**
60	3.25	3.61	26	Q9UJY5	ADP-ribosylation factor-binding protein GGA1	2	0.7717	0.927	0.6458	0.7861	0.776293622
61	20.02	20.42	60	Q9Y617	Phosphoserine aminotransferase	15	0.7914	0.7449	0.8025	0.7715	0.777264348
62	2.02	2.2	34.8	P13051	Uracil-DNA glycosylase	1	0.7731	1.0161	0.595	0.7909	0.779745122
63	5.8	6.35	44.3	Q12874	Splicing factor 3A subunit 3	3	0.7329	0.7826	0.7746	0.8372	0.780949263
64	2.22	2.45	52.5	Q9BT09	Protein canopy homolog 3	1	0.6798	0.799	0.761	0.9054	0.782146798
65	10.05	10.17	52.4	P20340	Ras-related protein Rab-6A	6	0.687	0.8036	0.7551	0.9014	0.782942147

66	12.18	12.24	45.5	Q9UK76	Hematological and neurological expressed 1 protein	7	0.7801	0.8777	0.697	0.8025	0.78667174
67	8.25	8.37	41.5	Q13011	Delta(3,5)-Delta(2,4)-dienoyl-CoA isomerase, mitochondrial	5	0.7636	0.8834	0.7013	0.8161	0.788256631
68	4.04	4.36	30.4	Q92615	La-related protein 4B	4	0.7895	0.7766	0.7982	0.8011	0.791292399
69	0.86	0.88	24	P85037	Forkhead box protein K1	1	0.809	0.8715	0.7166	0.7819	0.792795146
70	2	2.23	18	Q9Y2H6	Fibronectin type-III domain-containing protein 3A	1	0.7925	0.7201	0.8722	0.8027	0.795042522
71	2	2.5	16.6	Q6AI08	HEAT repeat-containing protein 6	2	0.6783	0.7842	0.8142	0.9534	0.801611105
72	4	4.04	32.5	Q9Y6W5	Wiskott-Aldrich syndrome protein family member 2	2	0.7107	0.8058	0.7971	0.9153	0.803984105
73	1.3	1.9	32	O75600	2-amino-3-ketobutyrate coenzyme A ligase, mitochondrial	2	1.2238	1.2821	1.1714	1.2429	1.229400652
74	2	4	42.9	Q71UM5	40S ribosomal protein S27-like	3	1.2556	1.1402	1.3289	1.2222	1.23485718
75	5.2	5.44	44.1	P20962	Parathymosin	3	1.2417	1.2308	1.2359	1.2385	1.236718558
76	2.03	4.24	38.7	P56545	C-terminal-binding protein 2	5	1.0786	1.2337	1.2445	1.4394	1.24254348
77	4.72	5.03	31.3	P07686	Beta-hexosaminidase subunit beta	2	1.5851	1.2436	1.2591	0.9985	1.254689947
78	6.09	6.74	19	Q09161	Nuclear cap-binding protein subunit 1	4	1.5102	1.2563	1.2592	1.0549	1.259964933
79	2.02	2.7	37.6	P28838	Cytosol aminopeptidase	1	1.2451	1.2136	1.3323	1.3185	1.27641086
80	5.88	6.01	60.9	O95721	Synaptosomal-associated protein 29	3	1.2468	1.2107	1.3091	1.3595	1.280254593
81	2	2.14	18.4	Q96ER3	Protein SAAL1	1	1.7563	1.247	1.307	0.9399	1.280724147
82	34.79	35.09	67.5	P12277	Creatine kinase B-type	34	1.3693	1.2386	1.3199	1.2034	1.281135837
83	2.01	2.05	51.4	P41223	Protein BUD31 homolog	1	1.3812	1.2838	1.2787	1.2037	1.285316896
84	4.05	13.68	60.1	P12236	ADP/ATP translocase 3	11	1.4428	1.2506	1.3154	1.1519	1.285876601
85	2.02	2.16	20.7	Q969X6	Cirhin	2	0.9438	1.3318	1.247	1.7821	1.292794146
86	3.36	5.04	30.5	Q7Z2Z2	Elongation factor Tu GTP-binding domain-containing protein 1	3	0.9331	1.2873	1.3019	1.8248	1.299721235
87	4.23	4.53	40.2	O95817	BAG family molecular chaperone regulator 3	4	1.3442	1.3211	1.271	1.2667	1.300333425
88	10.78	10.82	39	P35613	Basigin	12	1.5403	1.2327	1.3649	1.1039	1.300538819
89	52.9	89.24	75.5	P08107	Heat shock 70 kDa protein 1A/1B	101	1.324	1.3061	1.2908	1.2848	1.301336841

90	128.81	129.8	51.9	P21333	Filamin-A	89	1.3878	1.2428	1.3604	1.2301	1.303418234
91	2.07	2.14	28.1	Q96K37	Solute carrier family 35 member E1	1	1.2496	0.9791	1.7286	1.3717	1.305082387
92	11.14	11.45	79.8	Q92522	Histone H1x	7	1.3328	1.2661	1.3525	1.3002	1.312487292
93	32.34	32.79	93.4	P60174	Triosephosphate isomerase	35	1.4853	1.3226	1.3155	1.1837	1.322494273
94	2	2.1	27.7	Q9H3P7	Golgi resident protein GCP60	2	1.2542	1.3311	1.3249	1.4241	1.332217906
95	26.15	26.19	82.4	P04792	Heat shock protein beta-1	29	1.3908	1.2884	1.3996	1.3027	1.344438486
96	2	2.34	37.8	P07738	Bisphosphoglycerate mutase	1	1.3928	1.3986	1.3095	1.3318	1.357630852
97	2.12	2.43	39.1	Q99986	Serine/threonine-protein kinase VRK1	1	1.2731	0.8303	2.1928	1.4831	1.36165396
98	6.41	6.91	69.7	O95232	Luc7-like protein 3	4	1.5591	1.2675	1.4623	1.2022	1.365239314
99	3.5	4.13	33	O15269	Serine palmitoyltransferase 1	2	1.3834	1.2662	1.4649	1.3579	1.366254049
100	5.09	5.11	55.8	Q14165	Malectin	3	1.4348	1.364	1.378	1.3128	1.371713399
101	1.25	1.3	60.9	P52298	Nuclear cap-binding protein subunit 2	1	1.4767	1.2776	1.5287	1.3395	1.401967804
102	2.01	2.2	19.4	Q8NE86	Calcium uniporter protein, mitochondrial	1	1.2402	1.1433	1.7248	1.6104	1.408740852
103	2.02	2.19	25.2	P61916	Epididymal secretory protein E1	1	1.7381	1.3945	1.5166	1.2223	1.455913374
104	2.01	4.25	38.6	P11802	Cyclin-dependent kinase 4	2	1.6988	1.497	1.4152	1.263	1.460146076
105	2.02	2.16	29.3	Q96BN8	Ubiquitin thioesterase otulin	1	1.526	1.519	1.3955	1.4068	1.460557392
106	1.86	1.91	21	P63151	Serine/threonine-protein phosphatase 2A 55 kDa regulatory subunit B alpha isoform	1	1.652	1.3953	1.5484	1.3245	1.474528566
107	28.48	29.58	55.1	P04181	Ornithine aminotransferase, mitochondrial	18	1.5017	1.4897	1.4606	1.4657	1.479328403
108	2.29	2.85	20.6	Q9UI26	Importin-11	1	1.5487	1.7944	1.2829	1.5053	1.522038389
109	6.27	6.5	44.4	P40938	Replication factor C subunit 3	4	1.3854	1.1991	1.9559	1.6865	1.529998111
110	2.01	2.07	56	P21291	Cysteine and glycine-rich protein 1	1	1.1669	1.3818	1.6968	2.0348	1.536058667
111	3.51	3.82	16	Q03519	Antigen peptide transporter 2	2	1.4693	1.5015	1.6749	1.7141	1.586409176
112	2.04	2.39	37.3	Q9H6S3	Epidermal growth factor receptor kinase substrate 8-like protein 2	1	1.5919	1.3545	1.9575	1.6831	1.632588078

113	15.78	16.15	64.5	P29373	Cellular retinoic acid-binding protein 2	8	1.9344	1.479	1.8301	1.3994	1.645253362
114	2	2.32	20.7	O43747	AP-1 complex subunit gamma-1	1	2.8456	1.3202	2.1342	1.0028	1.6838979
115	2.06	4.18	26.5	Q14997	Proteasome activator complex subunit 4	2	3.0597	1.3841	2.7493	1.2596	1.956929927
116	2.1	2.54	16.9	Q8IZL8	Proline-, glutamic acid- and leucine-rich protein 1	1	2.3912	1.4326	3.4722	2.0375	2.218762411

Appendices III: Direct binding targets of triptolide by pull down assay

N	Unused	Total	% Cov	Accession #	Protein ID	Peptides (95%)	119:117	121:117	119:118	121:118	Geometric Mean
1	4.69	4.69	17.2	Q15427	Splicing factor 3B subunit 4	4	2.133	2.2241	2.304	2.4021	2.263626038
2	4.02	6.43	23.1	O75367	Core histone macro-H2A.1	3	2.689	2.153	2.4928	2.0203	2.323723944
3	3.5	5.32	11.4	P50453	Serpin B9	3	2.452	2.4889	2.2799	2.3147	2.382235027
4	4.04	4.31	8.5	Q9BUQ8	Probable ATP-dependent RNA helicase DDX23	3	2.378	2.1571	2.6328	2.393	2.384298767
5	5.16	5.18	21.4	Q9Y383	Putative RNA-binding protein Luc7-like 2	3	2.552	2.1076	2.7407	2.249	2.399550828
6	49.48	49.48	68.5	P68371	Tubulin beta-4B chain	59	2.797	2.2177	2.6436	2.0919	2.42009816
7	7.45	7.45	15.7	P50502	Hsc70-interacting protein	4	2.691	2.1025	2.8081	2.1921	2.429297249
8	6	6	9.9	P04040	Catalase	3	2.598	2.3182	2.5845	2.3069	2.447929119
9	23.24	23.36	57.1	P60842	Eukaryotic initiation factor 4A-I	13	2.832	2.2444	2.676	2.1266	2.452400279
10	6	6	28.5	P30050	60S ribosomal protein L12	4	2.907	2.3014	2.6322	2.0812	2.460466524
11	12	12	36.1	P62241	40S ribosomal protein S8	8	3.122	2.5035	2.5077	2.0185	2.507963473
12	6.2	6.38	24.4	P31689	DnaJ homolog subfamily A member 1	4	2.809	2.4222	2.6052	2.2472	2.512240043
13	7.8	8.16	17.1	Q9Y5B9	FACT complex subunit SPT16	6	3.135	2.5774	2.4425	2.031	2.516175714
14	13.37	13.37	22.6	Q07065	Cytoskeleton-associated protein 4	8	2.921	2.3627	2.677	2.1817	2.519682881
15	24.02	24.91	54.7	P00558	Phosphoglycerate kinase 1	16	3	2.359	2.7055	2.1235	2.525150398

16	9.44	9.44	50	Q71DI3	Histone H3.2	5	2.827	2.3429	2.7917	2.2971	2.552889707
17	**13.08**	**13.13**	**64.3**	**P63241**	**Eukaryotic translation initiation factor 5A-1**	**11**	**2.642**	**2.2452**	**2.8977**	**2.52**	**2.565431672**
18	2.22	12.61	52.6	P15531	Nucleoside diphosphate kinase A	7	2.449	2.2943	2.8682	2.6897	2.565890189
19	8.34	8.41	15.2	P04843	Dolichyl-diphosphooligosaccharide--protein glycosyltransferase subunit 1	6	2.895	2.2809	2.9388	2.3141	2.588670304
20	3.18	3.18	11.5	O60701	UDP-glucose 6-dehydrogenase	3	2.673	2.0807	3.1906	2.5312	2.588819744
21	9.9	9.9	73.3	P13693	Translationally-controlled tumor protein	6	2.684	2.2831	2.9502	2.5058	2.594336628
22	23.47	23.47	65.3	P63244	Guanine nucleotide-binding protein subunit beta-2-like 1	15	3.041	2.5787	2.6106	2.227	2.598480415
23	5.21	5.31	12.4	Q9BZZ5	Apoptosis inhibitor 5	3	2.351	2.3712	2.8457	2.8819	2.600292534
24	6.02	6.12	11.8	Q9BYT8	Neurolysin, mitochondrial	3	2.872	2.2108	3.0649	2.3708	2.60622124
25	8.11	8.13	23.5	Q96AG4	Leucine-rich repeat-containing protein 59	4	3.06	2.4624	2.7687	2.2133	2.606748027
26	4	4	14	P50579	Methionine aminopeptidase 2	3	3.288	2.672	2.5485	2.0702	2.609253659
27	20.51	20.51	25.1	Q00839	Heterogeneous nuclear ribonucleoprotein U	15	3.082	2.3812	2.8614	2.2101	2.610085605
28	2.91	2.96	37.6	P62913	60S ribosomal protein L11	3	2.465	2.3153	2.9497	2.7907	2.618055199
29	2	20.45	35.6	P12235	ADP/ATP translocase 1	11	2.955	2.6335	2.606	2.3223	2.61966577
30	4	4.5	11.7	Q99733	Nucleosome assembly protein 1-like 4	3	3.205	2.6178	2.6342	2.151	2.625810697
31	5.86	5.86	13.3	P78417	Glutathione S-transferase omega-1	3	2.827	2.2645	3.0337	2.4548	2.627675428
32	17.9	17.9	32.6	O75874	Isocitrate dehydrogenase [NADP] cytoplasmic	11	2.937	2.4812	2.784	2.3605	2.630629819
33	8.39	8.41	23.9	Q99536	Synaptic vesicle membrane protein VAT-1 homolog	5	3.058	2.5909	2.6691	2.2849	2.636513769
34	13.47	13.47	16.9	O43143	Putative pre-mRNA-splicing factor ATP-dependent RNA helicase DHX15	10	2.901	2.5275	2.7607	2.3992	2.639861488
35	4	4	22.4	Q9UI30	tRNA methyltransferase 112 homolog	3	3.022	2.3929	2.9039	2.3166	2.640966727
36	6	6.02	35	P63208	S-phase kinase-associated protein 1	4	2.844	2.5813	2.7071	2.4585	2.643842906
37	8	8.04	22.7	P20700	Lamin-B1	4	3.035	2.409	2.9105	2.3128	2.648654399

38	27.7	27.94	54.7	P48643	T-complex protein 1 subunit epsilon	21	3.062	2.4469	2.8785	2.2844	2.649353735
39	13.24	13.24	44.6	P40925	Malate dehydrogenase, cytoplasmic	9	3.015	2.336	3.0152	2.3252	2.650843864
40	33.45	34.79	45.1	P50990	T-complex protein 1 subunit theta	20	3.045	2.3817	2.9517	2.3106	2.651965283
41	9.7	10.43	16.8	Q09666	Neuroblast differentiation-associated protein AHNAK	7	2.982	2.366	2.9992	2.3897	2.666660928
42	15.54	15.73	19.9	P56192	Methionine--tRNA ligase, cytoplasmic	8	3.181	2.5706	2.7593	2.2451	2.667830269
43	**65.85**	**66.12**	**62**	**O43707**	**Alpha-actinin-4**	**45**	**3.038**	**2.4127**	**2.9638**	**2.3531**	**2.673899579**
44	4.89	4.96	14.7	P62333	26S protease regulatory subunit 10B	3	2.916	2.4026	3.0075	2.4633	2.684095623
45	39.44	56.76	58.7	P08107	Heat shock 70 kDa protein 1A/1B	38	3.203	2.5043	2.9372	2.2923	2.710891067
46	13.77	13.77	23.3	P11387	DNA topoisomerase 1	9	3.36	2.6865	2.7761	2.2222	2.731719438
47	6.38	6.4	13.4	O43290	U4/U6.U5 tri-snRNP-associated protein 1	3	2.855	2.228	3.3681	2.6176	2.736543711
48	8.07	8.07	19.2	O00154	Cytosolic acyl coenzyme A thioester hydrolase	4	3.272	2.7982	2.673	2.2963	2.737977708
49	12.25	12.74	12.2	O60763	General vesicular transport factor p115	7	3.415	2.7545	2.7189	2.199	2.738501526
50	6	6	12.2	Q9NQW7	Xaa-Pro aminopeptidase 1	3	3.176	2.7153	2.7761	2.3568	2.740716013
51	7.15	7.15	10.4	Q9BQ52	Zinc phosphodiesterase ELAC protein 2	4	2.981	2.6112	2.8936	2.534	2.748601663
52	10.39	10.53	10.7	O75694	Nuclear pore complex protein Nup155	7	3.291	2.6192	2.8832	2.2967	2.748646542
53	5.21	5.21	7.6	Q9NSE4	Isoleucine--tRNA ligase, mitochondrial	3	3.14	2.5435	2.9788	2.4261	2.756308715
54	12	12	29.4	Q9Y3F4	Serine-threonine kinase receptor-associated protein	6	3.168	2.4754	3.0915	2.4211	2.767917456
55	16.01	16.01	21.2	P23246	Splicing factor, proline- and glutamine-rich	12	3.328	2.6366	2.9111	2.3104	2.771679224
56	4.16	4.85	7.6	O15067	Phosphoribosylformylglycinamidine synthase	3	2.973	2.3712	3.2465	2.5886	2.774347531
57	33.78	33.78	46.9	P17987	T-complex protein 1 subunit alpha	19	3.475	2.7831	2.7662	2.2185	2.775598586
58	7.79	7.79	6.8	P46013	Antigen KI-67	5	3.18	2.5138	3.0543	2.4375	2.777496623
59	23.86	23.98	26.8	P33176	Kinesin-1 heavy chain	13	3.252	2.5249	3.0567	2.3736	2.778201666
60	11.66	11.66	41.4	P46777	60S ribosomal protein L5	6	2.951	2.3707	3.2839	2.6108	2.782930331
61	18.27	18.27	20.1	P25205	DNA replication licensing factor MCM3	12	3.425	2.6499	2.9265	2.2816	2.790098428

62	12.69	12.69	25.8	Q99873	Protein arginine N-methyltransferase 1	7	2.969	2.3575	3.3255	2.6189	2.794212568
63	6.47	28.16	48.4	Q9BUF5	Tubulin beta-6 chain	29	2.914	2.2987	3.4325	2.6551	2.79521886
64	5.16	5.17	17.9	P39748	Flap endonuclease 1	3	3.076	2.4398	3.2331	2.5604	2.807481341
65	11.07	11.16	20.5	P02786	Transferrin receptor protein 1	6	3.46	2.7021	2.9347	2.2886	2.81499599
66	**23.12**	**23.12**	**70.4**	**Q06830**	**Peroxiredoxin-1**	**14**	**3.444**	**2.359**	**3.3592**	**2.3259**	**2.822633529**
67	**8.96**	**8.96**	**58.5**	**P30041**	**Peroxiredoxin-6**	**5**	**3.41**	**2.7663**	**2.8919**	**2.3374**	**2.825806968**
68	17.38	17.38	26.6	P26639	Threonine--tRNA ligase, cytoplasmic	11	3.525	2.7821	2.8815	2.2812	2.833534215
69	9.54	9.54	19.9	P61158	Actin-related protein 3	5	2.921	2.4467	3.2949	2.7453	2.835541983
70	9.33	9.39	11.5	P42224	Signal transducer and activator of transcription 1-alpha/beta	4	3.279	2.5755	3.1249	2.4525	2.836364413
71	6	6	18.9	P00918	Carbonic anhydrase 2	3	3.323	2.7554	2.9208	2.4261	2.838124079
72	26.55	26.81	24.1	P49736	DNA replication licensing factor MCM2	15	3.686	2.859	2.8434	2.1963	2.848228165
73	6	6.06	11.6	P43490	Nicotinamide phosphoribosyltransferase	3	3.392	2.8205	2.8861	2.4044	2.854466894
74	14.53	14.53	31.4	P23381	Tryptophan--tRNA ligase, cytoplasmic	7	3.147	2.5862	3.151	2.5951	2.856211331
75	37.03	37.23	48.2	O60506	Heterogeneous nuclear ribonucleoprotein Q	26	3.571	2.8128	2.9032	2.2931	2.859612345
76	9.83	9.94	17.4	Q9Y262	Eukaryotic translation initiation factor 3 subunit L	5	3.417	2.9107	2.8216	2.3838	2.859907072
77	25.18	27.26	32.6	P34932	Heat shock 70 kDa protein 4	17	3.271	2.6919	3.0541	2.5046	2.86477339
78	11.26	11.39	38.7	Q8NC51	Plasminogen activator inhibitor 1 RNA-binding protein	7	3.072	2.4243	3.3884	2.681	2.867971062
79	26.71	26.71	29.7	Q13263	Transcription intermediary factor 1-beta	17	3.321	2.6004	3.1574	2.485	2.869070749
80	7.2	7.2	37	P46783	40S ribosomal protein S10	4	3.117	2.4755	3.3096	2.656	2.869794691
81	16.85	17.08	29.8	P40939	Trifunctional enzyme subunit alpha, mitochondrial	9	3.321	2.6236	3.1679	2.4594	2.870395778
82	15.75	15.88	29.6	P54577	Tyrosine--tRNA ligase, cytoplasmic	8	3.317	2.6728	3.075	2.4939	2.871501334
83	14	14	63.9	P04792	Heat shock protein beta-1	8	3.042	2.7662	3.001	2.7128	2.876945532
84	9.74	9.75	35	Q15417	Calponin-3	5	3.286	2.6604	3.1462	2.5003	2.879706565
85	15.42	15.72	29.2	P23526	Adenosylhomocysteinase	10	3.3	2.5912	3.2059	2.5152	2.881604294

86	31.96	31.96	34	P55072	Transitional endoplasmic reticulum ATPase	21	3.288	2.5318	3.2839	2.5253	2.882478169
87	5.31	5.38	17	P52888	Thimet oligopeptidase	4	3.323	2.6893	3.109	2.5145	2.891082526
88	10.16	10.16	46.7	P24534	Elongation factor 1-beta	6	3.116	2.5171	3.3201	2.6865	2.892071209
89	**10.01**	**10.35**	**61.1**	**P06703**	**Protein S100-A6**	**6**	**3.111**	**2.5885**	**3.2438**	**2.7008**	**2.898168746**
90	**68.26**	**68.26**	**78.1**	**P63261**	**Actin, cytoplasmic 2**	**93**	**3.154**	**2.7714**	**3.0424**	**2.6731**	**2.903675666**
91	8.47	8.47	27.3	Q16543	Hsp90 co-chaperone Cdc37	5	3.354	2.7035	3.1298	2.5142	2.906373735
92	3.84	4.77	6.5	Q14008	Cytoskeleton-associated protein 5	3	3.407	2.6578	3.1845	2.4864	2.909890658
93	37.36	44.36	51.8	P11021	78 kDa glucose-regulated protein	23	3.451	2.6884	3.1553	2.4575	2.912347929
94	13.16	13.16	18.8	P33991	DNA replication licensing factor MCM4	7	3.41	2.726	3.1578	2.5051	2.928346605
95	21.58	21.92	26.1	P06737	Glycogen phosphorylase, liver form	12	3.605	2.7906	3.0686	2.3975	2.933090335
96	23.14	26.24	63.2	P07195	L-lactate dehydrogenase B chain	18	3.549	2.7294	3.1574	2.4298	2.936083009
97	8.67	8.77	24.7	P00505	Aspartate aminotransferase, mitochondrial	7	3.389	2.7102	3.1935	2.5527	2.941608706
98	26.7	26.7	42.2	P06576	ATP synthase subunit beta, mitochondrial	18	3.361	2.6447	3.288	2.5816	2.94724624
99	10.36	10.36	50.2	P09429	High mobility group protein B1	7	3.462	2.666	3.2569	2.5114	2.947656556
100	4.23	4.25	9.6	Q9UHB9	Signal recognition particle subunit SRP68	3	3.788	2.977	2.9273	2.3005	2.952021858
101	16.45	16.5	21.7	P11586	C-1-tetrahydrofolate synthase, cytoplasmic	10	3.513	2.8813	3.0463	2.4874	2.959349322
102	23.83	23.96	32.4	P49588	Alanine--tRNA ligase, cytoplasmic	17	3.503	2.8361	3.0963	2.506	2.963100926
103	13.8	13.8	21.9	O00232	26S proteasome non-ATPase regulatory subunit 12	9	3.641	2.9236	3.0149	2.411	2.965870529
104	**17.65**	**38.98**	**40.9**	**P12814**	**Alpha-actinin-1**	**27**	**3.369**	**2.6949**	**3.2969**	**2.6434**	**2.982483718**
105	6.03	6.06	6.1	O60610	Protein diaphanous homolog 1	3	3.233	2.9946	2.9831	2.7477	2.984663762
106	8.68	8.71	15.7	P55884	Eukaryotic translation initiation factor 3 subunit B	4	3.276	2.5182	3.5375	2.7476	2.992409448
107	5.21	5.27	6	O14617	AP-3 complex subunit delta-1	3	3.387	3.2178	2.7918	2.6363	2.992701106
108	6	6.06	23.4	P35270	Sepiapterin reductase	3	3.475	2.945	3.0459	2.5749	2.993153772
109	25.43	25.43	16.7	P07814	Bifunctional glutamate/proline--tRNA ligase	17	3.338	2.6486	3.3972	2.6876	2.997416638

110	9.01	9.01	25.5	Q14247	Src substrate cortactin	6	3.188	2.4517	3.6816	2.8109	2.998934008
111	10.45	10.46	46.8	Q15293	Reticulocalbin-1	7	3.452	2.848	3.1603	2.6089	3.000537985
112	39.12	39.19	62	P49368	T-complex protein 1 subunit gamma	24	3.448	2.8729	3.1326	2.6153	3.001432328
113	16	17.06	29.5	P52292	Importin subunit alpha-1	11	3.504	2.8848	3.1398	2.5798	3.008097839
114	33.43	33.74	25.3	P41252	Isoleucine--tRNA ligase, cytoplasmic	17	3.565	2.8378	3.1965	2.5468	3.012504589
115	7.85	7.85	43.4	Q99497	Protein DJ-1	6	3.772	2.9655	3.0694	2.4053	3.014554141
116	4.03	4.03	15.5	Q9UK22	F-box only protein 2	3	3.691	2.9177	3.1397	2.4594	3.019781364
117	16.39	16.39	48.3	P31943	Heterogeneous nuclear ribonucleoprotein H	21	3.403	2.9581	3.092	2.6885	3.02451736
118	12.08	12.17	38	P62826	GTP-binding nuclear protein Ran	6	3.122	2.7034	3.3888	2.931	3.025876798
119	**6.05**	**6.05**	**27.7**	**O00303**	**Eukaryotic translation initiation factor 3 subunit F**	**4**	**3.595**	**2.8637**	**3.203**	**2.5507**	**3.028382192**
120	11.96	12	42.3	P52907	F-actin-capping protein subunit alpha-1	7	3.716	3.1134	2.9596	2.4631	3.030445111
121	28.5	28.56	38.1	P02545	Prelamin-A/C	20	3.319	2.6664	3.4533	2.7699	3.033246729
122	15.46	15.65	12.3	Q04637	Eukaryotic translation initiation factor 4 gamma 1	8	3.547	2.8877	3.1788	2.6062	3.03508635
123	10.23	10.23	23.1	Q9Y2X3	Nucleolar protein 58	5	3.428	2.9777	3.118	2.6884	3.041395772
124	**33.43**	**33.43**	**65.6**	**P04083**	**Annexin A1**	**19**	**3.619**	**2.9094**	**3.1811**	**2.5637**	**3.044101546**
125	6.12	6.12	17.7	Q8N163	Cell cycle and apoptosis regulator protein 2	4	3.771	3.0499	3.0344	2.4645	3.045341116
126	8.3	13.33	40	P52597	Heterogeneous nuclear ribonucleoprotein F	19	3.248	3.0966	3.0031	2.8625	3.049327742
127	**44.82**	**44.82**	**64.3**	**P07355**	**Annexin A2**	**28**	**3.147**	**2.8988**	**3.223**	**2.947**	**3.050976477**
128	63.41	63.48	76.4	P10809	60 kDa heat shock protein, mitochondrial	52	3.565	2.9554	3.1557	2.609	3.05183745
129	10	10	13.3	P47897	Glutamine--tRNA ligase	5	3.902	3.0177	3.0818	2.3967	3.053833561
130	8	8.38	19	P14868	Aspartate--tRNA ligase, cytoplasmic	4	3.216	2.6899	3.4814	2.8971	3.056274772
131	13.39	13.97	51.2	P21796	Voltage-dependent anion-selective channel protein 1	10	3.374	2.6707	3.5155	2.7722	3.061226481
132	**10.37**	**10.37**	**39.3**	**P30044**	**Peroxiredoxin-5, mitochondrial**	**6**	**3.5**	**2.7971**	**3.3517**	**2.6848**	**3.063643865**
133	37.31	37.47	28	P53396	ATP-citrate synthase	21	3.71	2.8662	3.2723	2.5332	3.064084573

134	6.22	13.44	15.9	Q92841	Probable ATP-dependent RNA helicase DDX17	7	3.261	2.8584	3.2962	2.8762	3.066031481
135	12.58	12.59	24.8	Q7KZF4	Staphylococcal nuclease domain-containing protein 1	8	3.511	3.0334	3.1043	2.6787	3.067694224
136	11.85	11.86	22.8	P49748	Very long-chain specific acyl-CoA dehydrogenase	6	3.454	2.8001	3.371	2.7221	3.069302377
137	7.57	7.57	24.1	Q9NUQ9	Protein FAM49B	5	2.868	2.7081	3.4675	3.2981	3.069948099
138	8.26	8.26	29.6	P47756	F-actin-capping protein subunit beta	4	3.405	3.2948	2.8263	2.8168	3.074185792
139	**6**	**7**	**6.8**	**P16144**	**Integrin beta-4**	**5**	**3.329**	**3.2164**	**2.9283**	**2.8525**	**3.075255949**
140	18	18	38	Q15084	Protein disulfide-isomerase A6	11	3.365	2.7519	3.4512	2.8209	3.08137024
141	14.79	14.79	32.7	P29401	Transketolase	13	3.173	2.5794	3.7006	2.9969	3.086620889
142	4.02	4.26	11.5	Q16401	26S proteasome non-ATPase regulatory subunit 5	3	2.972	2.4999	3.8327	3.2244	3.09550347
143	7.89	7.93	7.5	Q6P2E9	Enhancer of mRNA-decapping protein 4	4	3.717	3.2008	3.0144	2.5739	3.099637544
144	2.31	2.31	9.8	Q01780	Exosome component 10	3	3.48	2.8622	3.361	2.766	3.102058455
145	**8.66**	**8.67**	**40.7**	**P51148**	**Ras-related protein Rab-5C**	**4**	**3.718**	**2.9939**	**3.2835**	**2.5631**	**3.111088115**
146	7.2	7.2	45.3	O75947	ATP synthase subunit d, mitochondrial	5	3.648	2.8553	3.3999	2.6748	3.11972281
147	7.85	8.21	10.2	Q9Y6Y8	SEC23-interacting protein	4	3.606	2.8933	3.3604	2.7021	3.119808204
148	10.82	11.1	19.6	Q9BXJ9	N-alpha-acetyltransferase 15, NatA auxiliary subunit	9	3.543	3.079	3.1756	2.7589	3.126695931
149	2	4.27	16.1	P31150	Rab GDP dissociation inhibitor alpha	3	3.537	3.1823	3.0832	2.7743	3.132440457
150	4	4.02	14.2	P47985	Cytochrome b-c1 complex subunit Rieske, mitochondrial	3	3.333	2.5788	3.8058	2.9496	3.134119239
151	7.91	8.9	16.2	P05455	Lupus La protein	5	3.941	3.1672	3.1337	2.5097	3.147677923
152	6	6	9.5	O15371	Eukaryotic translation initiation factor 3 subunit D	4	3.953	3.1418	3.1674	2.5029	3.150017308
153	30.13	30.13	50.8	P78371	T-complex protein 1 subunit beta	22	3.887	3.0684	3.2384	2.5545	3.15166993
154	6.76	6.85	28.3	P13995	Bifunctional methylenetetrahydrofolate dehydrogenase/cyclohydrolase, mitochondrial	3	3.944	3.2125	3.1255	2.5039	3.15557954
155	4.01	4.1	19.2	P30040	Endoplasmic reticulum resident protein 29	3	3.286	2.7786	3.5975	3.0416	3.161543219
156	16.07	16.12	73.7	P22392	Nucleoside diphosphate kinase B	12	3.75	3.1848	3.1474	2.6933	3.172031752

157	12.39	12.47	43	P32322	Pyrroline-5-carboxylate reductase 1, mitochondrial	8	3.938	3.0672	3.2886	2.5588	3.175165013
158	26.2	26.37	66.4	P12277	Creatine kinase B-type	23	3.827	3.0349	3.3322	2.6306	3.176487721
159	8.72	8.76	18.5	P30740	Leukocyte elastase inhibitor	6	3.677	3.2575	3.1227	2.7486	3.184233924
160	6	6.01	12.4	Q53GS9	U4/U6.U5 tri-snRNP-associated protein 2	3	3.769	3.2073	3.2386	2.6267	3.184442246
161	6	6	14.9	Q14376	UDP-glucose 4-epimerase	3	3.71	3.0127	3.3945	2.7518	3.196543502
162	6.63	6.69	15.8	O95202	LETM1 and EF-hand domain-containing protein 1	5	3.925	3.1006	3.3009	2.6111	3.200260411
163	3.42	3.72	19.1	P28066	Proteasome subunit alpha type-5	3	3.38	3.1571	3.2482	3.0359	3.202829468
164	9.07	9.07	27.7	P14550	Alcohol dehydrogenase [NADP(+)]	5	3.683	3.1399	3.2711	2.7937	3.206252943
165	8.78	8.85	18.4	Q9UNM6	26S proteasome non-ATPase regulatory subunit 13	4	3.311	2.7764	3.7594	3.0638	3.207783442
166	5.23	5.24	18.2	Q9HC38	Glyoxalase domain-containing protein 4	3	3.968	3.137	3.2978	2.5899	3.211059647
167	21.9	21.95	20.2	P26640	Valine--tRNA ligase	14	3.771	3.0978	3.3359	2.7374	3.213773746
168	36.21	36.34	41.3	P12268	Inosine-5'-monophosphate dehydrogenase 2	19	3.886	3.0327	3.4166	2.6513	3.214373315
169	4	11.12	14.3	Q13310	Polyadenylate-binding protein 4	6	3.346	2.6003	3.9732	3.1075	3.21940222
170	11.64	12.02	45.1	Q02790	Peptidyl-prolyl cis-trans isomerase FKBP4	8	3.611	2.8935	3.5938	2.9057	3.231944641
171	6.06	6.66	8.5	Q92922	SWI/SNF complex subunit SMARCC1	3	3.43	2.7039	3.8701	3.0495	3.234512938
172	8.59	8.62	21.3	O00231	26S proteasome non-ATPase regulatory subunit 11	5	3.612	2.7977	3.747	2.8954	3.235826944
173	**7.86**	**7.86**	**37.1**	**P10599**	**Thioredoxin**	**5**	**3.898**	**3.2007**	**3.2947**	**2.7109**	**3.249032417**
174	4.74	5.3	28.5	Q9HB71	Calcyclin-binding protein	3	3.761	3.0024	3.5346	2.795	3.249926151
175	4.01	4.87	6.4	Q7L2E3	Putative ATP-dependent RNA helicase DHX30	3	3.585	3.5433	3.0124	2.9419	3.257312361
176	5.92	5.92	22.4	P43487	Ran-specific GTPase-activating protein	3	3.398	2.6647	3.984	3.125	3.258444003
177	21.48	21.48	32.5	Q92945	Far upstream element-binding protein 2	12	3.495	3.0883	3.423	3.0541	3.259223953
178	9.46	9.46	12.5	Q9H3U1	Protein unc-45 homolog A	5	3.84	3.062	3.47	2.7659	3.259309406
179	4.22	4.25	21.3	Q99615	DnaJ homolog subfamily C member 7	3	3.468	3.2585	3.2843	3.0693	3.266966969
180	4.06	4.06	11.7	Q6ZMU5	Tripartite motif-containing protein 72	3	3.867	2.9833	3.5887	2.7671	3.27158552

181	11.25	11.25	15.7	O75534	Cold shock domain-containing protein E1	6	3.742	2.9174	3.6579	2.874	3.273064687
182	5.18	5.2	32.7	P27695	DNA-(apurinic or apyrimidinic site) lyase	4	3.664	2.8597	3.7741	2.9398	3.283611608
183	6	6.05	13.7	P16435	NADPH--cytochrome P450 reductase	3	3.372	3.2427	3.1615	3.3665	3.284479349
184	**9.78**	**9.78**	**47.8**	**P51149**	**Ras-related protein Rab-7a**	**6**	**3.817**	**3.0249**	**3.5622**	**2.8321**	**3.285224223**
185	19.19	19.23	42.8	P61978	Heterogeneous nuclear ribonucleoprotein K	13	3.563	2.7981	3.8634	3.0287	3.286444078
186	28.35	29.12	13.1	Q92616	Translational activator GCN1	15	4.048	3.1986	3.3885	2.6868	3.295040952
187	31.14	31.98	48.7	P30101	Protein disulfide-isomerase A3	18	3.825	2.9836	3.6516	2.8496	3.301108392
188	6.04	6.06	17.2	P10515	Dihydrolipoyllysine-residue acetyltransferase component of pyruvate dehydrogenase complex, mitochondrial	3	4.202	3.4006	3.19	2.6174	3.304974363
189	21.32	21.32	49.8	O60664	Perilipin-3	13	3.708	3.2643	3.3426	2.9571	3.307273055
190	6.84	6.89	22.8	P07741	Adenine phosphoribosyltransferase	4	3.608	2.8354	3.9114	3.0152	3.314227411
191	8.23	8.23	45.2	Q16778	Histone H2B type 2-E	12	3.86	3.0227	3.6606	2.8627	3.325275373
192	6	6	23.1	P37802	Transgelin-2	3	4.32	3.337	3.3418	2.5865	3.341051905
193	9.85	9.85	16.4	Q15637	Splicing factor 1	5	4.04	3.2815	3.4313	2.7786	3.353008264
194	6.98	8.31	14.2	O60264	SWI/SNF-related matrix-associated actin-dependent regulator of chromatin subfamily A member 5	5	3.988	3.2651	3.4638	2.8217	3.358758826
195	6.08	6.08	25.6	O95816	BAG family molecular chaperone regulator 2	3	3.765	3.3637	3.3494	3.0154	3.362974278
196	7.43	7.46	11.3	P00367	Glutamate dehydrogenase 1, mitochondrial	4	3.675	3.2325	3.5119	3.0926	3.370275803
197	8.88	8.89	14.9	P48147	Prolyl endopeptidase	5	4.016	3.2715	3.4927	2.8828	3.391400709
198	1.57	1.61	21.5	O14929	Histone acetyltransferase type B catalytic subunit	4	4.214	3.2742	3.5336	2.7514	3.40324107
199	5.46	5.46	12.5	Q9Y305	Acyl-coenzyme A thioesterase 9, mitochondrial	3	4.285	3.4256	3.4263	2.6939	3.411721585
200	8.26	8.26	22.6	Q9NSD9	Phenylalanine--tRNA ligase beta subunit	6	3.707	3.0904	3.8141	3.1463	3.424186193
201	16.45	16.78	24.9	Q8WUM4	Programmed cell death 6-interacting protein	9	3.832	3.0258	3.8391	3.0948	3.425957199
202	6	6	31.3	Q02543	60S ribosomal protein L18a	3	3.558	3.1376	3.7685	3.275	3.426066876

203	**10.29**	**12.43**	**50.5**	**P32119**	**Peroxiredoxin-2**	**9**	**3.983**	**3.3509**	**3.5226**	**2.9617**	**3.435136844**
204	**9.74**	**9.85**	**49**	**P60660**	**Myosin light polypeptide 6**	**6**	**4.026**	**3.2748**	**3.6441**	**2.9532**	**3.451321561**
205	14.47	14.47	36.4	P50395	Rab GDP dissociation inhibitor beta	8	3.868	3.1055	3.8672	3.0769	3.457657752
206	4.55	4.62	17.2	Q01105	Protein SET	4	3.756	3.1691	3.8009	3.2072	3.47071141
207	5.12	5.12	18.6	Q9P258	Protein RCC2	4	3.822	3.7237	3.3254	3.2226	3.514219754
208	**8.84**	**8.84**	**37.9**	**P30048**	**Thioredoxin-dependent peroxide reductase**	**6**	**4.105**	**3.2069**	**3.8924**	**3.0374**	**3.532071674**
209	6.97	7.03	7.3	Q13435	Splicing factor 3B subunit 2	4	4.097	3.6418	3.4835	3.1032	3.563706336
210	**3.27**	**3.27**	**18.4**	**P61019**	**Ras-related protein Rab-2A**	**3**	**4.205**	**3.8733**	**3.3706**	**3.1051**	**3.613328827**
211	11.42	11.44	38.2	P35232	Prohibitin	6	4.252	3.7082	3.5437	3.0931	3.62578317
212	6.22	6.22	13	P35237	Serpin B6	3	3.71	3.1641	4.1809	3.5445	3.63171883
213	3.55	5.71	16.9	P30483	HLA class I histocompatibility antigen, B-45 alpha chain	3	4.467	3.646	3.697	3.0045	3.667444657
214	6	6.27	6.9	Q7L576	Cytoplasmic FMR1-interacting protein 1	3	3.783	3.3916	3.9949	3.5698	3.677881154
215	16.46	16.54	13.1	Q14980	Nuclear mitotic apparatus protein 1	9	4.06	3.2907	4.1488	3.3446	3.689948055
216	4.88	4.88	9.9	Q9BSJ8	Extended synaptotagmin-1	3	4.566	3.8438	3.6067	3.0517	3.728096427
217	14	14	16.4	P43243	Matrin-3	9	4.573	3.6209	3.9482	3.1193	3.778927026
218	6.04	6.04	11	Q9Y6M1	Insulin-like growth factor 2 mRNA-binding protein 2	3	4.628	3.5807	4.0389	3.1564	3.81244955
219	3.21	3.27	16.9	Q9BWD1	Acetyl-CoA acetyltransferase, cytosolic	3	4.698	3.6064	4.1085	3.1259	3.840708262
220	14.71	15.65	23.2	Q9P2E9	Ribosome-binding protein 1	9	4.171	3.7477	4.0062	3.5949	3.873522762
221	10.43	10.52	18.8	O00429	Dynamin-1-like protein	6	4.874	4.0291	3.8055	3.1474	3.916195008
222	6.8	6.82	10.2	P23921	Ribonucleoside-diphosphate reductase large subunit	4	5.042	3.9092	3.9588	3.0604	3.931045961
223	6	6	25.2	O75569	Interferon-inducible double-stranded RNA-dependent protein kinase activator A	3	4.746	3.9091	3.9635	3.2803	3.940934667
224	10.54	10.58	60.2	P84077	ADP-ribosylation factor 1	6	4.564	3.5553	4.3693	3.4196	3.945956247
225	49.07	49.07	43.1	O00410	Importin-5	41	5.168	4.0126	4.0491	3.1421	4.030247523

226	6.07	6.07	28.7	O95571	Persulfide dioxygenase ETHE1, mitochondrial	4	4.166	4.0015	4.153	3.9409	4.064198004
227	6.08	6.08	16.1	P49419	Alpha-aminoadipic semialdehyde dehydrogenase	3	3.822	3.6253	4.5761	4.3334	4.071362103
228	2.72	2.76	15.3	Q9H845	Acyl-CoA dehydrogenase family member 9, mitochondrial	3	4.899	4.139	4.0396	3.4127	4.088931504
229	15.59	15.59	48.3	Q15365	Poly(rC)-binding protein 1	12	4.979	3.8667	4.82	3.7567	4.320997743
230	20.8	20.8	63.6	P60174	Triosephosphate isomerase	14	5.103	4.0887	4.8862	3.9127	4.469044211
231	40.76	40.76	73.3	P05783	Keratin, type I cytoskeletal 18	31	5.286	4.5253	5.0246	4.2816	4.762889765
232	48.03	48.83	65.6	P05787	Keratin, type II cytoskeletal 8	35	5.391	4.7759	4.9042	4.3468	4.840225518
233	**9.3**	**9.31**	**42.4**	**Q9H773**	**dCTP pyrophosphatase 1**	**4**	**4.696**	**4.0305**	**5.9068**	**5.0451**	**4.873346202**
234	8.18	8.21	10.4	P28290	Sperm-specific antigen 2	5	5.573	4.9467	4.7219	4.3495	4.877981895
235	8.33	8.4	33.2	P30519	Heme oxygenase 2	5	6.542	5.7182	6.2086	5.4025	5.951680158
236	22.97	22.98	23.7	O95831	Apoptosis-inducing factor 1, mitochondrial	13	6.85	5.4901	7.5722	6.1311	6.464096416
237	18.32	18.32	35.9	P34913	Bifunctional epoxide hydrolase 2	16	7.261	5.6177	7.6744	5.9462	6.568402095

List of Publication

LI Jinglin, Wang Jigang, Lim Teck Kwang, LIN Qingsong. Quantitative Chemical Proteomics Approaches to Identify Triptolide's Binding Target, Annexin A1. (Manuscript in preparation)

Conference Presentation

The 7th International Structural Biology and Functional Genomics (SBFG) Conference *Singapore, 2013*